Bendix Instruments & Life Support Division

CRYOGENIC STORAGE SYSTEMS DESIGN, FABRICATION AND EVALUATION

FINAL REPORT

CONTRACT: NAS9-5491

VOLUME I

Prepared for

NATIONAL AERONAUTICS AND
SPACE ADMINISTRATION -
MANNED SPACECRAFT CENTER
HOUSTON, TEXAS 77058

Presented by

THE BENDIX CORPORATION
INSTRUMENTS & LIFE
SUPPORT DIVISION
DAVENPORT, IOWA 52808

Pub. No. 3861A-68
S.O. 33-11014
March 27, 1968

TABLE OF CONTENTS

SECTION A
PHASE I - CRYOGENIC STORAGE SYSTEM STUDY

SECTION B
PHASE II - VESSEL AND SHELL FABRICATION

SECTION C
PHASE III - PROTOTYPE THERMAL MODEL FABRICAION

SECTION D
PHASE IV - PROTOTYPE STRUCTURAL MODEL FABRICATION

SECTION A

PHASE I - CRYOGENIC STORAGE SYSTEM STUDY

1.0 INTRODUCTION AND TECHNOLOGY SUMMARY

The NAS 9-5491 program is to determine the applicable design concepts for long mission cryogenic storage tankage and to verify concept feasibility through hardware fabrication and test. The design, analysis and test results of work accomplished on NAS 9-2978 contract were used extensively as a basis for the extrapolation analyses for larger tank and longer mission characteristics. This was quite appropriate since that program is now recognized as the principal technology turning point to long duration cryogenic tank design. Technology development as it pertains to the space program is directly related to increasing the mission duration capability of the on-board systems. If the effective mission duration capability of the on-board systems is not progressively increased, earth orbital, lunar and planetary exploration will decline due to an inability to plan and meet progressive objectives. The direct and by-product rewards of this technology in terms of earth resource evaluation and management and earth-solar system resource evaluation would fail to develop. Cryogenic fluids, because of the purity, density and specific impulse are uniquely suited to the functions of atmosphere supply, power reactants, pressurants and propellants. Therefore, the development of long duration cryogenic storage and supply systems is a key factor to extending the mission duration capability of existing space systems.

Since cryogenic fluids must be protected from thermal environment to prevent pressure increase and premature loss of fluid, the thermal protection system is the principal design element. Thermal design cannot be compromised because the effectivity of thermal design influences mission duration. In all space systems, weight, structural integrity and reliability are critical factors and establish the technological criteria for obtaining optimum thermal performance while maintaining suitable weight and structural characteristics. An inseparable relationship between the thermal, thermodynamic and physical characteristics of a cryogenic storage and supply system and an orderly development evolution is constrained accordingly.

During the last three years, remarkable progress has been made toward increasing mission applications of cryogenic systems. This has been accomplished through thermal system development and improved understanding of thermal/thermodynamic system mechanics. As a result feasible mission limitation for the application of cryogenic storage systems is virtually nonexistant. This presents a new opportunity and greater flexibility to the planning of increased mission systems and programs with current state-of-the-art boosters and vehicles.

Chart I shows the thermal/thermodynamic features that constitute the practicable steps to obtain long mission duration capability using oxygen as the example fluid. The same design steps, in the same order, apply to all cryogenic fluids, although the mission duration characteristics will vary due to different fluid properties. Mission duration increases with the thermal and thermodynamic design arrangement and tank size.

The concept that "more insulation" will increase the mission duration capability rapidly reaches a practicable limit. In terms of effectiveness (weight, reproducibility, thermal management) this concept does not hold true. Specific insulation designs are effective only for specific temperature regions. Therefore, an effective thermal protection system design is comprised of several specific insulation designs with each design being selected for optimum performance in a specific temperature region.

Chart II shows the building block steps to obtain light weight cryogenic storage systems and is based upon a constant heat input flux of 0.5 Btu/ft^2-hr. at the inner vessel surface. A number of factors not noted on the chart control the stored system weight per pound of stored fluid. These are summarized below:

(a) As the heat input flux is decreased respectively to 0.4, 0.3 and 0.2 Btu/ft^2-hr., curves 1, 2 and 3 move rapidly upward on the relative weight scale.

(b) The only insulation design concept that holds a stable weight position at very low heat flux is curve 4. Therefore, this is the only design concept at this time that has the potential of effectively meeting the long mission system requirements.

(c) Curves 5, 6, etc. show the design technique for improving the weight of the basic curve 4 concept.

The data and design aspects of these graphs are explained in greater detail in the appropriate context of the ensuing report.

THERMAL – THERMODYNAMIC DEVELOPMENT OF LONG MISSION CRYO SYSTEMS (OXYGEN)

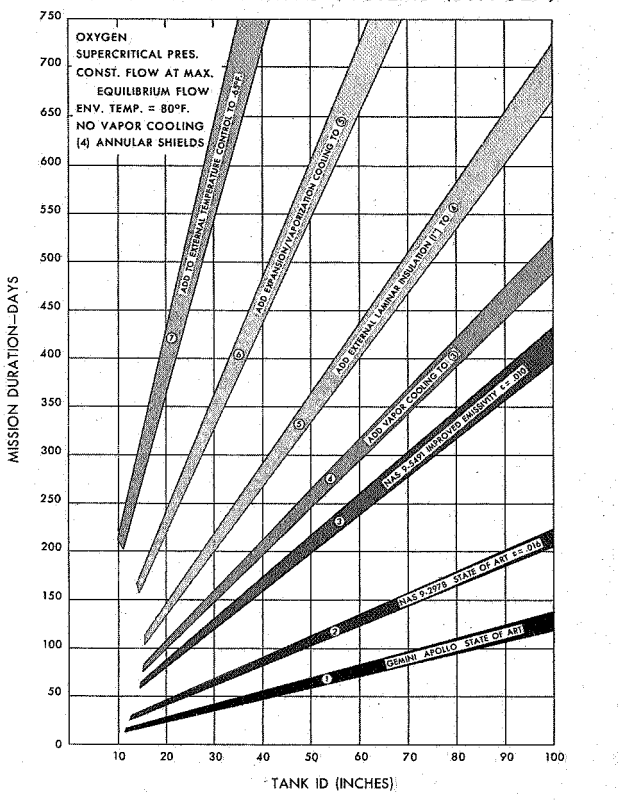

C-5005-68-2

THERMAL - PHYSICAL DEVELOPMENT OF LONG MISSION CRYO SYSTEMS (OXYGEN)

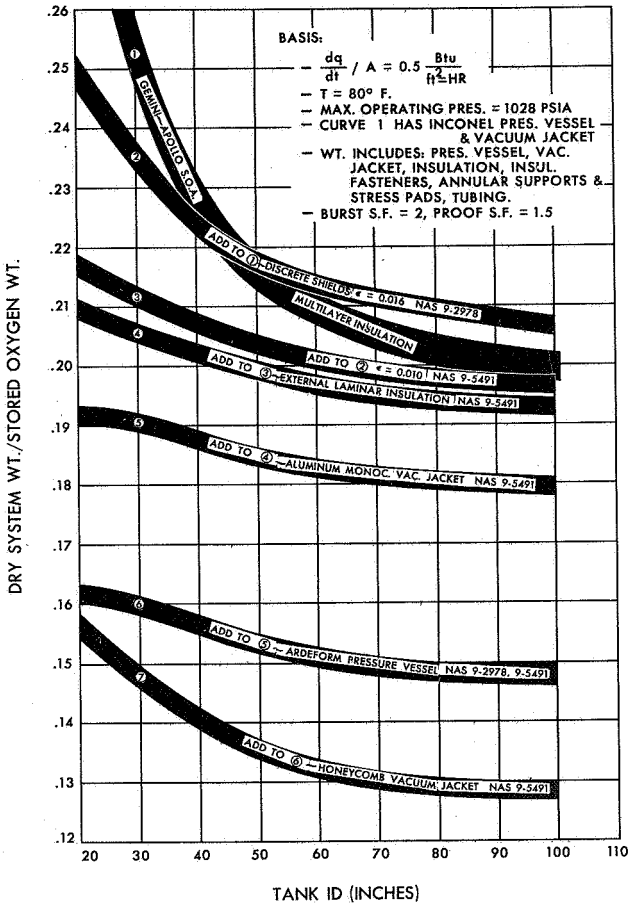

C-3790-67-8.2

2.0 CRYOGENIC VESSEL THERMAL/THERMODYNAMIC DESIGN PHILOSOPHY

Fluid storage supply systems are comprised of a storage vessel and components to provide pressure control, flow control, status monitoring, structural interfacing and service interfacing.

The major component of a normal fluid storage system from a design, fabrication and performance aspect is the pressure vessel. A cryogenic storage vessle requires, in addition, a sophisticated insulation package to preserve both the temperature and pressure of the cold, dense fluid.

A principle design consideration, therefore, is the property of the thermal insulation of the vessel; i.e., insulating quality, weight and volume.

The properties of different cryogens vary in terms of heat content, density, temperature and pressure. Therefore, a second design consideration, inportant to performance, is the thermodynamic characteristics of the integral thermal insulation - cryogen system.

Application of cryogenic system to flight vehicles imposes the requirements of minimum effective system weight and high structural integrity.

An experienced summarization of the design technology requirements for a cryogenic storage system in the order of imposed design constraints is therefore, thermal, thermodynamic and structural.

The cryogenic system is a thermodynamic machine that is powered, primarily, by the heat transferred from the surrounding thermal environment. A specific system will run faster or slower, respectively shorter or longer, depending upon the thermal environment and the thermal/thermodynamic design of the system.

The typical system performance parameters that establish the specific design for a certain environment are:

(a) Mission flow and duration -- quantity & basic size.

(b) No flow standby -- static thermal design.

(c) Minimum flow -- thermal/thermodynamic design.

(d) Maximum flow -- supplemental power and thermal/thermodynamic design.

It is seen that an inseparable relation exists between various design and performance aspects of the system.

The thermal insulation design establishes the basic static heat transfer characteristics of the system. Also, the basic vessel and insulation comprise the major weight and structure of the system. The difficult or unique technology is the attainment of a light weight, low heat transfer, high structural integrity-insulation tank system. Therefore, "thermal-physical" design provides the important basic thermal and physical properties.

The cryogen, at pressure and during flow, can be used by various processes of vaporization, expansion and direction of flow to perform heat interception and rejection. These processes supplement the static insulation package to further reduce the effective heat transfer to the system. This minimizes the static insulation required and becomes an addition to, or trade off with, the "thermal-physical" design. Therefore, the "thermal-thermodynamic" design provides the important functional properties.

System pressure determines the single or two-phase state of the contained cryogen. System weight due to cryogen pressure is minimal in the two-phase condition. Two-phase operation presents two fluid states, hence two distinct thermodynamic conditions. Management of the two-phases in a zero "g" environment requires a predictable method of phase collection and thermodynamic processing in the flow stream for control. The principle advantage of two-phase operation for small systems is the wide range of flow control that is possible through manipulation of the two thermodynamic states without supplemental power. In large systems, the advantages are a wide range of flow control and reduced weight.

The mission requirements of a system normally require a range of performance for the various functions such as principally non-operative standby and flow, within a varying thermal environment. Control versatility is obtained with a wide range between the "maximum flow per unit heat input" and "minimum flow per unit heat input" characteristics of the system. Therefore, the manipulation or management versatility of the thermal/thermodynamic function provides the important operation control properties.

System design and operation criteria are logically reduced to and treated as follows because of the interrelation of the various functions.

(a) Thermal-physical design - thermal & physical characteristics.

(b) Thermal-thermodynamic design - functional characteristics.

(c) Operational control - thermal/thermodynamic management.

The following sections treat the system in this order.

A further note is appropriate for appreciation of the order of criteria presented above. Recent Research and Development (R & D) programs have provided the lowest heat transfer system in terms of total heat transfer per unit temperature differential, unit thickness and unit weight of insulation. As the thermal requirements become more stringent, the thermal/thermodynamic designs become more sophisticated and the latitude in design approach becomes more limited.

2.1 Thermal-Physical Design

STATE-OF-THE-ART TODAY

Best application of available materials, available processes, available manufacturing techniques.

The concepts and data are generally derived from the design, fabrication and test experience on the NAS 9-2978 program, the manufacture of over 30,000 cryogenic systems, and twenty years continual research and development work on cryogenic tankage. The design concepts approach optimum due to the technological state-of-art and the apparent limitations of materials, processes and fabrication techniques.

HEAT TRANSFER

Surface Radiation
Support Conduction
Gas Conduction

The heat transfer to a cryogenic tank can be divided into surface radiation, support conduction and gas conduction.

Initial design consideration is generally concerned with the basic tank design philosophy. Typical tank designs for flight application are:

(a) Single wall tank - externally applied insulation.

(b) Dual wall tank - collapsible metal outer shell.

(c) Dual wall tank - rigid metal shells.

2.1.1 Single Wall Design

SINGLE WALL TANK WITH INSULATION

For application where the total heat transfer

This approach has been followed on large booster tanks and current R & D for large tanks applicable to cryogenic propellants for long mission vehicles. In this design the insulation is applied to the pressure vessel

is:

Small Tanks >2 Btu/ft^2/hr

Large Tanks >1 Btu/ft^2/hr

NON RIGID DUAL WALL TANK

Total Heat Transfer is:

>1 Btu/ft^2/hr

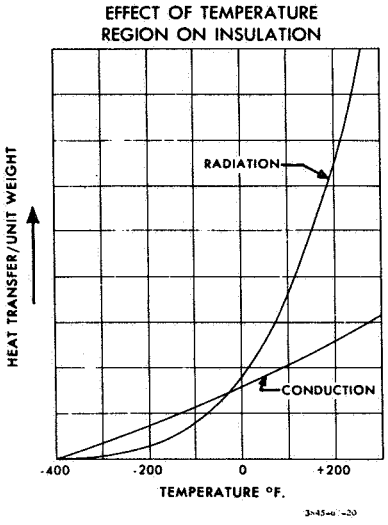

EQUATION FOR CONDUCTIVE HEAT TRANSFER

$$\frac{dQ}{dt} = 1\ KA\ \frac{dT}{dn}$$

wall with an outer protective bag or film. The pressure vessel is purged in a 1 g environment and naturally evacuated in a space environment. Problems of poor predictability, reproducibility, and quality preservation properties are apparent in this approach. If the total static heat transfer requirements (conduction & radiation) are less than 1 Btu/ft^2/hr, this concept is not applicable. If the requirement is less than 2 Btu/ft^2/hr the concept is marginal.

2.1.2 Dual Wall Design

The dual wall tank with a collapsible metal outer shell was extensively investigated and tested on the DynaSoar and Apollo programs. The thermal properties are comparable to the single wall design approach. In general, the dual wall tank has no practical application.

2.1.3 Rigid Dual Wall Design

The rigid dual wall tank has been used on all successful low heat leak design tanks for aircraft and space system applications. The principle advantage is that it provides a self contained protective environment for the complete insulation (conductive & radiation) package. Reproducibility, insulation quality preservation and predictability are maintained from manufacture through installation checkout and flight. At the current state-of-art, rigid dual wall construction is essential where the total static heat transfer requirement is less than 1 Btu/hr/ft^2 of cryogen vessel surface.

As the size of cryogenic storage tanks increases, the ability to achieve and maintain a stable and reliable vacuum in the dual wall tank design poses certain problems. In addition, the structural reliability and fabrication problems associated with large tankage point towards an alternative arrangement which, at the same time, retains the foregoing advantages of dual wall construction. R & D is currently proceeding on various alternate designs throughout the country; however, thermal properties which approach the rigid dual wall construction have not been achieved.

2.1.4 Gas Conduction Heat Transfer

In the rigid dual wall design, it is standard practice to evacuate the annular insulation package to a stable 10^{-6} torr. At this pressure and with the insulation spacing employed, the gas conduction heat transfer is extremely low. This mode of heat transfer is included in the Bendix computer programs and derived empirically

and theoretically for the data presented in the appendix. The gas conduction in a tank having discrete radiation shields must be computed for each intershield space utilizing the temperatures of the boundary shields.

2.1.5 Tube & Support System Conduction

The thermal conductivity heat transfer through a material varies directly as the temperature differential. This is a disadvantage, in the low temperature region, compared to radiation heat transfer since radiation heat transfer varies as the difference in the fourth power of the temperatures.

It was learned in aircraft and early space system development that the basic thermal conductivity mode of heat transfer must be minimized to obtain maximum efficiency from thermal and thermodynamic insulation improvements since these functions are most effective in the low temperature region. To accomplish this fluid lines and electrical leads were extended in length in the annular vacuum space to minimize the conductive heat transfer.

In search of lower conductivity, the tank support designs proceeded through the succession of posts, spokes, straps, springs etc. to the current radial bumper design. It is essentially a multiple point load device that is not integrally secured to either wall, and where thermal conductivity varies with load as shown at left. The bumper conductivity approaches "0" in a zero "g" environment.

The radial bumper design has been applied to several thousand qualified aircraft systems; NAS 9-2978, NAS 9-4634, NAS 9-7337, and NAS 9-5491 R & D tanks. Structural integrity, high "g" acceleration and impact properties are excellent. Most importantly the thermal conductivity is extremely low and precisely reproducible between tanks. This is extremely important in very low heat leak applications since the available vapor cooling refrigeration is not efficiently consumed in the rejection of conducted heat and nonoperative standby properties are greatly improved.

Radial bumper design has withstood production and development engineering re-evaluation for more than eight years. Through correlation of calorimetric and system test data, the discrete conductivity fraction of heat transfer into the radial bumper design tanks has been accurately isolated and identified and can be accurately predicted.

THERMAL CONDUCTIVITY AS A FUNCTION OF APPLIED LOAD

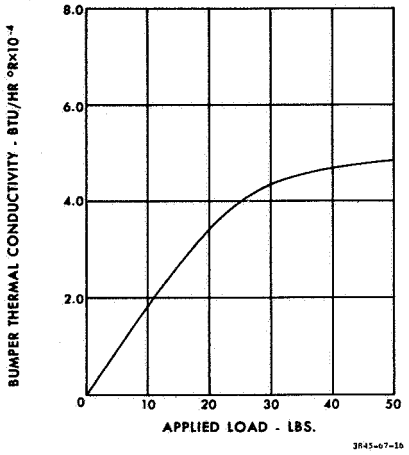

BUMPER CHARACTERISTICS

LOAD VS. DEFLECTION

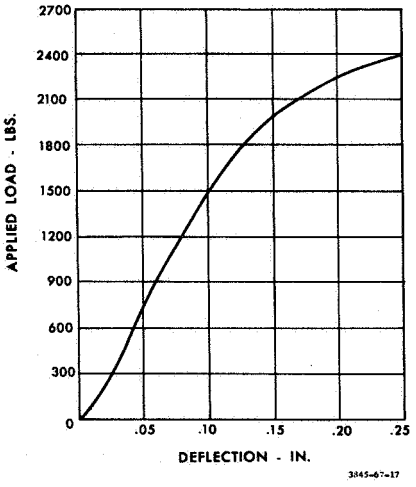

BUMPER SUSPENSION SYSTEM

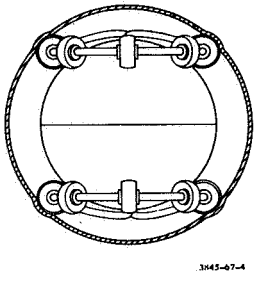

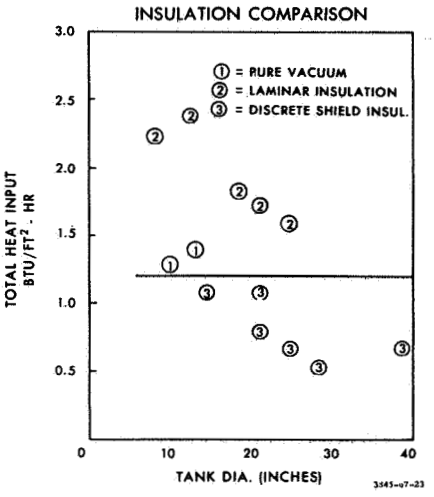

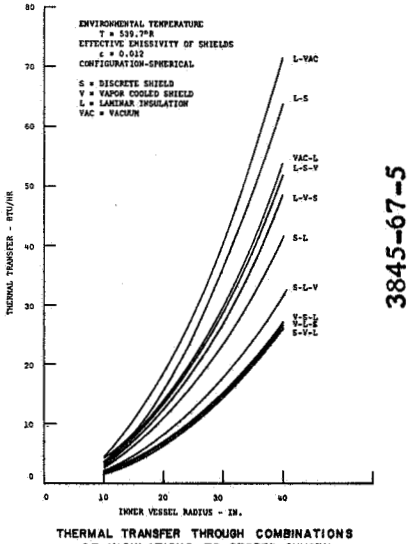

THERMAL TRANSFER THROUGH COMBINATIONS OF INSULATIONS TO STORED OXYGEN

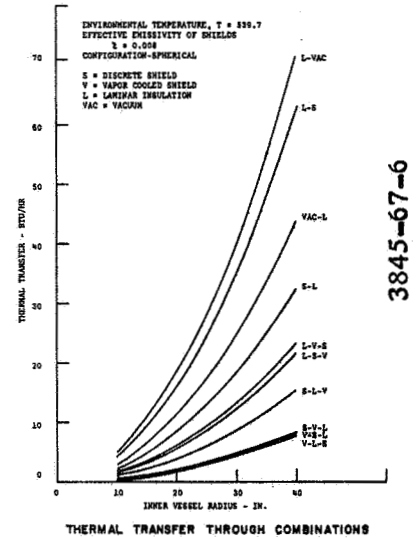

THERMAL TRANSFER THROUGH COMBINATIONS OF INSULATIONS TO STORED HYDROGEN

The dual wall tank design provided an excellent environment for evolution of the radial bumper design, integral fluid line penetration and electrical lead penetration.

The paramount factor in assessing an insulation design is the essential quality of controlling and minimizing the cold region thermal conductivity heat transfer. This is the major deficiency with the laminar insulation which is virtually uncontrollable in regions of tube and line penetrations.

2.1.6 Insulation Heat Transfer

Different insulation designs will vary from essentially a radiation mode of heat transfer to a combination of radiation and conduction heat transfer.

There are two basic considerations that influence the insulation selection and particularly the understanding of why certain insulation designs are superior to others. First, the temperature region of operation for the insulation package is essentially -400°F to +140°F. Insulation properties and designs are all sensitive to the temperature region of operation. Second, for a rigid dual wall tank design, the low emissivity annular space has a basic insulation property. A measure of supplemental insulation quality is the extent of thermal improvement to the basic dual wall design.

The graph at left shows the results of a study of 20,000 aircraft tanks and approximately 100 space system tanks including Gemini, Apollo and current R & D tanks. This data is for total static heat transfer properties without vapor cooling. The aircraft tanks identified by (1) have pure vacuum insulation with low emissivity surfaces (the best 10% of production). The tanks identified by (2) are laminar insulated tanks (SI-4 and NRC-2) and have a high conductive fraction of heat transfer. The tanks identified by (3) utilize discrete shields and in all cases the radiation mode proportion of heat transfer exceeds 80%. This analysis and presentation exposed the apparent heat transfer "obstacle" at 1.2 Btu/ft^2/hr for oxygen (1.0 Btu/ft^2/hr for hydrogen) through use of conductive mode laminar insulations in the cold temperature region.

Further analyses and actual system tests during the past three years have verified earlier predictions that the optimum insulation package must be designed for distinct temperature regions of operation. The optimum insulation package should have radiation mode

of heat transfer control in the cold region (shields) and essentially a conductive mode of heat transfer control in the warm region (laminar insulation). Insulation comparison data are included in the summary charts at left from the study performed in this program.

The effect of various thermodynamic processes upon the insulation design will be discussed in paragraph 2.2 of this section. Rigorous analyses and tests show that the most efficient static insulation system will provide the most efficient thermal/thermodynamic system because of the conservation of available refrigeration.

2.1.7 Radiation Heat Transfer

A radiation mode of heat transfer control is the most efficient cold region insulation scheme in the current state-of-the-art due to the qualities or limitations of available materials and processes.

Fortunately, a system that is essentially a radiation heat transfer system, when empirically verified, can be readily analyzed and predicted. This type of system is dependent upon the fabrication of very low emissivity surfaces. In retrospect, it was found that the techniques of obtaining low emissivity surfaces were well established on aircraft systems in the 1950-1960 period. Subsequent process development reflects further improvement in emissivity values.

The overall effective emissivity values which have been attained in full scale Bendix storage tanks along with some typical surface emissivity values for various materials as determined by the National Bureau of Standards are shown in the margin. Comparative data from calorimeter test programs indicate that a further improvement of the order of 30-50% is possible in large tanks with process technique development. This would appear to be consistent with National Bureau of Standards values since they are given for a low temperature corresponding to the boiling point of liquid nitrogen and the emissivity decreases with decreasing temperature of the surface.

A pure radiation insulation is accomplished by use of discrete isothermally mounted radiation shields. The shields are mounted in such a manner as to be thermally isolated from the inner and outer vessel walls and each other.

RADIANT ENERGY TRANSFER BETWEEN CONCENTRIC SPHERES AND CYLINDERS

1. $$Q=\frac{\sigma A_1 (T_1^4 - T_2^4)}{\{\frac{1}{\epsilon} + \frac{A_1}{A_2}(\frac{1}{\epsilon} - 1)\}(n+1)}$$

where

Q = Thermal Energy through a vacuum

σ = Stephan-Boltzman Constant

A_1, A_2=Areas, inner & outer

ϵ=Emissivities-inner, outer & shield surfaces

n=Number of discrete radiation shields

Typical Emissivity Values (NBS Data)

Material	ϵ_n
Aluminum(electro-polished)	0.018
Chromium (plated)	0.08
Copper (polished)	0.015
Gold (foil)	0.010
Nickel (plated)	0.03
Plantinum	0.016
Silver	0.006

Effective Emmissivities (F_e) in Bendix Tanks

Fluid Stored	F_e
LO_2	0.013
LN_2	0.011
LH_2	0.007

$$F_e = \frac{1}{\frac{1}{\epsilon_1} + \frac{A_1}{A_2}\left(\frac{1}{\epsilon_2} - 1\right)}$$

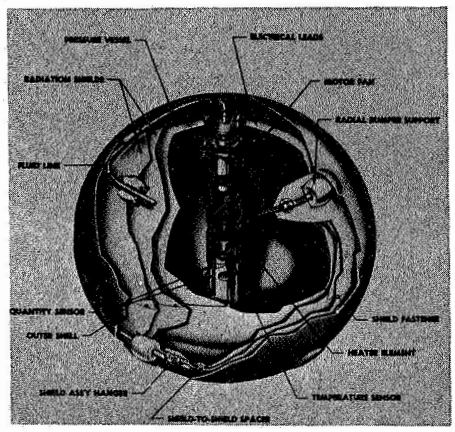

PRESSURE BUILDUP EQUATION

$$Q = m_2h_2 - m_1h_1 - m_2P_2V_2 + m_1P_1V_1$$

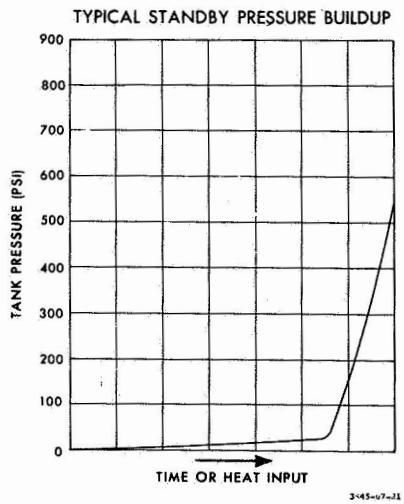

The isothermal discrete shield concept was first applied to flight design tanks at Bendix in 1962. Subsequent tanks have been fabricated on NAS 9-2978, NAS 9-4634, NAS 9-5491 and NAS 9-7337.

These tanks ranged in size from 15" to 40" diameter and contained one to four shields (vapor cooled and non-vapor cooled). The concept adheres well to theory, and is predictable.

Due to materials compatibility, the discrete shield provides a long term stable static vacuum. The shield has excellent structural (vibration) properties with no degradation of thermal properties due either to vibration or extended shelf life.

Shield mounting is by a multiplicity of low conductivity spools to sleeves on the fluid tubes and electrical lead bundles in the annular space. The low conductivity spacing of the spools acts as loose interfaces in vibration. Vibration throughout the complete 0-2000 CPS spectrum in both sinusoidal and random vibration shows effective damping of the shield system.

2.2 Thermal-Thermodynamic Design

This section treats the major fluid thermodynamic processes as applicable to system operation and supplemental insulation effects.

2.2.1 Pressure Buildup (Standby)

Generally, if the nonoperative standby is less than 100 hours (H_2) or 200 hours (O_2), the static insulation requirements are determined by the minimum flow requirements of the system. The equation for pressure buildup is given at the left. Also a typical cryogen pressure buildup curve is shown. The pressure buildup function is not a critical tradeoff factor between supercritical and subcritical pressure operation since the major standby time for either system has been achieved by 100 psia. Pressure rise within and above the compressed liquid region occurs rapidly with little heat input.

2.2.2 Stratification

The thermal stratification that occurs in cryogenic systems alters the thermodynamic processes, generally in an unfavorable way. For example, the pressure buildup time is reduced depending upon the extent of stratification. The curve at left shows an approximation of actual to theoretical buildup times from test data (no

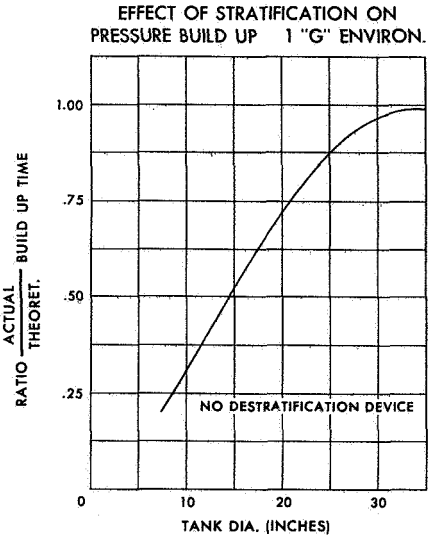

internal thermal conductors). The extent of stratification from test data appears to be influenced by tank size (mass to surface area ratio) and liquid phase to vapor phase interface area. One "g" temperature chamber tests show that stratification is almost independent of heat transfer rate for a given system. Conductor plates are fairly effective for destratification in small tanks (< 20" diameter) and fan stirrers are effective in larger tanks. Either are of questionable value to low gravity mission operation.

The type of stratification we observed is the convective concentration of low density fluid fractions which oppose thermal conductivity dissipation. This is enhanced or actually caused by the gravitational environment. However, the absence of convective concentration should allow more effective thermal conductivity dissipation. The equilibrium magnitude of stratification in zero "g" should be reasonably tolerable without destratification devices.

Numerous studies, including temperature profile measurements, pressure buildup and flow tests have been performed on aircraft liquid oxygen systems in order to describe the mechanisms of normal one "g" cryogenic fluid stratification. This work has been extended to rigorous analyses of zero "g" stratification and fluid thermal conductivity properties.

In one "g" environment, it appears that all heat which enters a small pressurized cyrogenic vessel is initially transported to the top vapor phase region. This has been ascertained by temperature measurement and pressure buildup tests. The process appears to vary (in part) with the fluid mass to tank surface area ratio and the liquid to vapor interface area. This results in non-ideal pressure buildup and flow properties and this abnormality appears to diminish with increased tank size.

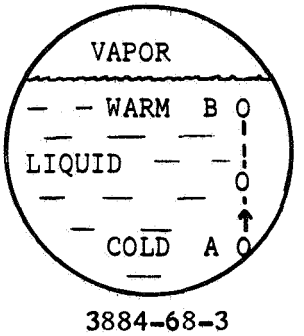

3884-68-3

The heat from the warm ullage region is conveyed downward through the liquid by thermal conductivity. Extreme temperature and density strata result since this process does not proceed uniformly in a one "g" environment due to a counteracting convection process.

A simple description of the convection process is shown at the left. A local unit heat input to the pressure vessel causes vaporization of bubble "A". The low density bubble rises through the successively warmer liquid stata "B", absorbs heat, and finally bursts into the ullage space. The downward conductivity heat transfer is counteracted by the upward movement and

heat absorption of low density fluid fractions (bubbles). The radiation and conduction heat energy in the ullage wall region is readily absorbed by the vapor and retained in that region. The total process in terms of rate and magnitude of heat energy concentration seems to be caused or enhanced by normal gravity convection. Therefore, stratification appears to be a stable configuration in a normal gravity environment, since the forces due to density differences are large, and in a self propogating direction.

Stratification is minimized in a gravity environment by use of conductor plates, mechanical mixing or vibration mixing.

In a zero gravity environment, density gradients play no role. The three forces exist which tend to preturb the strata are:

(a) Interfacial tension,

(b) Molecular diffusion, and

(c) Thermal diffusion.

Each of these forces has been examined separately with analytical models derived to compute their effect. From these models, the following may generally be concluded:

(a) Interfacial tension forces between various strata play no significant role in zero gravity systems.

(b) Molecular diffusion forces are significant, tending to eliminate stratification.

(c) Thermal diffusion forces are most significant, tending to prevent or dispel stratification.

(d) The latter two forces, molecular and thermal diffusion, reinforce one another, so that stratification should not persist.

In practice, a degree of stratification is expected to persist in a zero or low "g" environment. However, the processes of molecular and thermal diffusion in the absence of counteracting convection forces should result in a much lower order of stratification than observed in a normal one "g" operation. These factors in combination with the thermal characteristics of the dewar, the thermodynamic and physical properties of the fluid and the design of the internal fluid acquisition system may

INTERFACIAL TENSION

$$\frac{\gamma - \varepsilon}{\gamma_o - \varepsilon} = \frac{T}{T_o}$$

MOLECULAR DIFFUSION

$$\frac{NA}{A} = \frac{D_C}{RT_x} [(P_A)_1 - (P_A)_2]$$

THERMAL DIFFUSION

$$\frac{\partial t}{\partial \theta} = \alpha \frac{\partial^2 t}{\partial x^2}$$

EQUILIBRIUM FLOW EQUATION (supercritical)

$$dm/dt = \frac{dQ/dt}{\rho (dh/d\rho)_P}$$

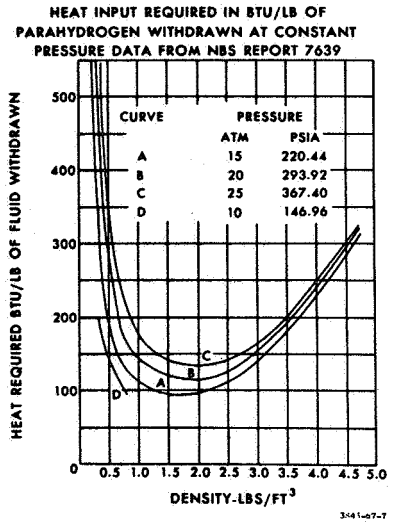

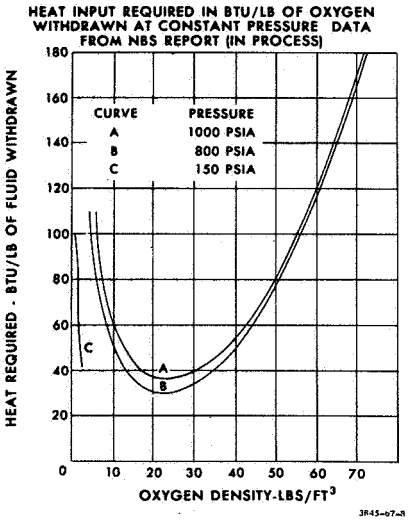

EQUILIBRIUM FLOW EQUATION
(Subcritical)

$$\frac{dm}{dt} = \frac{(dQ/dt)(\gamma g/\gamma \ell - 1)}{q}$$
(liquid flow)

$$\frac{dm}{dt} = \frac{(dQ/dt)(1-\gamma \ell/\gamma g)}{q}$$
(gas flow)

where:

- q = Heat of vaporization
- $\gamma \ell$ = Specific volume of liquid
- γg = Specific volume of gas

eliminate the need for additional destratification devices.

2.2.3 Equilibrium Flow

The equilibrium flow rate from a cryogenic system is a function of the heat inflow and fluid thermodynamic properties. Tank size has essentially no effect. The initial examination of equilibrium flow will exclude consideration of vapor cooling and expansion refrigeration.

Supercritical pressure operation results in an equilibrium flow according to the expression noted at left. The specific heat to flow for both oxygen and hydrogen is given for typical supercritical operating pressures. The minimum dq/dm flow determines the mission duration characteristics and the mission non-venting flow characteristics. Static equilibrium flow tests are important for evaluation of the thermal design integrity. Non-stable vacuum insulation designs usually do not show the expected receding flow rate in the low density region due to insulation outgassing as the cryogen warms.

Subcritical pressure operation can result in several equilibrium flow conditions depending upon whether liquid phase, gas phase or both phases are supplied.

If gas phase is acquired into the supply line (from the vessel contents) the flow rate will correspond to the vapor volume displaced by the liquid vaporization at the operating pressure and heat inflow.

If liquid phase is acquired into the supply line the flow rate will correspond to the liquid volume displaced by the internal liquid vaporization. It is seen that the mass flow rate ratio between gas phase flow and liquid phase flow at atmospheric pressure is approximately 1:200 for oxygen and 1:50 for hydrogen. This condition can be used to advantage in system control.

As explained previously, the delivery fluid can be used by expansion, vaporization and insulation precooling to extract, intercept and reject heat from the system. This is true in supercritical or subcritical operation. A comparative system analysis which includes Joule-Thompson expansion and insulation precooling for both systems, shows that the thermal tolerance of either system is essentially identical and relatively independent of operating pressure. Small differences occur in the process efficiencies in each system. The significant advantages for subcritical operation are:

(a) Reduced pressure vessel weight and

(b) High flow without supplemental power (improved control flow range).

2.2.4 Thermodynamic Processing of Supply Stream

2.2.4.1 Vapor Phase Acquisition-Supercritical Systems

In supercritical cryogenic storage systems, one phase is present and the acquisition of this fluid is unaffected by gravitational fields. The equilibrium flow rate has been discussed in paragraph 2.2.3 in detail.

2.2.4.2 Gas Phase Acquisition-Subcritical Systems

This process refers to the vapor phase within a subcritical storage vessel being expelled into the delivery line. The equilibrium flow rate is the rate of vaporization in the vessel at the conditions of heat inflow and pressure. This is the simplest and most effective process in a one "g" environment. The heat to flow for hydrogen is shown at the left. The heat to flow for oxygen vapor is shown in the margin below.

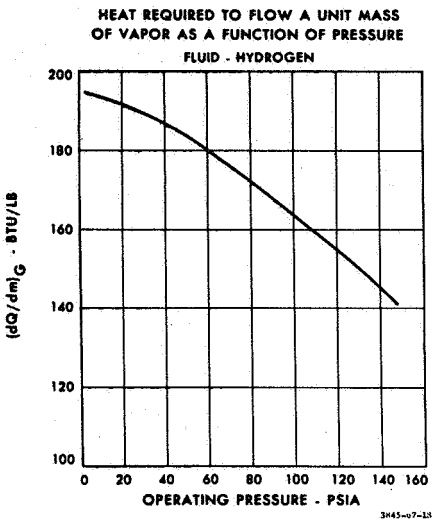

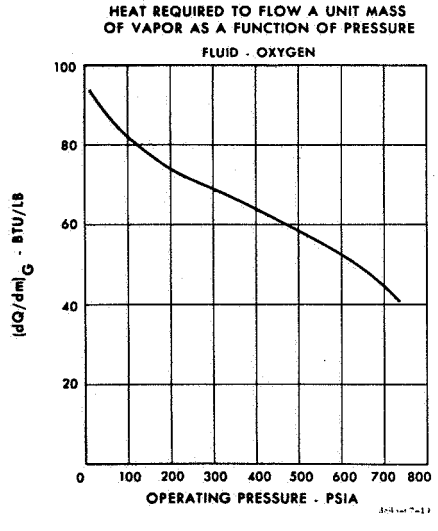

Due to low "g" phase orientation behavior, vapor phase acquisition cannot be predicted in a low "g" environment unless supplemental fluid acceleration is used. In a zero "g" environment the more dense liquid phase will wet and locate to the tank surface geometry, due to surface tension forces, and displace the vapor phase. Low "g" perturbations will constantly alter the vapor phase orientation. Therefore, a design concept based upon vapor phase acquisition (expulsion) is not practicable for a zero "g" environment.

Vapor cooling of the shield insulation for subcritical and supercritical systems is quite effective in that the static heat leak is reduced 10-15% for oxygen and 60-70% for hydrogen as verified by test.

2.2.4.3 Liquid Behavior in a Zero "g" Environment

It is known from thermodynamic analysis that the stable equilibrium state of a capillary system in an isothermal zero "g" environment is the state where the potential energy (P.E. = σA_c) has the smallest value. In this expression σ is the interface surface tension and A_c the capillary area.

The above statement can be used to determine where a liquid is most likely to be found in a container. Since

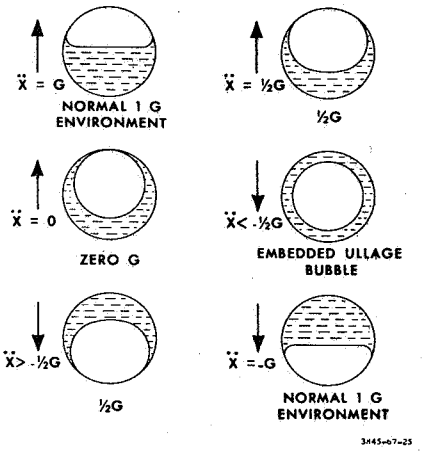

$$\sigma \frac{d}{ds} \left(r \frac{dh}{ds}\right) = \frac{dr}{ds} (P_g - P_l)$$

where:

P_g = gas pressure

P_l = liquid pressure just below surface

r,h = Dimensional parameters of liquid/gas interface

σ = Interface surface tension

surface tension depends only on temperature, σ is constant in an isothermal system and we need only investigate the condition which minimized the capillary area A_c.

Geometrical calculations have been made for the case of liquid in a spherical tank which shows that in every case both the liquid and gas bubbles are wall bound in the preferred configuration. However, with wetting liquids in large quantity, the ullage bubble sometimes becomes embedded due to inertial effects. The maximum acceleration force required to eliminate this condition and ensure a wall bound condition can logically be argued using the following diagrams.

The diagrams at left show that an acceleration of something less than 1/2 "g" is necessary to eliminate the embedded bubble configuration. The consensus of opinion points in the direction of very small "g" loads causing bubble drift toward the wall bound condition. Configuration of the assumed fluid movement in the diagrams can be found in stability considerations. These show that the meniscus in an "inverted" spherical tank is always unstable causing the liquid to flow in the direction of the gravitational field.

The shape of the menisci in any given gravitational field can be determined from the solution of the governing differential equation which assumes an axisymmetric wall-bound liquid-gas configuration.

2.2.4.4 Liquid Phase Acquisition and Control

From a versatile system operation and control aspect, it is desirable to have a wide range of flow operation (without supplemental power) with self-contained thermal/thermodynamic compensation or response. This becomes one of the principle advantages of subcritical storage and a characteristic of the versatility of aircraft storage systems.

The objectives are to obtain:

(a) Minimum flow per unit environmental heat input and

(b) Maximum flow per unit environmental heat input.

The "minimum flow" requires delivery of fluid from the system at "the highest energy state (vapor) with the lowest net heat input to the pressure vessel". The "maximum flow" requires delivery of fluid from the system at "the lowest energy state (liquid) with the highest net heat input to the pressure vessel". The net

heat input to the vessel is the important factor since this will vary with different insulation designs. Effluent fluid temperature cannot be used as a sole criteria for this reason.

It is readily seen that vapor phase must be excluded from the acquisition system if maximum control versatility is to be obtained. Alternately, electrical power or gas feedback heat input can be used to provide pressure control if vapor phase is acquired into the supply circuit during the high flow operation. This complicates both system design and reliability.

It has been shown previously that vapor phase acquisition cannot be assured in zero "g" environment due to random vapor phase orientation. For the same reason, the unpredictable orientation of the vapor phase, the normal fluid port designs in a tank will not predictably exclude gas phase. Under these circumstances a system must be designed for acquisition of 100% liquid phase, 100% vapor phase or any fraction of each phase. As the fraction of liquid phase in the tank diminishes during the mission, the probability of a normal port design acquiring vapor phase increases. Irrespective of expansion or shield cooling, it is probable that supplemental heating will be required, in the normal port design, to maintain pressure control for all flows above minimum and during the latter mission period. Emptying the tank will require excessive power.

These considerations led to the conclusion that a high assurance liquid acquisition feed system should be designed. Liquid phase behavior and orientation is such that it can be acquired with high assurance.

A successful liquid acquisition feed system was designed and tested in a subcritical oxygen system on AF33(615) 2308 contract. The acquisition system consisted of seven capillary-wick devices interconnected with supply line tubing. Six of the capillary-wick units were equally spaced 90° apart at the inner preiphery of the pressure vessel. The seventh wick was placed in the center of the sphere and has since been determined as unnecessary. The wicks provide the ideal mechanism for liquid phase adhesion and exclusion of the gas phase. The wick-capillary bundle interface determines the liquid capillary retentive force, the liquid phase flow rate characteristics and the gas phase break-through or flow resistance characteristics. It is well known by analysis and test that liquid phase will wet and orient to the vessel walls. Geometry and low "g" accelerations

will cause random vapor phase orientation at the wall proximity. The capillary-wick aquisition system is designed so that if only one wick is wetted by liquid phase, only liquid phase will flow into the supply network. This allows the evaluation of both the orientation and acceleration effects of the fluid on the feed system.

Equally important to the capillary-wick acquisition development was the development of a test procedure to evaluate the feed system performance. A part of AF33(615)2308 contract effort was the further development of the oxygen-nitrogen mixed gas test procedure for subcritical system evaluation. The purpose of this test procedure is to provide a quantitative method of determining the phase quality acquired into the feed supply network for evaluation of phase exclusion efficiency and the phase sensitive thermodynamic processes. This is accomplished with the mixed gas procedure because of the vapor pressure differences of the two gases. If a liquid air mix is used, the liquid phase will be 80% N_2 - 20% O_2, and the vapor phase will be 92% N_2 - 8% O_2. Nitrogen analysis of the effluent gas will identify whether vapor phase, liquid phase or a mixture was acquired into the feed-supply line.

The oxygen-nitrogen mixed gas test procedure is considered essential as a development evaluation tool and as an acceptance test procedure for subcritical storage systems.

$$\Delta M_{L/M} = \frac{1}{\left(\frac{\upsilon_g}{\upsilon_l} - 1\right)}$$

2.2.4.5 Liquid Phase Expulsion and Cooling

Liquid expulsion from a tank is by volumetric displacement of vapor phase at the rate of liquid vaporization to the ullage. The mass of liquid which must be vaporized to expel a unit mass of liquid ($\Delta M_L/M$) is given in the equation at left. The heat input required is a function of the heat of vaporization at the operating pressure.

If q represents the heat of vaporization, then the heat required to expel a unit mass of liquid at constant pressure is given by:

$$(dQ/dm)_L = q\ (\Delta M_L/M)$$

The attached figures shows a comparison of the heat required to expel a unit mass of liquid or vapor at equilibrium conditions.

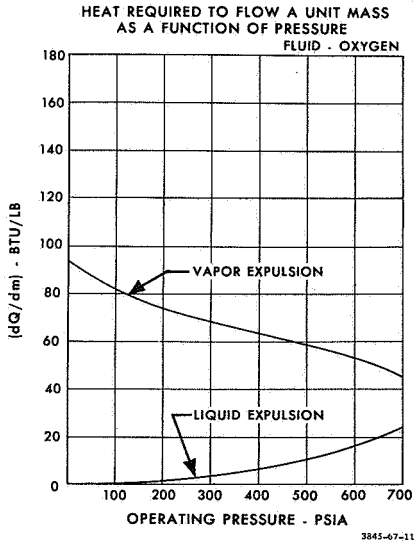

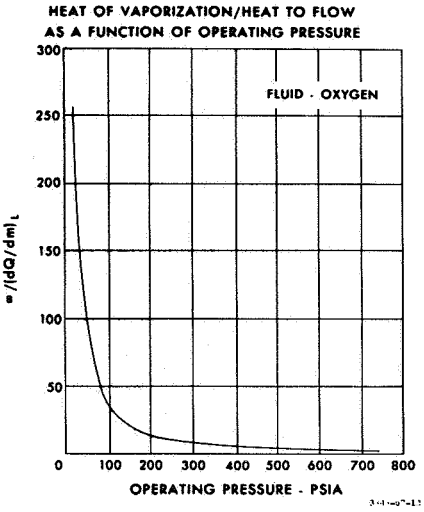

Theoretically, if the liquid expelled from the tank is utilized by complete vaporization in a shield to intercept the heat inflow, the equilibrium flow rate will approach a vapor vented system. However, the specific heat to flow is extremely low at low pressures, therefore an extremely high ratio of heat interception to heat transmission is required at the low pressure region in order to approach this optimum. This is shown on the figure at left.

Tests have been conducted at Bendix on shield design tanks and on tanks in which a liquid shroud surrounds the pressure vessel. In no instance thus far has the heat transfer to the inner vessel been eliminated or completely reduced as theoretically indicated.

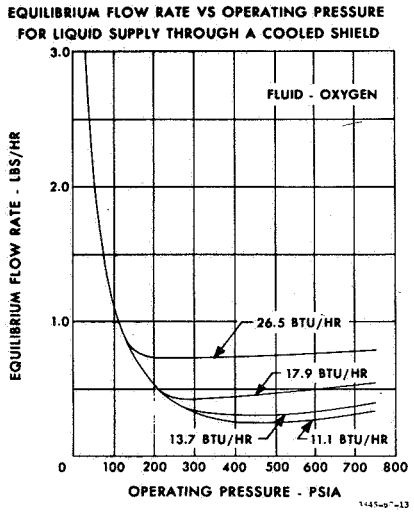

An approximation method has been derived for calculating the equilibrium flow rate at various pressures for liquid expulsion through a liquid cooled shield in a vessel having various numbers of shields. Account is taken of the conductive heat transfer to the pressure vessel and a certain portion of uncooled shield as estimated from empirical data.

The adjacent figure shows the theoretical equilibrium flow rate versus operation pressure for liquid expulsion of oxygen. Four different heat leak tanks are used as examples with the innermost shield cooled in each case.

A comparison of the theoretical liquid and vapor expulsion, equilibrium flow rates and the minimum dq/dm supercritical flow rate for a particular tank is shown at the left. The liquid expulsion is through a liquid cooled shield without shield vapor phase cooling in the examples.

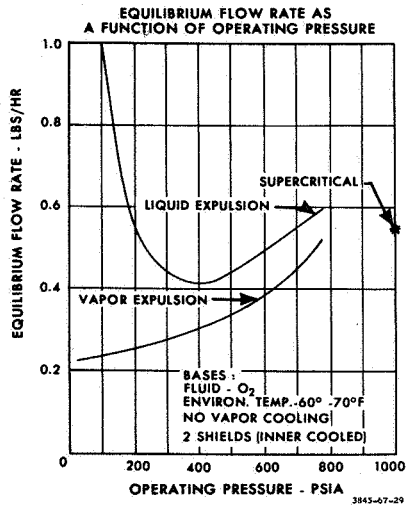

Liquid expulsion with liquid shield cooling can significantly reduce the flow rate over a non shield cooled system. This method is extremely sensitive at low operating pressure and requires extremely efficient vaporization heat transfer and heat interception. Prototype tests indicate that extreme heat transfer design problems would be encountered.

2.2.4.6 Joule-Thompson Expansion

Sufficient test work has been performed on shielding and shrouded tanks to realize that it is virtually impossible to intercept all heat transfer into the pressure vessel with a reasonable weight insulation system.

The expansion cooling process provides a means of absorbing internal heat energy and rejecting it from the system. In the process, shield vapor cooling can be accomplished. The process is ideally suited to the concept of liquid phase acquisition and expulsion.

Prior R & D contracts have utilized an internal expansion (throttling) valve. The advantage of the throttling valve is that it can accommodate a wide range of flow resulting from a single or two-phase supply. Operational reliability for long term missions and failure problems have been encountered in the prior systems.

Bendix is currently performing F33615-67-C-1954 contract for a subcritical oxygen system which embodies a capillary-wick liquid acquisition and expulsion device followed by liquid flow through an orifice throttling device. The reason for the orifice design is to eliminate the moving valve mechanism in the cryogenic environment and improve the reliability of the function.

A wide range of flow is not actually required with the liquid acquisition system, since the expansion heat exchange function is only required at the low end of the system flow range by virtue of the system thermal design.

The Joule-Thompson effect is an enthalpic throttling process whereby a fluid of specific pressure, volume and temperature is throttled (expanded) adiabatically to a lower pressure, larger volume and lower temperature state.

The diagram on the following page shows the region of interest and the thermodynamic paths of the fluid during operation. State point A represents the initial fluid condition after tank filling. Tank pressure buildup follows path ABCD. Points B, C, and D are three possible operating pressure points to present various operating conditions. Fluid throttling occurs from point B to B-1, C to C-1 or D to D-1 depending upon the operating pressure. The expanded fluid B-1 is two phase and vaporizes in the internal heat exchanger along path B-1 to B-2 at which point it is completely vaporized. The vapor continues to absorb heat along path B-2 to B-3. At B-3 the fluid is again at its original temperature at the lower pressure established by the orifice device and is completely vaporized. In application, the latter portion of the vaporization process and subsequent warming of the vapor will occur in the vapor cooled shield. The available refrigeration is utilized both to absorb internal heat and intercept incoming

OXYGEN STORAGE

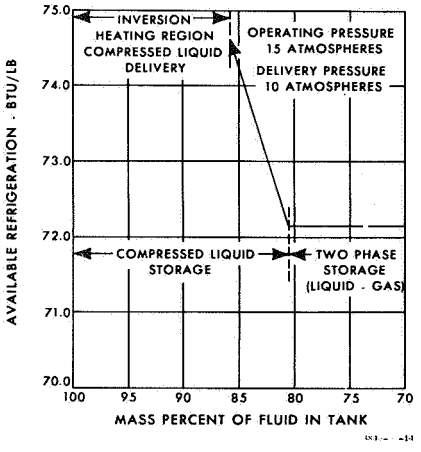

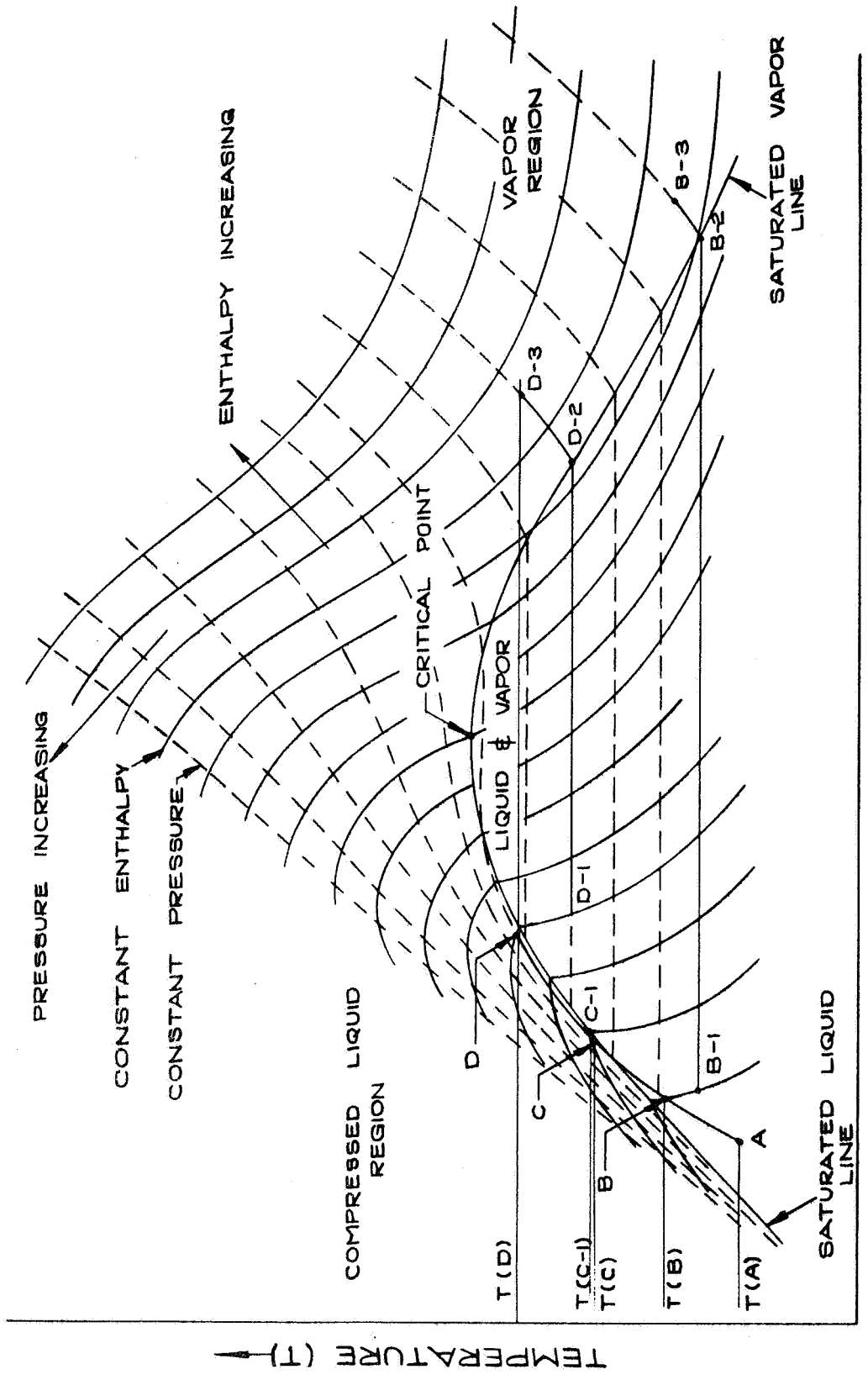

3746-67-2

TYPICAL TEMPERATURE - ENTROPY DIAGRAM

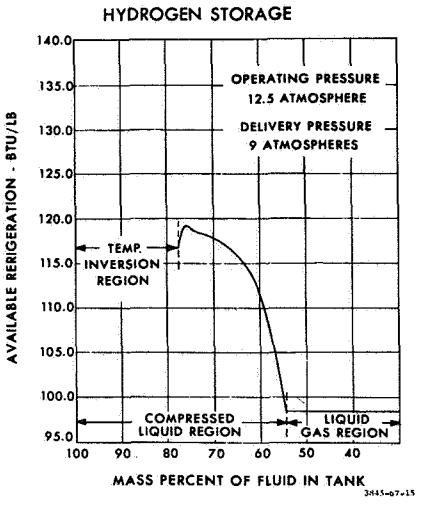

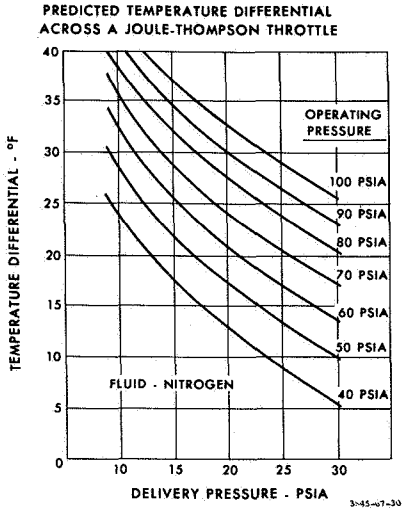

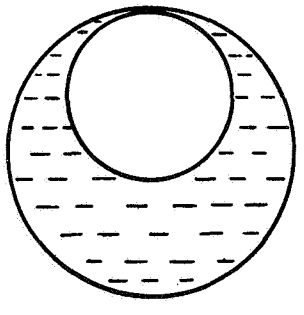

3884-68-4

heat. This is a practical approach since the internal throttling process is not perfectly adiabatic and the heat exchange process is not perfectly isochoric.

The available refrigeration is shown on the adjacent figures for hydrogen and oxygen, with representative operating and delivery pressures.

The preliminary test work on F33615-67-C-1954 contract to determine the temperature differential across an orifice device under various conditions is complete. The orifice devices tested consist of a multiplicity of in-line and parallel orifices with different flow rate characteristics. Both vapor and liquid phase tests were run. The predicted temperature differential with different Δ P conditions is shown on the botton adjacent chart. Excellent agreement with the predicted values was attained at pressure differentials of 35 to 80 psi and liquid nitrogen flow ranging from less than 0.2 lbs/hr to over 4 lbs/hr.

2.2.5 Tank Baffles

Baffles can be designed into a cryogenic tank to assist low "g" liquid phase orientation and dampen high amplitude liquid sloshing due to random acceleration forces.

2.2.5.1 Baffles for Liquid Phase Orientation

Phase orientation control is a problem that is generally associated with system flow and pressure control. The primary considerations are:

(a) Phase expulsion control,

(b) Expulsion efficiency, and

(c) Weight & complexity of phase oreientation equipment.

The position of the liquid/gas interface in a spherical tank without baffles subjected to zero "g" conditions was previously discussed in 2.2.4.3. This type of phase orientation is expected throughout the zero and very low "g" mission profile.

The vapor phase bubble as shown at left will be displaced randomly around the tank wall as the acceleration environment and liquid quantity varies. Under these conditions a conventional design (open tube) expulsion port will acquire liquid or vapor phase in a random or unpredicatable manner. Baffle shells, rings or screens can

be applied to orient the fluid phase in zero or very low "g" environment. It is apparent that the weight of the baffling required will increase significantly with tank size and acceleration environment.

The capillary-wick feed system eliminates the need for baffle orientation to obtain predictable phase expulsion because of the quadrant (multiple) positioning of the wick supply ports. In practice, the capillary-wick feed system is a method of applying a multiplicity of supply ports (in parallel) in the tank so as to assure liquid phase expulsion even though only one capillary-wick port is exposed to liquid phase. This is desirable to minimize or eliminate baffle weight for phase expulsion control.

Baffles also appear to present an expulsion efficiency problem by orienting or trapping liquid remote from the supply ports. In view of this problem, all internal protuberances should be designed so that liquid phase will "wet" and flow freely to the supply port regions.

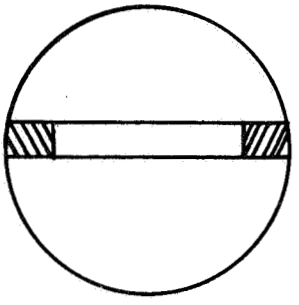

3884-68-5

2.2.5.2 Baffles for Slosh Control

Sumner[1] has shown that appreciable reductions in "sloshing" within spherical tanks can be achieved by using a single ring baffle as shown at left. A further increase in damping or reduction in sloshing amplitude is possible by using a single flexible baffle as opposed to a rigid ring.

The baffle flexibility is governed by the equation.

$$F = \left(\frac{W}{t}\right)^3 (1-\nu^2) \frac{\rho W^2}{ET^2}$$

where F = Flexibility of baffle
W = Baffle width
t = Baffle thickness
T = Period of liquid oscillation or sloshing
ρ = Fluid density
ν,E = Poisson's ratio and Young's modulus of baffle material.

---

(1) Sumner, Irving E., Experimental Investigation of Slosh-Suppression Effectiveness of Annular-Ring Baffles in Spherical Tanks. NAS TND-2519, 1964.

An ideal design flexibility value would appear to be F = 0.02.

Because a ring baffle will restrict the ideal liquid phase orientation at low "g" conditions, some compromise must be reached between the ideal flexible baffle configuration and the configuration necessary to allow zero "g" wetting of the pressure vessel wall and liquid flow to the supply ports.

2.3 Operation & Control - Thermal/Thermodynamic Management

The thermal and thermodynamic elements of the system can be managed in consonance to provide a wide range of performance, control and duration values.

The boiler plate tank developed under this contract is used as an example in part of the following discussion. This tank is spherical, contains 1200 lbs of oxygen and has a vapor cooled shield for insulation.

2.3.1 Typical Tank Flow Performance-Supercritical

Graph I below shows the equilibrium and constant flow predictions for the boiler plate tank. Subsequent tests confirm this performance.

EQUILIBRIUM FLOW RATE & MISSION DURATION CHARACTERISTICS OF OXYGEN & HYDROGEN TANKS NAS 9-5491 (NTP)

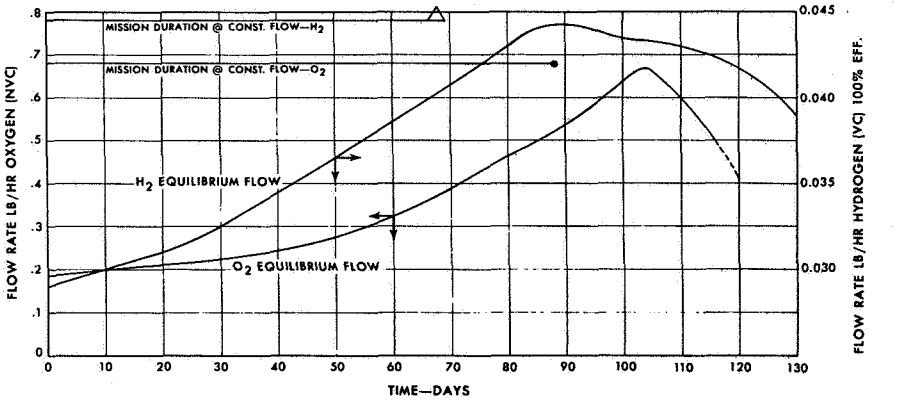

GRAPH I

B-3884-68-213

In the Graph I presentation, mission duration is estimated on the basis of constant flow at minimum dq/dm conditions. This is a minimum mission duration capability based upon the equilibrium flow constraint.

2.3.2 Flow and Relief - Subcritical

Subcritical aircraft oxygen systems are designed to provide a high range of flow control and accomplish a pulsing flow on a demand basis for personnel breathing. This is accomplished by fluid circuit design that performs a self compensating management of the thermal thermodynamic processes of the system. Minimum to maximum flow rates of 1:50 are readily accomplished.

The subcritical oxygen system that is currently being fabricated under F33615-67-C-1954 contract will utilize the capillary wick liquid acquisition concept for vapor exclusion of the initial supply fluid.

The minimum flow rate requirement is accomplished by liquid phase flow through a Joule-Thompson orifice and internal heat exchanger.

The maximum flow requirement is accomplished by liquid phase flow directly to the external circuit. Switching between the two flow circuits is accomplished automatically on a supply line pressure demand basis. The system circuitry is quite similar to aircraft circuitry. Flow response and pressure control performance are expected to be of the same order.

The ratio of minimum to maximum continuous flow rate without supplemental power is expected to be 1:10 or greater in the equilibrium region. This provides a good range of control for most space system applications.

An important aspect of flow control, particularly for subcritical systems, is the pressure relief function. System pressure relieving can occur for many reasons from initial acceptance test through integration checkout to final mission operation. The function is needed and it is critical in terms of reliable, low leakage, repetative, performance for long mission systems. In many applications the power level may be reduced for some reason to an unusually low level for a significant period of time. It is desirable that the cryogenic system level out at some equilibirum flow below a nominal system operation level. Maximum thermodynamic refrigeration must be applied to the relief flow circuit which requires a reliable relief valve resealing function.

2.3.3 Effect of Environment Temperature Control

If the emitting surface of the outer shell is cooled from 70°F to -65°F the total vessel heat input will be reduced by a factor of 0.60 to 0.67. This has been con-

HEAT LEAK AS A FUNCTION OF OUTER SHELL TEMPERATURE

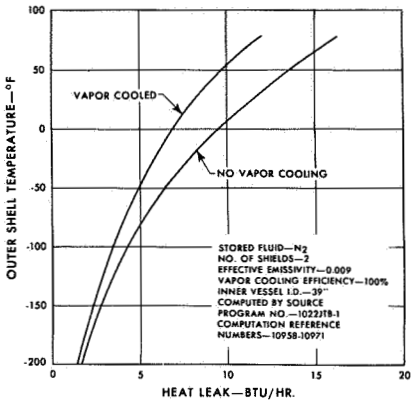

A-3884-68-209

HEAT TO FLOW OXYGEN

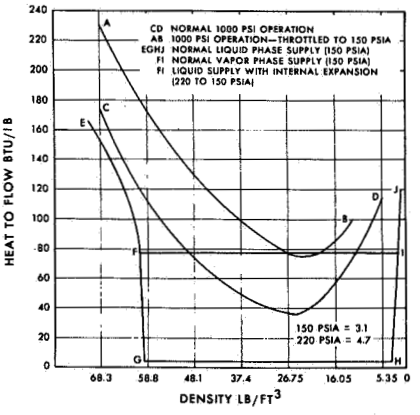

A-3884-68-210

firmed by cold box, refrigeration and insulation tests on the NAS 9-2978 program. This can be accomplished by:

(a) A refrigeration coil on the outer shell,

(b) Laminar insulation on the outer shell,

or in part by

(c) Gold plating of the outer shell.

The constant flow mission duration is increased by the value of heat input reduction by 2.5 to 3 times. Graph II shows the effects of outer shell temperature on the heat leak of the thermal model dewar fabricated on this contract.

2.3.4 Effect of Joule-Thompson Throttling

Graph III shows internal Joule-Thompson throttling of the expulsion fluid. Supercritical pressure fluid or liquid phase subcritical fluid, will double the heat to flow as compared to non-throttled supercritical fluid expulsion. This process can double the mission duration capability. Joule-Thompson expansion and heat transfer efficiency of a supercritical fluid is a point in question and requires further test work.

2.3.5 Effect of Vapor Cooling in the Shields

Tests indicate that vapor cooling in the shield insulation can be expected to reduce the effective heat input to the pressure vessel by:

(a) 10 - 15% for oxygen and nitrogen and

(b) 50 - 80% for hydrogen.

Therefore, this process will increase the constant flow mission duration capability by these amounts.

2.3.6 Environment Temperature Control, Throttling, Vapor Cooling Effects

The effects of internal thermodynamic heat exchange, shield vapor cooling and outer shell temperature control are additive in terms of controlling the effective heat input or increasing the mission duration characteristics. Internal thermodynamic heat exchange and shield vapor cooling in series can be self compensating; however, the efficiencies of these processes are important and generally appear as follows:

50% --- Practicable

70-80% --- Feasible

> 80% --- Subject R & D

2.3.7 Thermal Tolerance of Subcritical vs Supercritical Operation

The intercept of supercritical curve AB and subcritical line FI on Graph III is a point in question. Further test data is required to resolve these process efficiencies.

The specific thermal tolerance of the various concepts must then be analyzed in over-all system context as described in Graph IV. The mission duration characteristics of a supercritical tank system can be increased about 35% when applied in a 3-tank cluster by offsetting the thermodynamic operation of each tank. This feature is also additive to items (2.3.3) (2.3.4) and (2.3.5) above. There is no apparent mission duration advantage to clustering subcritical tanks.

COMBINED FLOW CHARACTERISTICS OF THREE 9-2978 OXYGEN TANKS

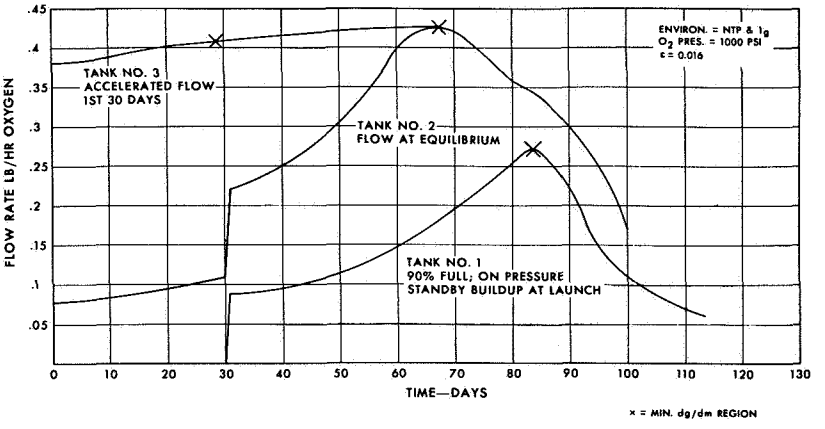

B-3884-68-214

2.3.8 Thermal Sensitivity of Subcritical vs Supercritical Operation

Graph V shows the flow rate per unit of heat input for supercritical and subcritical operation.

The ratio of flow between throttled and non-throttled subcritical liquid expulsion (over 15:1) has significant control potential, particularly for emergency EVA, cryo power and propulsion applications.

The very low heat to flow indicates the sensitivity of the system to thermal insulation variance. System

COMPARISON OF FLOW RATE SUPERCRITICAL VS. SUB-CRITICAL OXYGEN

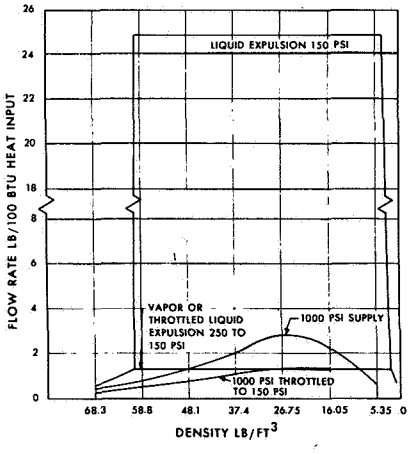

A-3884-68-211

3.0 CRYOGENIC STORAGE SYSTEM DESIGN AND FABRICATION EVALUATION

Longer mission cryogenic storage systems require larger tanks because of the generally larger fluid quantities. This has an impact on the design and fabrication of the tankage system due to the critical technologies involved.

A cryogenic storage vessel must withstand both high pressure and very high vacuum. This integrity must be maintained from the cryogen fluid temperature of -400°F to the vacuum processing temperature of +300°F. Fluid tubes and electrical lead joints, structure weld joints and shell wall characteristics must be highly controlled to provide the requisite quality. Materials selection and properties must accommodate the extreme temperature environments with extremely low outgassing to maintain a stable high vacuum property.

With increases in tank size, many of the normally important design and processing factors become critical in terms of probability. The problem associated with linear length of welds, number of penetration joints, vacuum exposed surface area, thermal and structural stress all increase. Selection of propulsion materials, design features, fabrication processes and control procedures become extremely important.

A significant part of the contract study was to evaluate fabrication and design procedures that can be successfully applied to large, long duration, tank systems. It would be difficult to summarize this data, particularly the fabrication data, since different procedures apply to different design and size tanks depending upon the application and objectives.

This data is presented in the appendix and a review of that material will be useful to those engaged in the design and fabrication of cryogenic storage systems.

thermal quality, long term thermal predictability and reliability in the control circuit are important factors.

4.0 RECOMMENDATIONS

4.1 Thermal-Thermodynamic Design

The thermal design approach has been to differentiate the heat transfer modes and then to maximize the control of each basic heat transfer mode. This approach fits the evolutionary development upgrading.

The basic static heat input into the dewar can be converted to a lower effective heat input, resulting in lower flow, by utilizing the thermodynamic refrigeration of the supply stream. For any given flow there is a maximum available thermodynamic refrigeration. Minimizing flow (or maximizing mission duration) is a direct function of the conservation and effective application of the available thermodynamic refrigeration.

The throttling and heat exchange within the pressure vessel depend upon the efficiency of that specific process.

The effective heat transfer as a result of vapor cooling is more complex. Vapor cooling of the insulation causes an increase of the environment heat transfer into the insulation system due to an increased ΔT in that outermost insulation region. Heat transmission to the pressure vessel is reduced due to a reduced ΔT in the insulation adjacent to the pressure vessel.

When this is converted to supply stream thermodynamics in the insulation region, the total enthalpy change in the supply stream is not the only criteria for system efficiency, but rather, the enthalpy change per unit reduction of heat transmission into the pressure vessel. For example, an enthalpy change of 5 Btu/lb. in the shield adjacent to the pressure vessel is just as effective as a 25 Btu/lb. change in an outer sheild. On this basis, for a given vapor cooling function, the lowest enthalpy change maximizes the conservation of thermodynamic refrigeration and more cooling functions can be performed.

To obtain the maximum advantage from the available vapor cooling it is generally found that:

(a) Vapor cooling is most effectively applied to a radiation mode heat transfer.

(b) Vapor cooling should be applied first to the innermost cold insulation regions.

(c) Vapor cooling is inefficient when applied to a conductivity mode of heat transfer due to the high ratio of heat absorbed to heat transmission. This is due to the available material properties and the conductivity mechanism.

Since radiation heat transfer constitutes a large portion of the heat ultimately transfered to the cryogen it lends itself for consideration to improve the mission capabilities of the storage system. Analysis of test data indicate net heat transfer to be essentially proportional to the effective emissivity of the radiative surfaces. Further improvements in lowering radiation heat transfer can evolve around the determination of the basic physical characteristics that produce low emissivities. These concepts should be analyzed and methods investigated to prepare and preserve these surfaces.

Design interpretation of this information supports the discrete shield-radial bumper concept, since it is essentially a radiation mode design. It also points up the importance of minimizing the basic thermal conductivity to the lowest possible value prior to vapor cooling the conductive (bumper) elements for an efficient operation.

The tank designs on NAS 9-2978, NAS 9-4634 and NAS 9-5491 contracts have no vapor cooling of the bumpers and are thermally isolated from vapor cooling. This was done to obtain test and statistical evidence of the actual thermal conductivity values.

Further thermal improvements can evolve through vapor expansion cooling in the insulation region, multishield vapor cooling and vapor cooling of the conductivity elements. This should be accomplished in the vacuum annulus region designated as the radiation mode control region of the insulation package, i.e., the inner cold region most suited to a radiation mode of heat transfer control.

When the above thermal/thermodynamic features have been optimized (since these impose low weight), we must look to control (temperature) of the outer annulus radiation emitting surface for improvement. This is accomplished by the following methods in singular or combined application.

(a) Tank to ship thermal isolation mount

(b) Gold plate of the external surface of the outer shell

(c) External laminar insulation design

(d) Refrigeration of outer shell

(e) Final vapor cooling of the outer shell and slip to tank structural attachments

The present state-of-the-art coupled with the above improvement recommendations provide the design features for extension of Cryogenic Storage Systems mission capabilities to an excess of two years.

As the tank sizes increase, the standard rigid dual wall design imposes a continuously increasing weight penalty due to the buckling constraints of the outer shell. Further design work on alternate insulation design approaches are recommended which would be directed toward stabilizing the insulation weight/ft^2 of tank surface with increased tank size. It is extremely important, however, that the thermal/thermodynamic design technology reported herein is rigidly adhered to and embodied in the alternate design(s) if any overall weight improvement is to be accomplished.

4.2 Thermal-Physical Design

Cryogenic Storage System weight is dependent upon the thermal design. If the thermal/thermodynamic design is reliable and predictable, then the weight is predictable.

Significant weight improvement steps for the Cryogenic Storage System are shown in the Thermal-Physical Development diagram in paragraph 1.0 and are further identified as follows:

(a) Continued improvement of shield emissivity values.

(b) Continued improvement of vapor cooling and throttling expansion efficiencies in internal and shield heat exchangers.

(c) Continued development of a reliable feed system for low pressure subcritical storage.

(d) Continued development of higher strength pressure vessel materials and fabrication techniques.

(e) Continued development of sandwich contruction outer vacuum jacket.

(f) Continued development of intermediate temperature region laminar insulation shields.

(g) Continued development of warm region laminar shield insulation wraps.

(h) Increased development effort on design and test of alternate insulation schemes for larger size tanks.

SECTION B

PHASE II - VESSEL AND SHELL FABRICATION

1.0 PRESSURE VESSEL FABRICATION

The lower pressure cylindrical vessels were fabricated from low silicon 301 stainless steel by the Ardeform process. The spherical vessels for both high and low pressures were constructed from Inconel 718 using the inturgescent bulge forming process. Outer shells were also formed by this process using 6061 Aluminum.

1.1 Ardeform Pressure Vessels

1.1.1 Description of Ardeforming

Arde, Inc. of Paramus, New Jersey, has developed a proprietary process known as Ardeforming. This process involves the stretching or swelling at cryogenic temperatures of undersized preforms into full size pressure vessels using a modified 301 stainless steel. Stretching is performed by submerging a preform into liquid nitrogen and pumping liquid nitrogen into the preform.

In the fabrication of pressure vessels for aerospace applications there are several potential advantages in using this process.

(a) The cryoformed material has a higher strength/weight ratio than most other materials and still maintains other desirable characteristics, particularly for cryogenic tankage applications.

(b) The modified 301 stainless steel material has a lower cost than competing materials.

(c) The modified 301 stainless steel is relatively easy to form and weld into a preform.

(d) The cryoforming process is a strength test of the vessel. A vessel with a significant flaw will fail during cryoforming and not proceed along a schedule to final failure after more money and time have been expended.

1.1.2 Program Objective

As the size of cryogenic tankage becomes larger the above listed potential advantages assume added importance. NASA/MSC and Bendix have recognized this factor and have been interested in the development of the

Ardeform process. Two earlier programs were completed. In one program Arde, Inc., was funded directly by MSC for the development of a spherical 25" diameter vessel. In a second program Arde, Inc., was funded through Bendix by MSC for the development of pressure vessels for cryogenic oxygen and hydrogen.

Significant success was achieved in each of these programs, but certain shortcomings were also revealed. Consequently the present program was initiated with the objective of overcoming these conditions. Four of these objectives are listed below.

(a) In the earlier program schedule delays and failures were attributed to unclean material. Contaminants entered the material during melting and processing. These contaminants cause defects that result in failures during welding or stretching. Consequently an ojbective was to obtain a vacuum melted material which would produce a cleaner metal.

(b) In a cryogenic dewar, where the pressure vessel is located within and supported from an outer shell, dimensional accuracy becomes quite important. In early programs Arde's stretching technique involved performing this operation in the free state (unrestricted). In theory this should produce a completely symmetrical vessel. Under actual conditions wall thickness variation, weld thickness, fitting boss restrictions, etc., occurred. As a result vessels would vary from nominal dimensions as much as one-fourth inch. An objective was to develop a technique to fabricate a vessel whose contour was accurate to within $\pm$ 0.06.

(c) A third objective was to upgrade quality control, better documentation of parts and processes to provide visibility of the vessel configuration.

(d) A fourth and most significant objective was to establish methods of fabrication and handling the considerably larger parts that were involved in this program.

1.1.3 Program Description

The contract between Arde, Inc. and Bendix involved the design and fabrication of a cylindrical vessel with approximate hemispherical ends. The requirement was for a vessel 39.00 inches in diameter and 63.50 inches long. The vessel was to be designed for use with liquid hydrogen with a minimum burst pressure of 600 psi.

The material used was a low silicon AISI-301 stainless steel, Arde Specification AES 256. This material displayed excellent properties at liquid hydrogen temperature. In order to improve the cleanliness of the material a vacuum melted material was specified. To further establish the capability to produce a clean material and protect the success of the program, two separate heats of material were specified. Each heat was sufficient to provide the entire requirement. Eastern Stainless Steel of Baltimore, Maryland, was selected to produce and roll the material to the required thickness.

In order to improve dimensional accuracy and repeatability, it was decided to stretch the vessel in a completely enclosed die permitting the final stretching to swell the vessel out against the walls of the die. It was expected that this technique would provide a more accurate vessel than would an unconfined free stretch.

Bendix directed Arde to prepare, implement and document an inspection and test plan to insure that fabrication and stretching of the preform and finishing and testing of the final vessel would be in accordance with the design requirements. This plan was reproduced and is included in Appendix II of this report.

The contract also required that Arde fabricate four preforms using parts and procedures established and approved by Arde. Bendix made periodic reviews and audits to determine that Arde was following its established specifications and procedures. Following completion of the four preforms the contract required Arde to successfully stretch and deliver two cylindrical vessels per Bendix requirements.

1.1.4 Program Results

Arde effort was initiated on April 6, 1966. A purchase order was issued to Eastern Stainless Steel Corporation for two 2,000 pound heats of low silicon AISI 301 vacuum melted material. Eastern provided heat number 96269 and 96296. The first, 96269, met Arde's specification AES-256 in all respects. The second was discrepant in that an analysis indicated an oxygen content of 64 parts per million while the specification limits the oxygen to 60 ppm maximum. A review revealed that a requirement of 60 ppm was well below limits that had been successfully used in welded and stretched vessels. This figure was above the maximum level that their supplier felt he could meet. Consequently, it was agreed that heat 96296 would be accepted.

The most significant preform manufacturing step was fabrication of the hemispherical preforms with an inside diameter of 36.76 inches. After investigating several companies for fabrication of this part, Arde selected the B. H. Hubbert Company of Baltimore, Maryland. This company uses a deep draw process with a male punch and draw ring. Considerable development effort was involved in establishing the technique of forming a thin walled shell without excessive wrinkling. However, Arde and Hubbert developed necessary procedures and controls, and satisfactory hemispheres were provided.

During hemisphere development, Arde also undertook the fabrication of one full-size preform of 304L stainless. The primary purpose of this vessel was to establish techniques to handle these large parts and assemblies through cleaning, annealing, stretching, polishing, machining, etc., and to develop welding procedures and setups.

The initial plan for fabrication of the enclosing stretch die involved deep drawn hemispherical ends and a rolled cylindrical section. The cylindrical section was welded to one hemisphere, and a bolt flange was welded to the open end. A second bolt flange was welded to the other hemispherical end. Welding had caused some distortion of the part which caused a machining problem. When machined, the resulting die wall in some areas was too thin for the design loads. It was necessary to refabricate most of the die which resulted in an extended delay in the program.

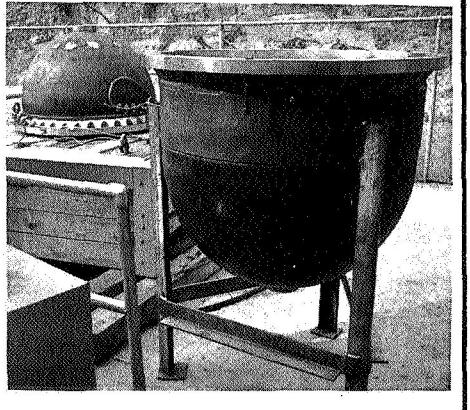

COMPLETELY CLOSED
CRYOSTRETCH DIE

The revised die was made up of segmented welded ends rather than one piece deep drawn ends. This resulted in a more uniform wall thickness in the finished die. The finished completely closed cryostretch die is shown on the left.

The first preform was stretched in early May 1967. One major objective of this stretch was to determine whether the length of the cylindrical portion of the preform was accurate. Arde was concerned that the cylindircal length was too long. Therefore, it was decided that the first preform would be stretched in a "stovepipe" die, one which restricts the cylindrical expansion but not the hemispherical ends. With this technique the vessel was successfully stretched using a pressure of 745 psi. The final dimension versus Bendix requirements are tabulated.

CRYOFORMED CYLINDRICAL VESSEL DIMENSIONS

		Spec	Actual
Diameter	IN	39 ± .06	39.02
Length over bosses	IN	*	65.5
Volume	IN^3	58,000 min.	58,622

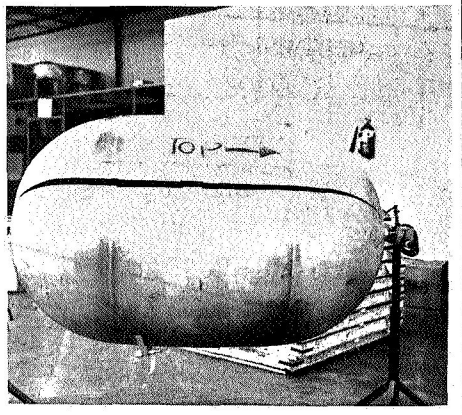

FAILURE PATTERN OF CRYOSTRETCHED CYLINDER

The vessel was then age hardened and polished in accordance with Bendix requirements and was subsequently hydrotested until it failed. The burst pressure was established at 645 psi with a 0.17 percent offset yield of 623 psi. These values are equivalent to stress levels of 247,000 psi and 238,000 psi, respectively. The 0.17 percent offset is equivalent to a 0.2 percent offset for uniaxial test. The hydroburst test results of this pressure vessel was reproduced and is included in Appendix II of this report.

Upon completion of the closed stretch die a second preform was installed in this die and stretched. The vessel burst at 710 psi. After the vessel was removed from the die, it was learned that the vessel had split lengthwise through the cylindrical section next to the longitudinal weld and into each hemispherical end. The failure pattern of the cylindrical pressure vessel is shown at the left.

Arde was unable to firmly establish the cause of failure in a preliminary failure analysis. However, there were several possible reasons:

(a) Weakness in the weld affected zone -- No evidence could be found.

(b) Contamination of the material -- No evidence could be found.

(c) Material thickness not according to specification -- Measurements at the rupture showed 0.048 to 0.049 while Arde's calculations indicated that thickness could be as low as 0.044.

---

*Bendix dimension over bosses was 64.00. However, actual dimension cannot be compared because bosses were not completely machined.

(d) Error in design calculations for preform size and shape -- A complete review revealed no errors in calculations or computer program.

(e) Some unaccounted stress due to use of closed die -- A complete review indicated nothing.

Arde and Bendix reviewed all of these factors without positively identifying a failure cause. It was then decided that a third preform would be stretched in the "stovepipe" die (open ends) to a pressure of 660 psi. This pressure was established by reducing the applied effective stress during stretch in the vessel by 5 percent.

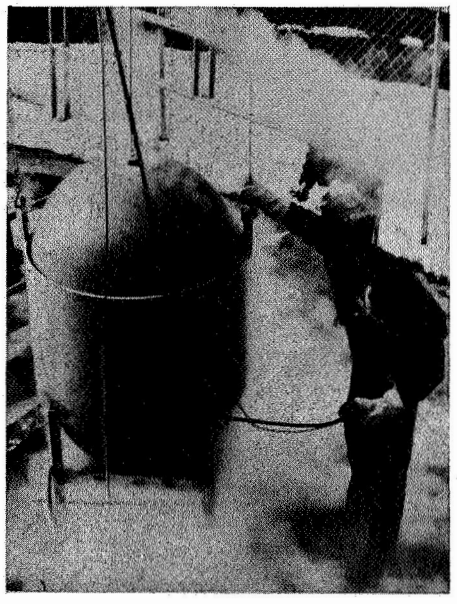

PRESSURE VESSEL & STOVEPIPE BEING RAISED FROM N_2 TANK

The vessel stretched and failed at 590 psi. The failure pattern was the same as for the preceding vessel, longitudinally through the length of the cylindrical section parallel to the weld extending into both hemispherical ends.

A similar failure analysis revealed no specific cause of failure, and the only conclusion made at that time was that failure was due to an undetected flaw in the vessel.

It was concluded that the likelihood of a similar flaw existing in the fourth and last preform was remote, and Arde and Bendix agreed to stretch this preform to a pressure of 660 psi in the "stovepipe" die. This was accomplished successfully.

Following that, this vessel was age hardened, polished, proof tested to specification, machined, and delivered to Bendix. The characteristics of this vessel are as follows:

CHARACTERISTICS OF DELIVERED PRESSURE VESSEL

			Specified	Actual
a.	Volume	IN^3	58,000	57,750*
b.	Proof	PSI	440 ± 10	440
c.	Weight	LB	111.5	122**

* Volume was slightly small due to stretch pressure lower than originally planned which diminished total stretching of vessel.

** Higher weight due to fittings not completely machined. For initial pressurization, Arde uses a relatively heavy boss fitting which would be largely removed to reach specified weight.

Following the completion of stretching, Arde engaged in a comprehensive detailed failure analysis. This analysis was reported in Arde, Inc. Report No. AMR 250 which has been reproduced and is included in Appendix II.

1.1.5 Conclusions

The question of how to obtain material with sufficient cleanliness so as to be usable in the Arde forming process has not yet been completely resolved. Originally, air melted material was used, but it proved to have too much contamination. Arde then specified vacuum melted material to improve cleanliness. While this has been accomplished, the degree of cleanliness obtainable, at least from the supplier on this program, is indeaquate. Arde is presently evaluating different sources for material and is evaluating double vacuum melted material. Only time and completion of these evaluations can determine whether this will result in a suitable material.

During the time span of the contract between Arde, Inc. and Bendix, Arde established a good quality control organization and system for material, parts, and process control. They maintain good documentation and visibility of the material as it is processed to a deliverable piece of equipment.

Bendix believes that good dimensional accuracy and repeatability can be achieved by using the Ardeform process and an enclosing stretch die. Unfortunately, due to limitations in the preforms that were available, this could not be fully evaluated. However, this program did produce much useful information both as to the fabrication and use of enclosing stretch dies.

This program did demonstrate conclusively that vessels of the size involved can be successfully fabricated, handled and stretched. Since these vessels are significiantly larger than Arde had previously built, this is considered to be a most important achievement. The fabrication of thin wall large hemispheres, welding of these hemispheres without unacceptable distortion, heat treating, cleaning, stretching and polishing of vessels of this size are all accomplishments important to the government's future need for large pressure vessels.

1.2 Inconel Pressure Vessels

1.2.1 Inturgescent Forming Process

Inturgescent forming is an improved version of hydraulic bulge forming with a greater depth to diameter ratio capability. All forming results in tension stress in the blank. Relative movement between the part and the cavity surfaces after initial contact is nonexistant. The process is capable of very close dimensional control, extremely good surface finish and large diameter to thickness ratios.

1.2.2 Inconel 718 Pressure Vessels

The pressure vessels fabricated for this contract were formed using hot rolled Inconel 718 alloy plate, purchased to Bendix Specification ECL 201. The 39" diameter hemispheres were formed by inturgescent technique, using a 56" diameter blank. Flat blanks and taper ground blanks have been used. The 0.200" thick flat blanks severly challenge the machine capability to maintain sufficient draw ring pressure to accomplish a hydraulic seal. The taper ground blanks reduce the bulge pressure requirements. Fully developed taper ground blanks will yield a wall thickness sufficiently uniform to preclude any post chemical milling requirements.

Interstage annealing is performed in accordance with Bendix specification MCI 168 which includes post annealing and pickling requirements. Annealing is accomplished in an air atmosphere furnace with the surface protected from excessive oxidation by coating with a trade name product called "Turco-Pre-treat." The annealing temperature, 1850°F., was determined by evaluating formability of material with a 1750, 1850 and 1950°F anneal. The 1950°F anneal produces noticable grain growth while the 1750°F anneal produces lower elongation and higher yield strength. The 1850°F temperature produces the optimum combination of lower yield and higher elongation without appreciable grain growth (undesirable "orange-peel" surface condition). The "Turco-Pre-treat" coating limits the loss of gauge to approximately .001" per anneal and the oxide formation to an easily removed thin scale.

1.2.2.1 Low Pressure Spherical Oxygen Vessels

These are 39" diameter spherical pressure vessels for oxygen with a minimum burst strength of 600 psi.

Two vessels were fabricated of Inconel 718, age hardened to an ultimate strength above 180,000 psi. Hemispheres for these vessels were formed from flat sheet by the inturgescent forming process. Boss fittings were machined from pancake forgings of Inconel 718.

The boss fitting-to-hemisphere weld and the vessel girth weld were made by a hand TIG process. Age hardening of the complete vessel was performed by Scott Ford, Inc. of Rock Island, Illinois in accordance with Bendix instruction MCI-174. This process involves pretreating the exterior of vessel with "Turco-Pre-treat" and purging the inside of the vessel with argon. The vessel is then held for 8 hours at 1325°F then furnace cooled to 1150°F and held at this temperature for a total heating period of 18 hours. The vessel is then subjected to a proof test at 450 psi for 15 minutes. This is equivalent to a safety factor of 1.5 times maximum operating pressure of 300 psi.

1.2.2.2 High Pressure Spherical Oxygen Vessels

These are 39" diameter spherical pressure vessels for oxygen with a minimum burst strength of 2040 psi.

Two vessels were fabricated using Inconel 718 age hardened to an ultimate strength exceeding 180,000 psi. Hemispheres for these vessels were formed from flat sheet by the inturgescent forming process. Boss fittings were machined from pancake forging of Inconel 718.

On the first vessel the boss fittings were welded into the hemisphere by hand TIG welding. The girth weld joining the two hemispheres was made by the same process. This vessel was ultimately used in the structural model tank which is discussed elsewhere.

Welding of the second vessel was performed by Arde, Inc., using a semi-automatic TIG procedure. This effort was under the cognizance of Bendix technical representatives.

Age hardening of these vessels was performed in the same manner as indicated for vessels under paragraph 1.2.2.1 above. Proof testing was performed at 1530 psi representing a safety factor of 1.5 times maximum operating pressure. The first vessel was ultimately used in the structural model tank and the second vessel was used in the thermal model tank. These tanks are discussed elsewhere.

1.2.3 Cylindrical Hydrogen Pressure Vessels

These are 30" diameter by 63.5" length cylindrical pressure vessels for hydrogen with a minimum burst strength of 600 psi.

Two vessels were fabricated of AISI 301 stainless steel by the Ardeform process. Details of this program are discussed elsewhere.

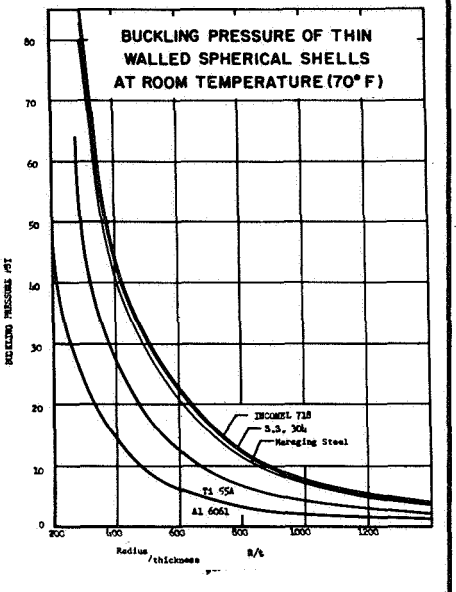

2.0 OUTER SHELL FABRICATION

The aluminum hemispherical outer shells for the monocoque and honeycomb structures were formed by the inturgescent process.

2.1 Aluminum Monocoque Shells

2.1.1 Spherical Vessels

These are 41.5" O.D. spherical monocoque shells for oxygen with a buckling pressure differential of 23 psi.

Two shells were fabricated of 6061 aluminum alloy. Hemispheres for these shells were formed from flat sheet by the inturgescent forming process. In order to establish the buckling pressure the attached curve was used. This curve is empirical and results in a modification to the classic (Zoelly) buckling equation. By using the room temperature curve and R/t ratio of approximately 340 is required for a buckling ΔP of 23 psi. The equation is then:

$$t = \frac{R}{340} = \frac{D/2}{340}$$

$$= \frac{41.5/2}{340} = .061" \text{ min. thickness.}$$

One outer shell was used on the thermal model tank and second vessel was used on the structural model.

The 41.5" diameter spherical aluminum outer shells have been produced from warehouse material, 6061-0 aluminum, .090 thick. The following problems occured:

(a) Finished parts near or below print thickness tolerance in the "pole" area.

(b) Shoulder folds due to too much material being drawn into the cavity as a result of attempting to solve problem (a).

To aid in solving the above problems, a new draw ring and wear plate have been fabricated from heat treated aluminum (7075-T6). This aluminum makes a good bearing surface in mating with the body steel sandwich used in the draw operation. The lower friction forces allow draw to be accomplished at a lower bulge pressure thereby resulting in less thin-out in the pole region.

Future material will be procurred from a mill and have more control exercised on those properties which effect draw.

2.1.2 Cylindrical Shells

These are 41.5" O.D. by 66" length cylindrical monocoque shells with hemispherical ends with a buckling pressure differential of 23 psi.

Two shells were fabricated of 6061 aluminum alloy. Hemispheres were formed from flat sheet by the inturgescent forming process. The wall thickness of the hemispheres was established in a manner identical to that described in paragraph 2.1.1.

The cylindrical section was formed by rolling and welding a sheet of 6061 aluminum alloy. Fabrication was performed to Bendix requirements by Arde, Inc.

Wall thickness of the cylindrical section was established by using the classical critical buckling pressure equation for thin cylindrical shells (shown in Appendix I). The resulting thickness of the cylindrical shell having a buckling pressure differential of 23 psi is 0.125 inches.

2.2 Honeycomb Hemispherical Outer Shells

Two (2) hemispherical honeycomb sandwiches were fabricated by Bendix in compliance with NAS 9-5491 Contract. Honeycomb structures of this type are being considered for the outer shells of cryogenic storage vessels in an attempt to optimize on strength-to-weight characteristics. As the size of dewar-type cryogenic tankage becomes larger, buckling stresses on the outer shell become greater. This buckling stress results from the pressure gradient between ambient pressure on the outside and the vacuum annulus on the inside of the spherical shell. A monocoque outer shell would become increasingly heavier with a thicker wall section as the vessel size increases; whereas a honeycomb sandwich would have strength properties to provide adequate buckling safety and still be weight optimized for consideration as flight hardware.

Buckling tests were performed on simulated test samples and the hemispherical honeycomb sandwiches. The test results appear to show some agreement.

2.2.1 Honeycomb Fabrication

2.2.1.1 Vacuum Bag Process

The hemispherical honeycomb sandwich is fabricated by the vacuum bag process. As vacuum is applied to the inside of the bag, external atmospheric pressure of 12 to 14 psi will exert a compressive force on the honeycomb sandwich elements. The vacuum bagged honeycomb assembly is placed in an oven at the prescribed temperature and for the time required to cure the adhesive which bonds the flexcore to the facings. A vacuum gauge is advisable to monitor vacuum pressure, and a thermocouple should be inserted inside the vacuum bag for temperature readout on the honeycomb sandwich. Time and temperature observations are important because there is a critical time period for the adhesive film to reach its bonding temperature.

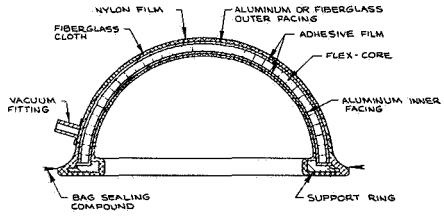

VACUUM BAG ASSEMBLY TECHNIQUE

A3861A-68-3

Prior to curing the adhesive film, the sandwich elements (inner facing, outer facing and flexcore) are in a very flexible or non-rigid state. For this reason, a support member or back-up plate is necessary to prevent distortion of the honeycomb sandwich during the vacuum bag operation. One very successful way of preventing warpage is by using a support ring. This ring is located on the inside diameter of the inner shell and flange facing.

The complete honeycomb sandwich can be fabricated in one operation, or the flexcore can be assembled to the inner facing and then the outer facing added as a separate "vacuum bag" procedure. The latter method allows for a more precise individual treatment of the inner and outer facings due to the lay-up techniques involved when applying the adhesive film. If the two-stage method is used in the honeycomb sandwich fabrication, the support ring is needed for both vacuum-bag operations because rigidity of the honeycomb structure is not achieved until the sandwich is completely bonded to the inner and outer facings.

Materials and suppliers used in the making of a vacuum bag are listed below.

2-mil nylon film	Richmond Paper Company
Fiberglass cloth	Owens Corning Fiberglass Co.
Bag sealing compound	Schnee-Morehead Chemicals, Inc.

The honeycomb sandwich components are mounted to the support ring and a layer of fiberglass cloth is wrapped around this lay-up. Fiberglass cloth serves the function of a "wick" to assure sensing of the vacuum pressure at all parts of assembly. This material is considered a reusable item for subsequent vacuum bag operations because the adhesive curing temperature of 250°F is less than the 1000°F temperature maximum of the glass cloth. The 2-mil nylon film serves as the "vacuum bag" and has proven to be ideally suited for this purpose since it can withstand vacuum-bagging temperatures in excess of 350°F. This material is not considered reusable because the nylon hardens at the 250°F use temperature and a puncture may occur wherever the material is creased or folded.

A leak-tight bag is formed with the nylon film by means of "bag sealing compound". This is a highly tenacious putty-like material which seals onto the nylon film with no leakage. The vacuum fitting is assembled to the nylon bag also by use of the bag sealing compound. This is a versatile approach to this method of honeycomb sandwich fabrication because it is ideally suited to experimental and prototype work where final sizes and shapes are not definitely determined.

2.2.1.2 Hemispheric Fabrication

The honeycomb sandwiches consisted of the following components.

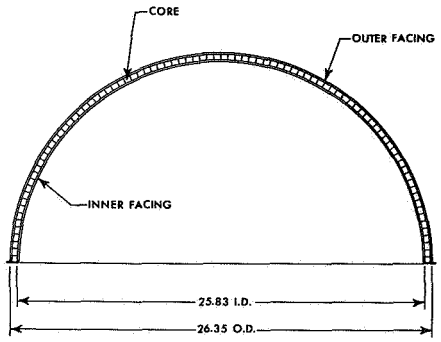

HEMISPHERICAL HONEYCOMB SANDWICH

A-5001-68-1

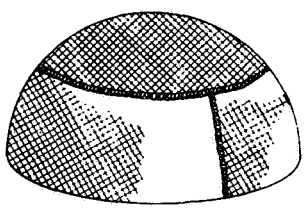

FLEX-CORE SPLICED AND ASSEMBLED TO HEMISPHERICAL FACING

(a) Outer facing - aluminum hemisphere, 6061 alloy, 0.022 inch material thickness.

(b) Inner facing - aluminum hemisphere, 6061 alloy, 0.022 inch material thickness.

(c) Core material - Flexcore (Hexcel Co.), 5052 aluminum alloy, 0.0019 inch ribbon thickness, 0.200 inch core thickness, 40 cells per foot.

The above components were cemented together using epoxy film, 3M AF-111, between the facings and the core. Bonding pressure was obtained by the vacuum bag process. The curing cycle was for one (1) hour at 250°F while maintaining approximately 14 psi vacuum bag pressure.

Flexcore was chosen as the core material for this project because of its ability to conform to a non-planar shape. Instead of a hexagonal cell geometry, as is the case with conventional honeycomb, flexcore is comprised of a wavy cell structure. Thus, flexcore was readily formed to a hemispherical shape without causing the cells to collapse due to overstress. A splicing epoxy (Shell Epon 924) was used to join the flexcore together.

The hemispherical facings used in this program were formed by the "Inturgescent Process" at the Bendix facility in Santa Ana, California. After the forming operation, these aluminum hemispherical shells were trimmed to the required radial height and flanged. Exact dimensional checks of the facing diameters with respect to the core thickness were made to assure a proper fit-up of the final sandwich. If the flexcore fits too loosely between the facings, this lack of intimate contact will not permit the epoxy adhesive film to "wet" properly and the overall sandwich strength would be impaired. Conversely, if the dimensional build-up causes a tight fit of the sandwich components, the outer facing will become difficult or impossible to assemble. To help assure a minimum tolerance build-up and maintain an optimum fit-up and bond of the overall honeycomb sandwich, the flexcore material is held to a $\pm$ 0.005 inch core thickness. The epoxy adhesive film thickness must also be taken into account when calculating the fit-up of these components. For example, 3M AF-111 film is .015 inch tick. A honeycomb outer shell with an aluminum outer facing is most sucessfully constructed in two stages - (inner facing cured to the flexcore, outer facing cured to this subassembly). During the inner facing-to-flexcore subassembly, the epoxy film "melts" down to create a honeycomb-to-facing contact. In this manner, the only dimensional build up

for epoxy film is in conjunction with the outer facing at the time of final honeycomb sandwich assembly.

A cautious procedure of material handling must be inaugurated for the fragile aluminum facings as well as for the flexcore honeycomb. When the facings and flexcore are in transit, adequate packaging must be provided to prevent denting and when the epoxy and honeycomb are being applied, care should be taken not to deform the facings. The flexcore ribbon is a delicate article about 0.0019 inch thickness requiring careful handling. Furthermore, care should be exercised when cleaning the facings to prevent "rack marks" as a result of the holding fixture. Large hemispherical facings must be immersed into the cleaning tanks with care to avoid buckling or denting the delicate aluminum facings.

It is necessary to store the epoxy adhesive film at approximately 0°F to prevent degradation of the adhesive properties and insure a longer shelf life. Upon removal from 0°F storage, storage life should not exceed one week and the temperature should not exceed 80°F. If these precautionary steps are not taken, degradation of the adhesive may well result in subsequent lowering of the overall strength properties of the honeycomb sandwich. To accomplish the layup, the adhesive film should be pre-cut into spherical triangle sections. These sections are numbered in sequence so they will fit their proper places at the time of assembly. A center piece of the adhesive film is then cut to size and placed at the upper junction of these sections.

Excess grit and oil are removed from the facings by wiping with a cloth soaked in trichloroethelene. Chemical cleaning consists of a quick (approximately one-half minute) immersion in hot caustic followed by a nitric acid dip lasting 40 to 60 minutes. These chemical treatments are interspersed with water rinses and the facings are blown dry with clean dry air or nitrogen and/or dried in an oven at 120°F for 20 minutes. The facings must be checked for "water break" after final rinse to check cleanliness. If the water film pulls away leaving dry zones, contamination exists on the aluminum surface and the cleaning operation should be repeated. As soon as possible after the chemical cleaning procedure, the facings are "primed" with a solution such as 3M PD-3901 and allowed to air dry in a contaminent-free atmosphere for one hour. The advantages of priming are to preserve the cleaned aluminum facing free from further oxidizing for a period of one week, and permit easier "tacking" of the epoxy adhesive film.

The process of "tacking" is aided by a hot air blower gun. Excessive overlap of the epoxy adhesive may contribute to a dimensional build-up problem and make it difficult to assemble the outer aluminum facing. Trimming of flexcore honeycomb is a procedure which must be skillfully controlled to prevent mutilation of the delicate ribbon. Each individual cell can be cut with a pair of scissors; or with acquired skill the flexcore can be trimmed more rapidly with a special honeycomb cutting serrated knife. Processing and assembly of honeycomb sandwich components must be conducted in an atmospheric environment free from oil and excess dust and humidity. Temperature above 80°F should be avoided during subassembly to prevent rapid aging of the epoxy adhesive film.

The completed hemispherical honeycomb shells were 26-3/8 inches in diameter and weighed 6 pounds 6 ounces each.

2.2.2 Honeycomb Testing

2.2.2.1 Preliminary Testing

Considerable background work was performed in evaluating sample honeycomb panels for strength and adhesion. T-peel testing was used to establish techniques for obtaining highest bond strengths. The resulting values for T-peel using various fabrication methods for the honeycomb sandwiches are shown in Table I. Optimum fabrication techniques learned from these data were applied to the hemispherical honeycomb sandwiches.

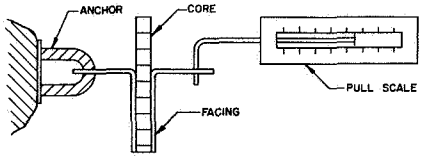

T-PEEL TEST

A-5001-68-6

There are other methods of testing for honeycomb sandwich bond integrity. These include the "ultrasonic" and "infrared" techniques. When a precision honeycomb sandwich is manufactured for such applications as outer shells of dewar vessels used in aerospace missions, positive assurance of no defects in the sandwich bonding is required. Such defects as intermittent "wetting" of the core to the facings would result in a deterioration of overall strength properties. This could result in a buckling failure. By combining proven manufacturing techniques, rigid control standards and highly reliable nondestructive testing sequences, it is felt that quality outer shells can be successfully fabricated. This nondestructive test procedure would entail 100% inspection of each completed hemispherical and cylindrical sandwich. One method of testing is with ultrasonics. The honeycomb specimen is immersed in water when performing the ultrasonic scanning operation. An ultrasonic tracing is then made on special paper to show the faulty honeycomb bonding. The infrared technique of non destructive

honeycomb sandwich testing is based on heat penetration, and is a function of the core-to-facing bond quality. This "thermal map" is usually observed on a picture tube. An attachment is also available to record non destructive honeycomb sandwich test results on a special paper.

2.2.2.2 Spherical Segment Testing

Numerous simulated buckling tests were performed on spherical honeycomb segments versus spherical monocoque segments. This was believed to be a means of predicting buckling pressures for hemispherical honeycomb sandwiches. A honeycomb sandwich spherical segment is shown (margin) in the process of testing. A one inch diameter metal rod, with a 1-1/8 inch diameter by 1/8 inch thick hard rubber bumper cemented to the end, was used as the impinging tool. The base fixture was 5 inches in diameter with the outside edge rounded to prevent sharp contact with the test specimen. The pieces used as test specimens were from a hemisphere having a diameter of 13-5/8 inches.

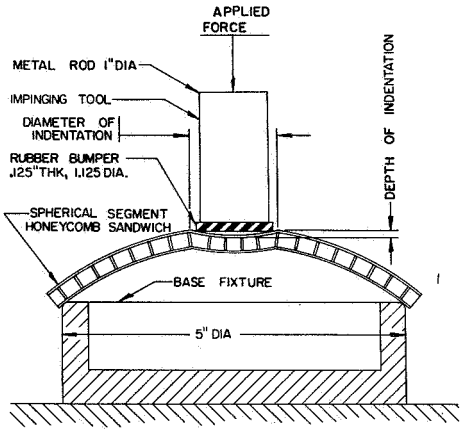

SCHEMATIC FOR COMPRESSION TESTING A HONEYCOMB SANDWICH

A5001-68-7

The honeycomb sandwich spherical segment was placed on the test fixture and sufficient force applied to the metal rod to cause a slight indentation in the honeycomb. This operation was readily conducted on a Riehle universal testing machine. An indentation of 0.020 to 0.025 inch with about one inch diameter was achieved with a force of 150 pounds. For the monolithic segment, testing was performed on a Toledo scale by pushing the metal plunger rod by hand. A similar indentation was achieved with a force of 13-1/2 to 14 pounds. Therefore, the force ratio to obtain similar indentations was about 11:1. This data was verified by repetitive testing. In another test, the honeycomb segment was indented with a force of 240 pounds to a diameter of 1-7/8 inches and depth of 0.138 inch. A similar indentation on the monocoque segment required a force of 25 pounds resulting in a force ratio of about 9.6:1. It is believed that the former data is more realistic, because a slight dimpling or discontinuity as described in the first instance would be sufficient for buckling of a monocoque sphere.

Materials for the honeycomb sandwich segment described above were 6061 aluminum spherical segments 0.017 inch thick for the facings and flexcore honeycomb 5052 aluminum with a 0.200 inch core thickness by 0.0019 inch ribbon thickness. The honeycomb sandwich was fabricated by the vacuum bag process using 3M AF-111 adhesive film to bond the facings to the flexcore at 250°F for 60 minutes. The monocoque test specimen

comprised one of the facing segments used in the honeycomb sandwich.

2.2.2.3 Hemispherical Buckling Tests

After the honeycomb hemispheres were fabricated, they were subjected to full vacuum testing for buckling characteristics. The sandwiches were subjected to a vacuum pressure of 14 psi minimum for a period of 30 minutes at room temperature. There was no tendency of the hemispheres to buckle during this vacuum test.

To obtain higher buckling pressures, the two hemispherical honeycomb sandwich shells were tested on the Bendix inturgescent forming machine at Santa Ana, California. These were destructive tests conducted with hydraulic pressure in order to determine buckling characteristics. The schematic at left and the following description explain the test method used.

SCHEMATIC OF HONEYCOMB BUCKLING APPARATUS

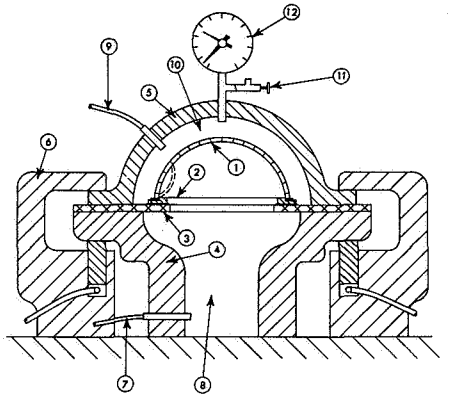

A-5001-68-2

Honeycomb hemisphere (1) is assembled to support ring (2). A rubber sealing gasket and vacuum grease are used between these parts to prevent leakage during the buckling test. Hydraulic fluid is pumped through line (7) into cavity (8). The honeycomb hemisphere and support ring are then placed on ring (3) and sealed with another rubber gasket and vacuum grease. Hydraulic clamps (6) are positioned around the periphery of the inturgescent forming machine and hydraulic pressure is applied to firmly seal upper cavity (5), ring (3) and base (4). At this time the hydraulic fluid in cavity (8) is pumped out through line (7), leaving a partial vacuum under the honeycomb hemisphere and causing the gasket seals to be firm and leak tight. Without this "water vacuum", the honeycomb hemisphere would float when hydraulic fluid is applied in chamber (14). Hydraulic fluid is then pumped through line (9) and into chamber (10) while valve (11) is open. Valve (11) is closed when chamber (10) is filled. Gage (12) registers increasing pressure and is equipped with a stop hand to indicate maximum pressure.

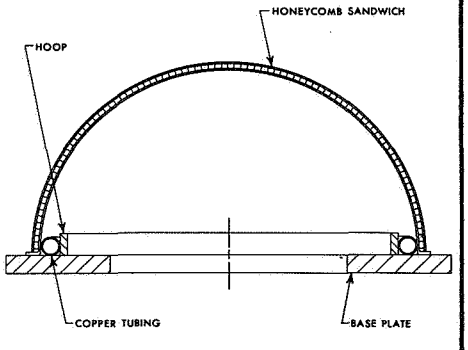

HONEYCOMB HEMISPHERE WITH SUPPORT RING #1

A-5001-68-8

Since buckling pressures were only 14-1/2 psi for this test, there was no giving way of the support ring. No premature failures were experienced when testing with higher pressures on the inturgescent equipment at Bendix, Santa Ana.

Hemisphere #1 buckled at 53 psi differential pressure. A set-up showing hemisphere #1 mounted to its support ring is shown in the margin. An aluminum hoop served as an inner support with a copper tubing spacer between

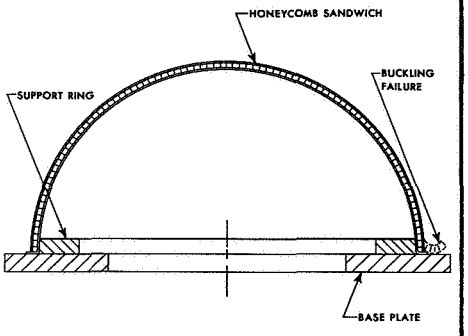

HONEYCOMB HEMISPHERE WITH SUPPORT RING #2

A-5001-68-9

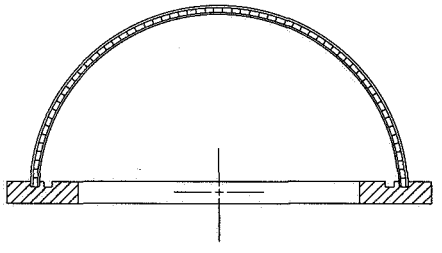

HONEYCOMB HEMISPHERE WITH CONSTRAINING SUPPORT RING

A-5001-68-4

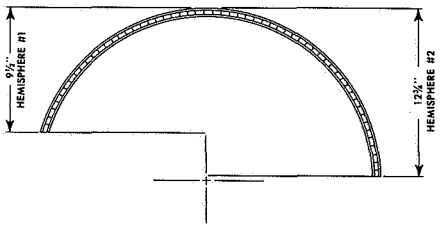

HEMISPHERICAL HONEYCOMB SANDWICHES (REWORKED AFTER INITIAL BUCKLING TEST)

A-5001-68-3

the hoop and the honeycomb hemisphere. This copper tubing was curved to the prescribed hemisphere inside diameter, butted together and tightly wedged in place. The hemisphere sandwich with this inner support was placed on the base plate and sealed with a rubber gasket. At a hydraulic pressure of 53 psi, the honeycomb hemisphere buckled prematurely at its base because the inner support ring gave way. That is, the copper tubing spacer became separated at the butt joint, causing failure of the honeycomb sandwich at that position.

In order to correct the inadequate support ring design described above, a modification was made for the testing of hemisphere #2. This is illustrated in the margin. A solid support ring machined to snugly fit the inside honeycomb hemisphere diameter replaced the hoop and copper tubing. When hydraulic buckling pressure was applied to the outside of hemisphere #2, buckling again occurred at the base of the hemisphere. This second test showed a buckling pressure of 83 psi. The honeycomb sandwich failed by moving outward in the form of a "J" as depicted.

Since both of the above buckling failures occurred at the base of the hemisphere, the support ring was further modified in an effort to cause buckling on the dome portion. The new type constraining support ring shown in the margin was designed to permit the hemisphere to fit into a groove. When buckling pressure is applied, the base is firmly held to prevent both inward and outward movement. Buckling must, therefore, occur on the dome portion. This type support ring eliminates local discontinuities at the hemisphere base and likens the testing to that of a complete sphere. Putty, to serve as a sealing gasket, was placed in the support ring grooves to prevent leakage during the application of hydraulic buckling pressure.

In order to conduct testing with the new support ring, the hemispheres already buckled, were machined to remove the deformed sections. The heights of the resulting hemispheres are shown at the left.

Hemisphere #1 was shortened to a height of 9-1/2 inches. For the buckling test, this sandwich was placed in the inner support ring groove and buckling occurred at 55 psi differential pressure in the dome portion of the hemisphere. The cave-in amounted to a dent diameter of 13-1/2 inches.

Hemisphere #2 was shortened to a height of 12-3/4 inches to remove deformities caused during the initial buckling test described above. For this second buckling test, the sandwich was placed in the outer support ring groove. Buckling occurred at 73 psi differential pressure. The cave-in amounted to a dent diameter of 12 inches and was located in the dome section of the hemisphere.

2.2.2.4 Conclusions

Hemisphere #1, when mounted to the support ring, buckled at approximately the same pressure during both tests. The testing of hemisphere #2 showed that it buckled at a 10 psi lower pressure during the second test. It was anticipated that the buckling pressure would be higher when using the constraining support ring. Weakening or delamination of the honeycomb sand- which due to pressures applied may have occured during the first tests. This was not likely because the buckle dent appeared normal, and no evidence of flaws existed in this vicinity. It is concluded that the hemispherical honeycomb sandwiches were nearly at their buckling pressures when they failed at their base during the first tests.

Both hemispheres were slightly damaged at their poles during the first buckling tests. This was caused by a pipe fitting projecting from gage (12) to the inside of upper cavity (5). As the buckling test was concluded and hydraulic pressure released, the honeycomb hemisphere floated upward creating approximately a one inch diameter by 1/4 inch deep dent. These dents were carefully smoothed out before the second series of tests were conducted. However, the original scars still existed. When the second buckling tests were run neither hemisphere dented in the vicinity of these scars. This indicates that a honeycomb sandwich is not nearly as dent sensitive as a monocoque structure.

If the monocoque spherical segment is considered a portion of a complete spherical vessel, the buckling pressure for this vessel would be approximately 14.25 psi. The fact, that an apparent similarity exists between the force applied to indent the monocoque spherical segment and the buckling pressure of a spherical vessel, is noteworthy. If it is assumed that the ratio of forces required for indenting a honeycomb and a monocoque structure is the same as their buckling ratios, then the buckling pressure for a spherical honeycomb sandwich 13-5/8 inches diameter would be 157 psi. The buckling pressure of a 26" diameter monocoque hemisphere of 6061 aluminum 0.022 inch thick is approxi-

mately 6.2 psi. With a force ratio of 11:1 for honeycomb versus monocoque, a honeycomb buckling pressure of 68.2 psi is predicted. Since the average buckling value for the hemispheres fabricated was 68 psi, it appears that this may be a valid approach for predicting the buckling pressure for honeycomb structures.

The weight of a hemispherical honeycomb shell, 26-3/8 inches in diameter with an approximate buckling pressure of 68 psi, is 6.4 pounds. The weight of an aluminum monocoque shell having similar characteristics is 7.1 pounds. It is, therefore, evident that honeycomb outer shells with diameters greater than 26 inches weigh considerably less than comparable monocoque outer shells.

TABLE I

HONEYCOMB BONDING EVALUATION

5052 Aluminum Flex-Core .0019" Ribbon Thickness x .200" Core Thickness Used as Noted. Bonding Accomplished by Vacuum Bag Process. Facings are 6061 Aluminum 1-3/8" Wide x 4-1/2" Long x .008" Thick. Minimum Industry Standard is 14 lbs/in T-Peel.

CLEANING PROCEDURES	ADHESIVE	CURE TEMP. (°F)	CURE TIME (Min)	T-PEEL TEST (lbs/in)
A	1	250 (a)	60 (a)	10.2 (f)
B	1	250 (a)	60 (a)	11.3 (f)
B	2	250 (b)	60 (b)	10.2 (f)
D	2	250 (b)	60 (b)	11.7 (f)
C	2	250 (b)	60 (b)	14.2 (f)
C	3	250 (b)	60 (b)	15.3 (f)
E	2	250 (b)	60 (b)	4.7 (hc)
F	2	250 (b)	60 (b)	5.1 (hc)
G	2	250 (b)	60 (b)	16.8 (hc)
B	2	250 (b)	60 (b)	13.6 (hc)
G	2	250 (b)	60 (b)	15.3 (f)
B	2	250 (b)	60 (b)	13.8 (f)
G	2	250 (b)	60 (b)	13.1 (f)
B	2	250 (b)	60 (b)	13.1 (f)
H	2	250 (b)	60 (b)	11.3 (hc)
I	2	250 (b)	60 (b)	> 26.0 (hc)

A. Vapor degrease only
B. Vapor degrease, hot caustic etch 5 min., muriatic acid 5 min., nitric acid 3 min.
C. Vapor decrease, sulfuric and dichromate @ 150°F for 20 min.
D. Vapor degrease, nitric acid 3 min.
E. Vapor degrease, hot caustic 5 min., nitric acid 10 min.
F. Vapor degrease, hot caustic 5 min., nitric acid 10 min., Oakite 34 10 min., nitric acid 1 min.
G. Vapor degrease, nitric acid 10 min.
H. Vapor decrease, hot caustic 1/2 min., nitric acid 40 min.
I. Vapro degrease, nitric acid 40 min.

1. 3M AF-111, one side primed w/3M 3901, other side unprimed.
2. 3M AF-111, both sides primed w/3M 3901.
3. 3M AF-111, unprimed.

a. Took 40 minutes to reach temperature.
b. Took 30 minutes to reach temperature.
f. Facing cemented to facing (no honeycomb used).
hc. Honeycomb used in conventional manner between facings.

SECTION C

PHASE III - PROTOTYPE THERMAL MODEL FABRICATION

1.0 INTRODUCTION

This section discusses the major tasks required to fabricate the thermal model on this program. The development of fabrication techniques, processes and solutions during the fabrication effort are also discussed herein.

2.0 SYSTEM DESCRIPTION

The dewar is a 41.5 inch spherical diameter double-walled container with a pure vacuum annulus between the Inconel 718 39 inch diameter pressure vessel and the aluminum outer shell. Two thin aluminum radiation shields are suspended between the pressure vessel and outer shell. The inner shield contains a vapor cooling coil. To minimize radiant heat transfer all surfaces in the vacuum annulus are plated with low emissivity metallic coatings. The radial bumper suspension technique is used to support the pressure vessel within the outer shell. Eight equally spaced bumpers of Kel-F material are employed on the bottom and eight on the top of the pressure vessel to provide adequate load carrying capacity and low thermal conductivity characteristics.

There are three fluid tubes running from the pressure vessel to the outer shell. On the bottom the fill tube exits from the pressure vessel at the pole and rises up to the bumper plane where it then passes through four of the radial bumpers and exits from the outer shell by passing through a stainless steel to aluminum bi-metal transition joint. The vent tube is identical to the fill tube and is located on the top of the tank. The vapor cooling tube exits from the top pole of the pressure vessel and runs to the top underside of the inner shield. It then winds its way down the inside surface of the shield to the bottom and exits from the outer shell thru a transition joint located at the bottom of the tank.

Eleven metal sheathed electrical leads from the instrumentation package exit through the top pressure vessel closure fitting and eleven leads exit

through the bottom closure fitting. The leads are formed into a .312 inch diameter bundle and are routed through the vacuum annulus in the same manner as the fluid tubing. A stainless steel to aluminum transition fitting is used to exit through the outer shell.

The pressure vessel instrumentation package is supported within a 1.750 inch diameter thin wall stainless steel tube. This assembly is located in the center of the tank and extends from top to bottom of the tank. The dewar assembly drawing 1620553-1 shows the location of components in the assembly. The assembly includes two motor fans located at opposite ends of the tank for destratification of the cryogen. Six Calrod type electrical heaters, three on each end, are silver brazed to the outer surface of the support tube in the form of a triple helix. Two thermocouples are attached to the support tube at the upper end for monitoring dewar temperature.

A capacitance type density measurement probe is located inside the support tube and extends from a point approximately 4.5 inches above the tank bottom to a height sufficient to measure 97.8% fill. Two thermostats (cut-off switches) are provided at the bottom end of the instrumentation assembly between the motor fan and the capacitance probe to prevent overheating of the dewar by de-energizing the electrical heaters.

The external hardware, shown in schematic drawing 1621192 consists of three manual valves for the vapor cooling, fill and vent line. Two pressure switches sense system pressure in the vent line and serve to control heater and motor fan operation. Each pressure switch controls three heaters and can operate independently or simultaneously. A pressure gauge, with a range of 0-3000 psi, is provided to indicate system operating pressure. The Bendix FR-131 relief valve is plumbed into the vent line and is capable of relieving excess system pressure.

The cryogen heat input is controlled from the control panel. Heaters and destritification fans can be energized individually or in any combination from the control panel. Bendix drawing 1620899 provides electrical details of the system.

Dewar operating pressure is maintained automatically by pressure sensitive switches which apply voltage to the heater and fan ralays (K_1 through K_8) whenever system pressure drops below a predetermined level.

Individual switches on the control panel apply the ground connection for a selected relay.

Pressure switch bypass control switches (SW_3 and SW_{10}) on the panel permit control of the heaters and fan independent of the pressure switches.

A meter on the control panel provides fluid density data when used in conjunction with a Bendix GZ-46 analog capacitance servo. The meter indicates the percentage of useable cryogen in the vessel. A three-position switch changes the meter scaling to conform to the cryogen being used.

Additional detail physical characteristics of the thermal model are presented in table I.

TABLE I. THERMAL MODEL PHYSICAL CHARACTERISTICS

DRY SYSTEM WEIGHT (Including Transport Cart)			563.7
Dewar Dry Weight		268.0	
Pressure Vessel (less components)	177.0		
Outer Shell Assy	39.9		
Outer Shield Assy	16.8		
Inner Shield Assy	19.1		
Misc. Components	15.2		
External Components		17.7	
Transportation & Handling Cart		278.0	

DEWAR

OUTER SHELL	
Female	P/N 1620848-1, S/N 12
Male	P/N 1620849-1, S/N 13
Material	Aluminum 6061-0
	QQ A 250/11
Thickness	0.065" nom.
Outside Diameter	41.460" nom.
Plating (inner surface)	Copper Vapor Plated
OUTER SHIELD (non-vapor cooled)	
Female	P/N 1620763-1, S/N 26
Male	P/N 1620762-1, S/N 30
Material	Aluminum 6061-0
	QQ A 250/11
Thickness	0.031" nom.
Outside Diameter	40.900"
Plating (both surfaces)	Silver Vapor Plated
INNER SHIELD (vapor cooled)	
Female	P/N 1620773-1, S/N 21
Male	P/N 1620774-1, S/N 23
Material	Aluminum 6061-0
	QQ A 250/11
Thickness	0.025" nom.
Outside Diameter	40.470"
Plating (both surfaces)	Silver Vapor Plated
Vapor Cooling Tube	
Material	Copper
Size	0.250" O.D. x 0.030" wall
Length	56' approx.
Length Soldered to Shield	54.50'
Stainless Steel Tube Length	
Pressure Vessel to Vapor Cooling Tube	13.0"
Vapor Cooling Tube to Outer Shell	10.5"
V.C. Tube Bend Schedule	

TABLE I (con't)

Radius	No. 90° Bends
1.00	9
2.00	8
2.28	2
3.86	4
4.00	3
1.50	2

PRESSURE VESSEL	
Hemisphere	P/N 1620764-1
Hemisphere	S/N 13 & 14
Material	Inconel 718 (aged)
Thickness	0.120" nom.
Outside Diameter	39.0" nom.
Volume	17.5 cu. ft.
Operating Pressure	1020 psi
Proof Pressure	1530 psi
Boss Fittings	P/N 1620739-1
Material	Inconel 718 (formed)
Plating (outer surface)	Silver Vapor Plated
FLUID FILL & VENT TUBING	
P/N 1620779-1	
Material	Stainless Steel 304L
Size	0.312" O.D. x 0.020 wall
QUANTITY SENSOR	
Type	Concentric Tube Capacitor
Manufacturer	Bendix, I & LS Division
Size	1.250" O.D. x 31.0" Length
Capacitance	
76°F Air	201.60 pico farads
Liquid Oxygen	289.2 pico farads
TEMPERATURE SENSOR (2)	
Type	Thermocouple-Copper Constantan
Manufacturer	American Standard
MOTOR FAN (2)	
Type	Cryogenic Destratification
Manufacturer	Globe Industries Inc.
Mfg. P/N	19A1993
Mfg. S/N	0021 & 0022
Weight	13.5 oz.
Size	1.683" O.D. x 2.887" Length
Input	115 V AC line to neutral 3Ø

TABLE I (con't)

Speed in Air	400 Hz 20.3 watts max. 6030 PRM max.
HEATER (6)	
Type	Electrical Resistance
Manufacturer	American Standard
I & LS Division P/N	1620742-1
Material	
Element	Constantan
Lead	Copper, Nickel Clad
Insulation	Magnesium Oxide
Sheath	Inconel 600
Size	.109" dia. x 120 Long
Input	28 V DC
Power	
Heater Element	122 watts max.
Leads	96 watts max.
ION PUMP (2)	
Manufacturer	Varian Associates
Mfg. P/N (pump)	913-0008
Mfg. P/N (Magnet)	913-0011
Capacity	1 L/S
Input	3.5 KV DC
RUPTURE DISC	
Type	1" Reverse Buckling Rupture Disc
Manufacturer	Black, Sivalls & Bryson, Inc.
Mfg. P/N	77-BEN-025
Rupture Pressure	95± 13
THERMOSTAT (2)	
Manufacturer	Metals & Controls Inc.
Mfg. P/N	11041-117-1
I & LS Division P/N (modified)	1620511-1
Operating Temperature	
1) Energize	53°F
De-energize	82°F
2) Energize	51°F
De-energize	84°F
Contact Rating	4.0 amps DC

EXTERNAL COMPONENTS

PRESSURE SWITCH (2)

TABLE I (con't)

Type	Metal Diaphragm Sealed Case, SPDT
Manufacturer	Southwestern Industries Inc.
Mfg. P/N	PS-5906
Mfg. S/N	25241
Opening Pressure	883-887 psia
Closing Pressure	860-857 psia
Mfg. S/N	25240
Opening Pressure	881-884 psia
Closing Pressure	856-857 psia
RELIEF VALVE	
Type	Gauge Pressure
Manufacturer	Bendix I & LS Division
Mfg. P/N	FR-131
Port Configuration	MS33656-5 .312 dia. flared tube
Crack Pressure	1000 psi
Seal Pressure	980 psi
Leak Rate at Seal Pressure	4 cc/min
Proof Pressure	1240 psi
MANUAL VALVE (3)	
Type	Ball Valve
Manufacturer	James Bury
Mfg. P/N	1/4" HPO-36MT
Port Sizes	1/4" Internal ANPT
Valve Leakage (closed*)	0
Proof Pressure	2100 psi

* No measurable leakage across 1/2" dia. with leak-tak film.

2.1 Internal Instrumentation Package

All internal dewar components are mechanically attached and/or silver brazed to a thin wall tubular structure as depicted in figure C-1. The support structure consists of two similar tubes, each with an end plate for mounting the motor fan and connecting to the pressure vessel boss fitting. The tubes join together at the center of the structure by means of a slip joint as shown in figure C-2. Calrod type electrical heaters are silver brazed to the outer surface of the structure as shown in figure C-3. Metal sheathed electrical leads for the motor fan, temperature cutoff switches, capacitance probe and thermocouples are also silver brazed to the structure. Figure C-4 depicts the four lower motor fan leads, heater lead routing and temperature cutoff switch leads. Figures C-5 and C-6 show the thermocouple and electrical leads for one switch respectively.

The components that make up the instrumentation package are illustrated in figures C-7 through C-12. The dual cutoff switch housing and one switch is depicted in figure C-7. The capacitance type density measurement probe, shown in figures C-8 and C-9, is fabricated of three concentric stainless steel tubes supported by non-metallic spacers between the tubes that are mounted inside the support structure. Figure C-10 depicts a motor fan destratification unit. Each end of the support tube is attached to a closure fitting as illustrated in figure C-11. This fitting is comprised of three different parts that are manually welded together utilizing TIG welding. Figure C-12 illustrates the closure fitting.

Figures C-13 through C-16 depict the various components installed in the support structure. The motor fan installed inside the support structure and the method used to secure the capacitor within the structure is shown in figure C-14. Figure C-15 illustrates the sheathed lead to component electrical connection for the motor fan and temperature cutoff switch. A closure fitting, assembled to the support structure and electrical leads, is shown in figure C-16. The manner in which the electrical leads are installed is depicted in figure C-17. Figures C-18 and C-19 illustrate the brazing of the electrical leads to the closure fitting.

Following assembly, cleaning and electrical checkout, the instrumentation package is installed within the

pressure vessel through a 2.025 diameter opening in the pressure vessel boss fitting as shown in figures C-20 and C-21. Welding the package into the vessel is detailed in the pressure vessel assembly discussion.

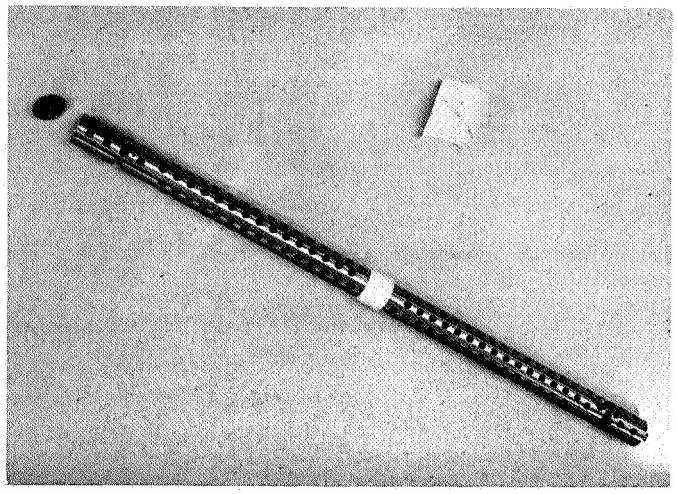

Figure C–1

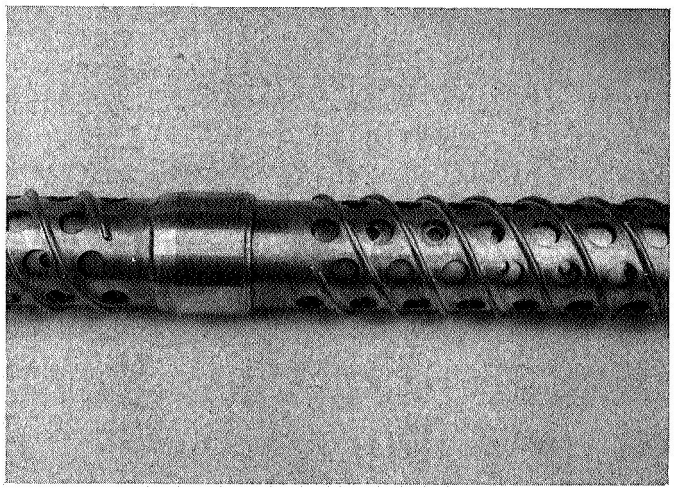

Figure C–2

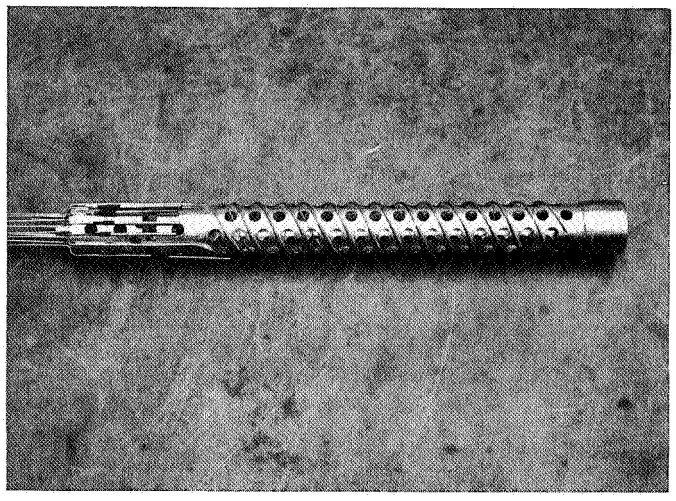

Figure C–3

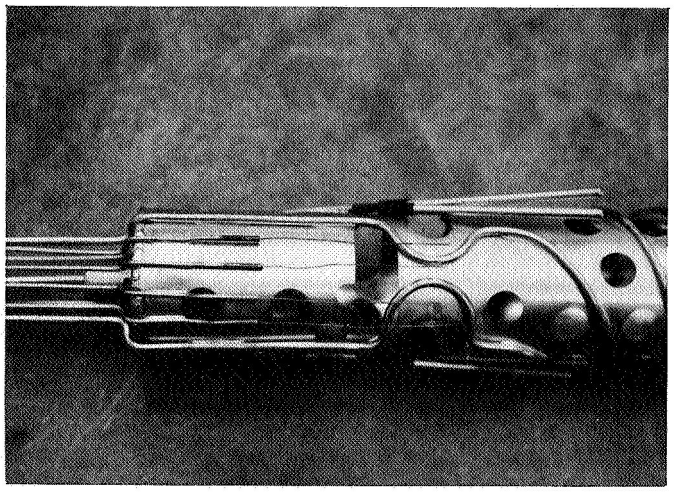

Figure C–4

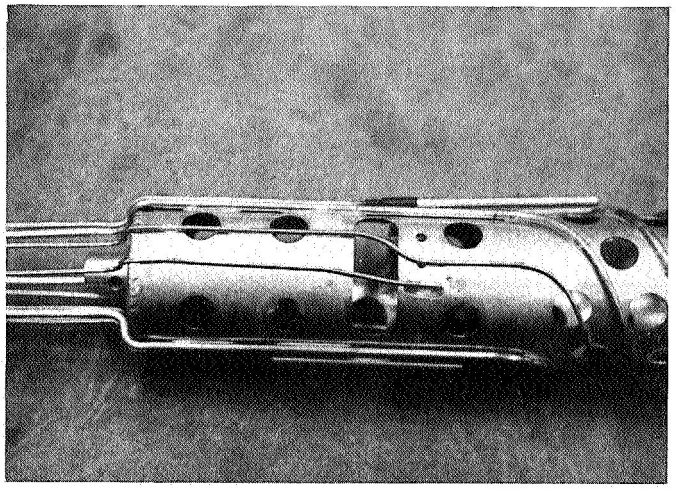

Figure C–5

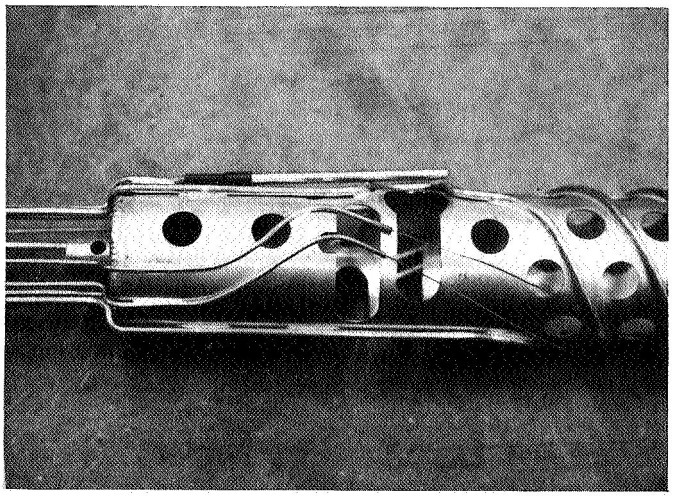

Figure C–6

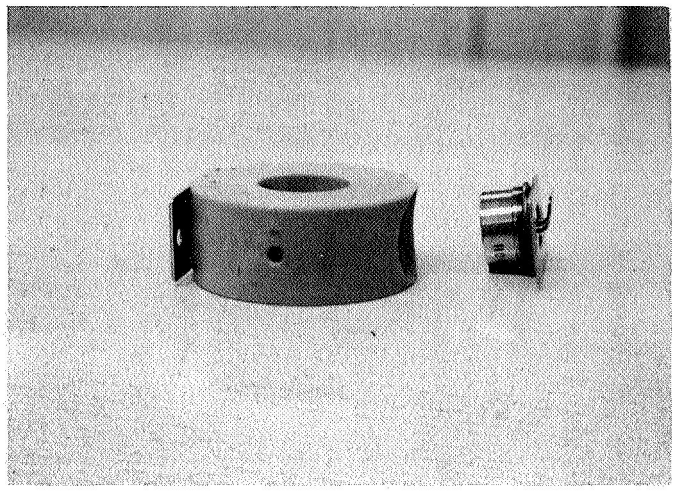

Figure C–7

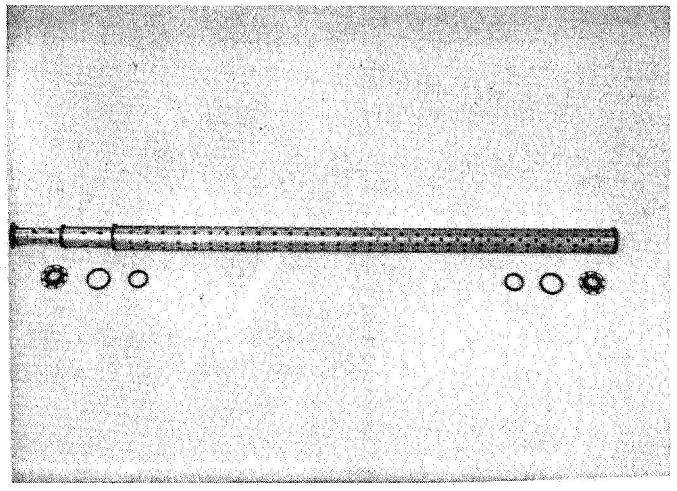

Figure C–8

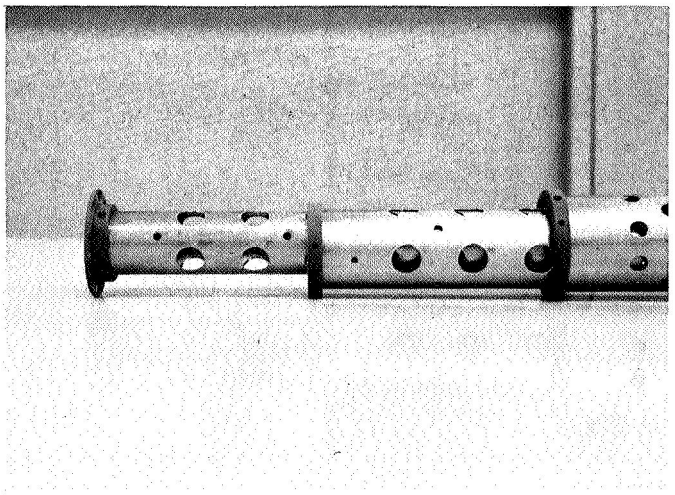

Figure C–9

Figure C–10

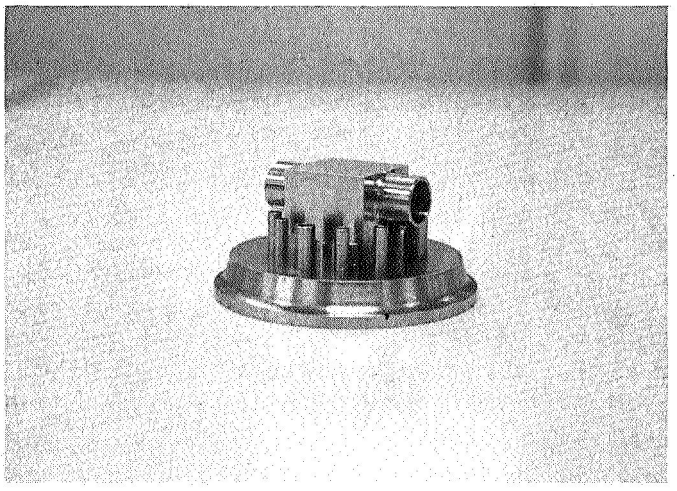

Figure C–11

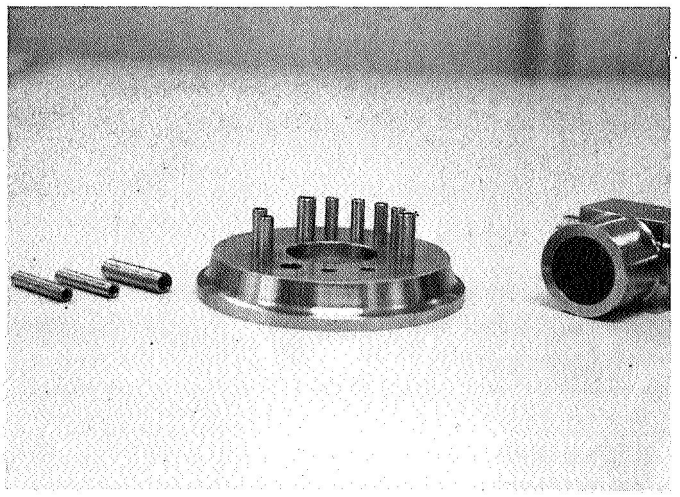

Figure C–12

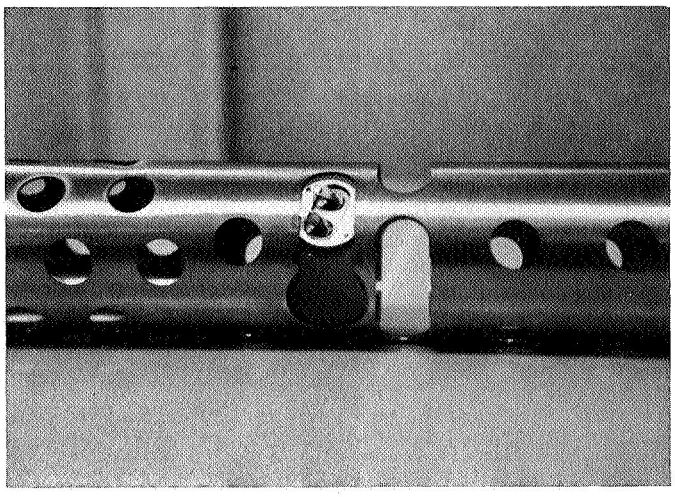

Figure C–13

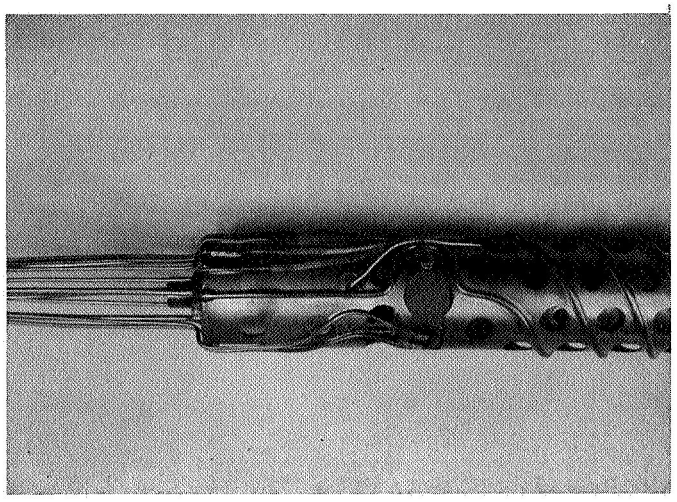

Figure C–15

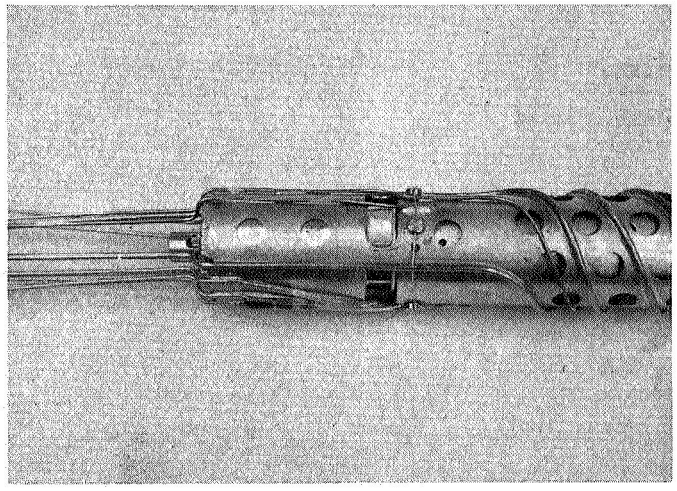

Figure C–14

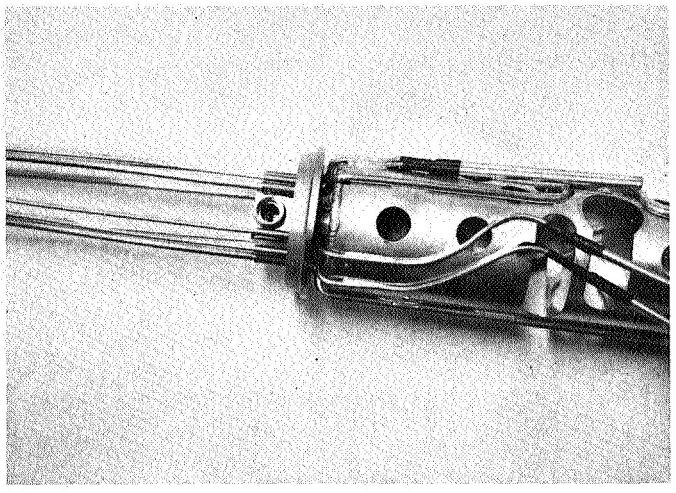

Figure C–16

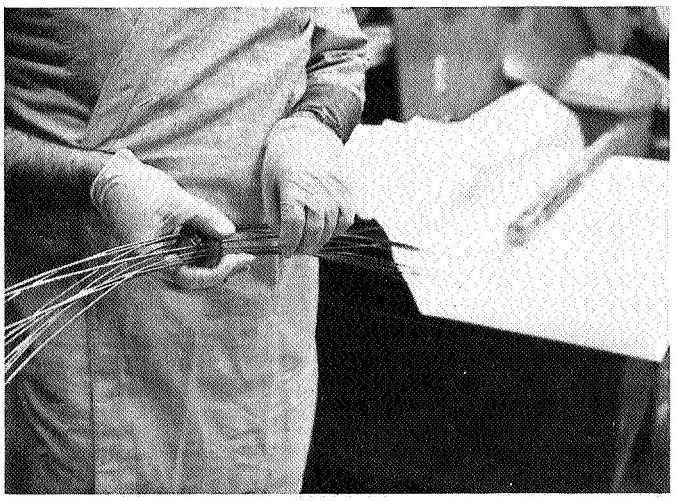

Figure C–17

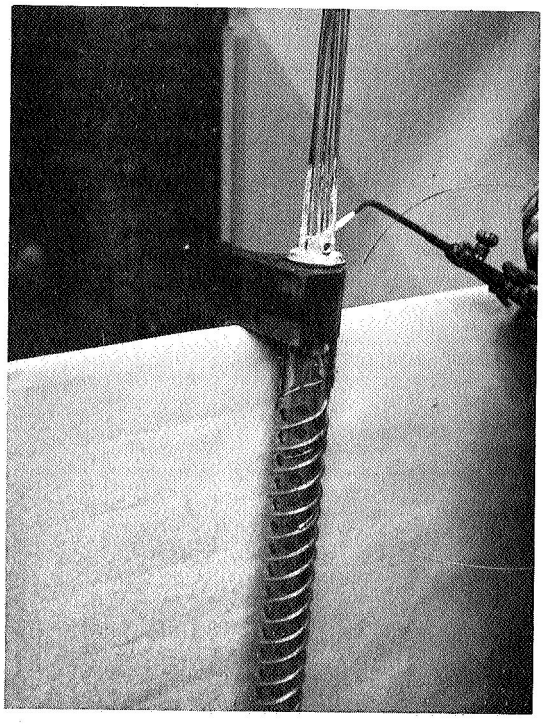

Figure C–18

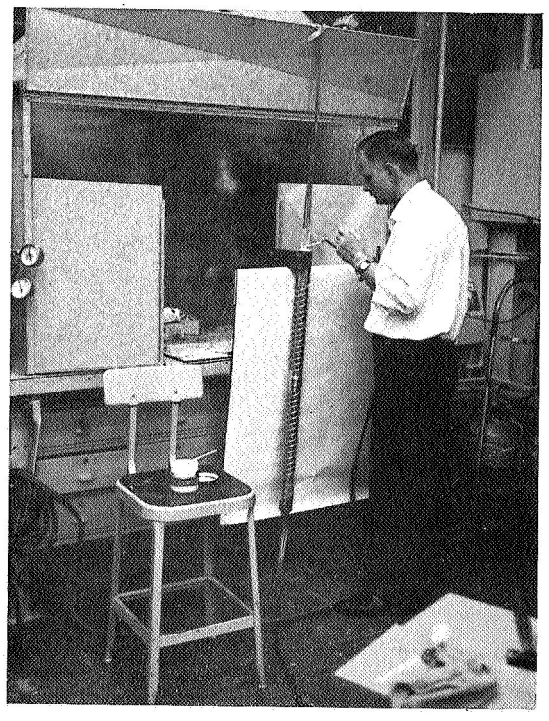

Figure C–19

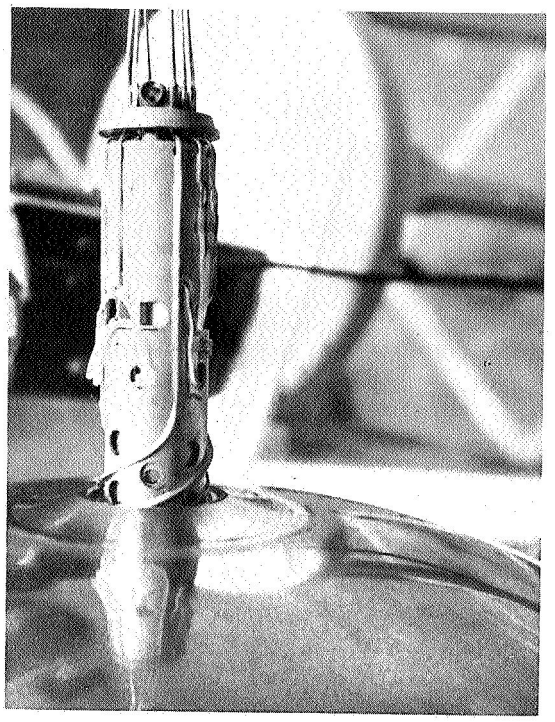

Figure C–20

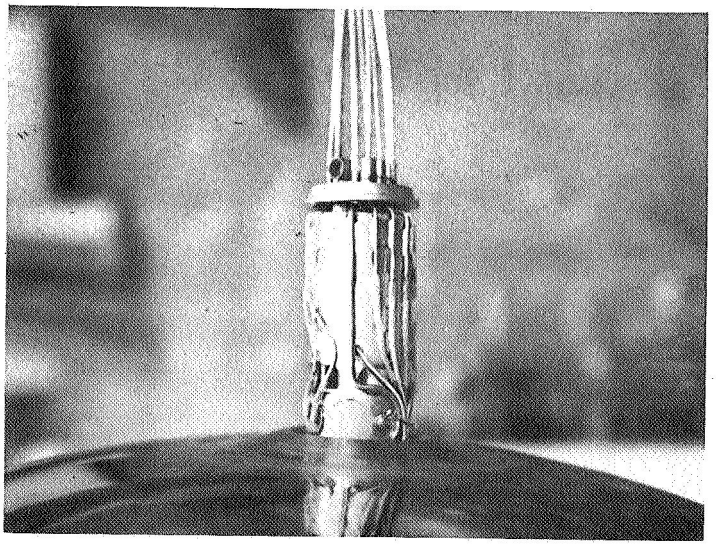

Figure C–21

2.2 Pressure Vessel Assembly

The hemispheres for the pressure vessel were formed from Inconel 718 by the inturgescent forming process. After the hemispheres were formed, they were given a thorough inspection to detect any minor imperfections, a vidigage inspection to determine shell thickness as shown in figure C-22 and a complete check for height and diameter. After the hemispheres were inspected and found to be satisfactory they were ready for the milling operation. The flange was trimmed off and holes machined for the boss fitting as illustrated in figures C-23 and C-24. To insure a flat edge for welding the girth area was ground as depicted in figure C-25. After the above tasks were performed the two hemispheres were again dimensionally checked.

The hemispheres were cleaned with trichloroethylene, an electrocleaner bath, rinsed with water and finally rinsed with methyl alcohol prior to the welding operation. The boss fittings which had been machined from Inconel 718 forgings were welded into the hemispheres as depicted in figure C-26. The girth weld was then made. All welding was by the cold wire TIG automatic process using slight positive argon backup pressure. All weld areas were checked with a dye penetrant, 100% x-ray inspection and finally a dimensional check. The dimensional check indicated that the vessel had shrunk both pole to pole and around the girth slightly during welding. This situation was improved by hydrostatically pressurizing the vessel with water.

The next step in manufacture of the pressure vessel was to polish the outer surface with a belt sander and buffer wheel. Figure C-27 illustrates the polishing.

The pressure vessel was now ready for age hardening. In order to minimize oxidation of the outer surface during the aging process, the shell was thoroughly cleaned with trichloroethylene, electrocleaned, rinsed with water, rinsed with methyl alcohol and then sprayed with a coating of Turco Pre-Treat.

In order to prevent oxidation on the interior of the vessel, it was purged with argon for several hours prior to heating and then purged continually during the heat cycle until the vessel was back to approximately room temperature. The aging operation was carried out in a radiant heat tube, pit type, gas fired furnace. The vessel is shown in this furnace prior to start of

the heat cycle in figure C-28. Thermocouples were attached to the vessel top and bottom in order to monitor the temperature during the aging cycle.

To remove the slight amount of scale that formed during the aging cycle, the pressure vessel was next pickled in a bath containing vitric, hydrofluoric and hydrochloric acids and rinsed in water.

The next step was to hydrostatically proof pressure test the vessel to 1530 psi as illustrated in figure C-29. The exterior of the vessel was then brightened by polishing with the belt sander and buffing wheel. The interior of the vessel was brightened by tumbling with polishing stones (figure C-30). The weld area of the boss fittings was polished with Scotch Brite. The entire vessel was again electrocleaned, rinsed with water and alcohol, and the weld areas wiped with acetone. The pressure vessel was ready for insertion of the instrument package at this point (figure C-31 and C-32). After inserting the instrument package, the vessel was evacuated and backfilled with argon several times and then purged with argon for several hours prior to welding. The welding of the instrument package into the pressure vessel is shown in figure C-33. A moist cloth was placed on the pressure vessel near the closure fitting to help prevent heat buildup during the welding.

The electrical leads were next formed into an electrical pigtail (figure C-34), and the fluid pigtails were brazed into a closure fitting. At this point the pressure vessel assembly including fluid pigtails was hydrostatically proof tested to 1530 psi, using Ucon fluid. The exterior of the pressure vessel was cleaned with solvents using benzene, trichloroethylene and acetone. After cleaning, the pressure vessel was placed in a plastic bag for shipment to the vapor plater.

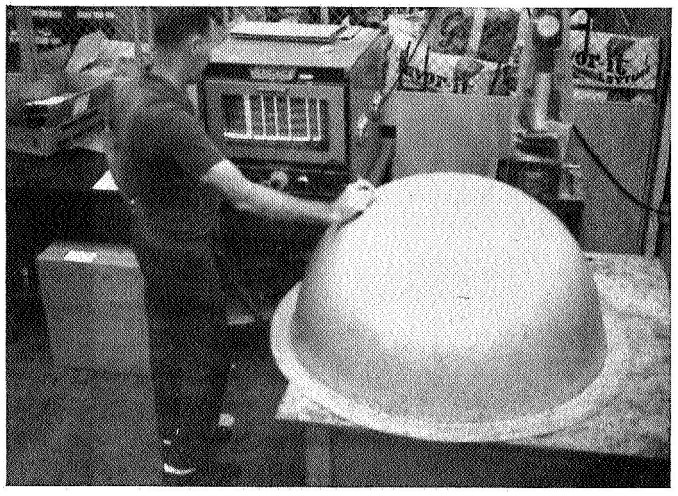

Figure C–22

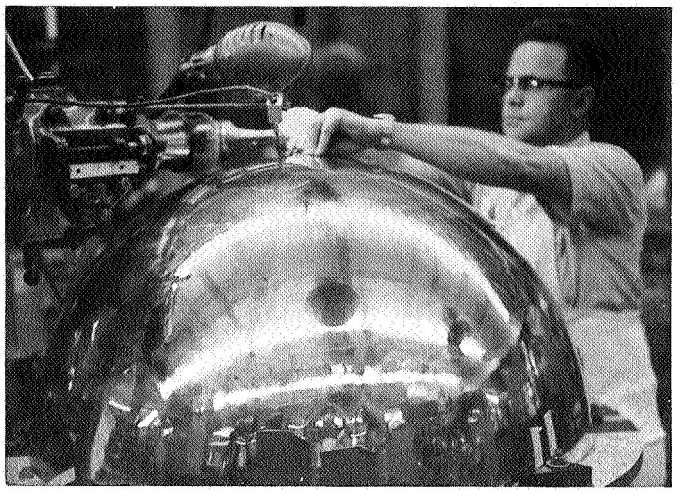

Figure C–24

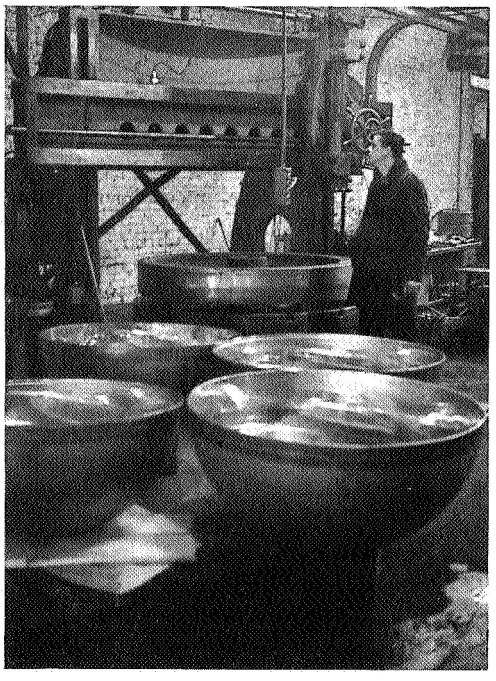

Figure C–23

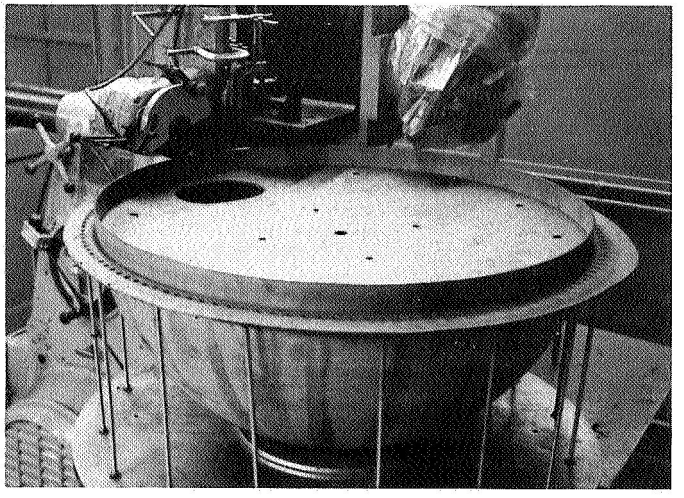

Figure C–25

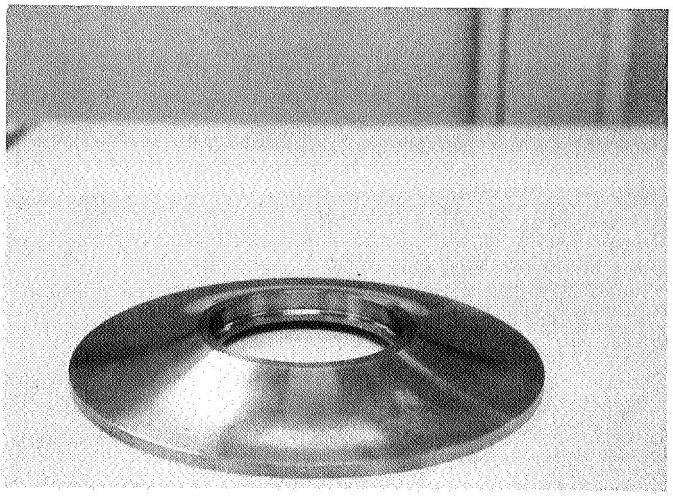

Figure C–26

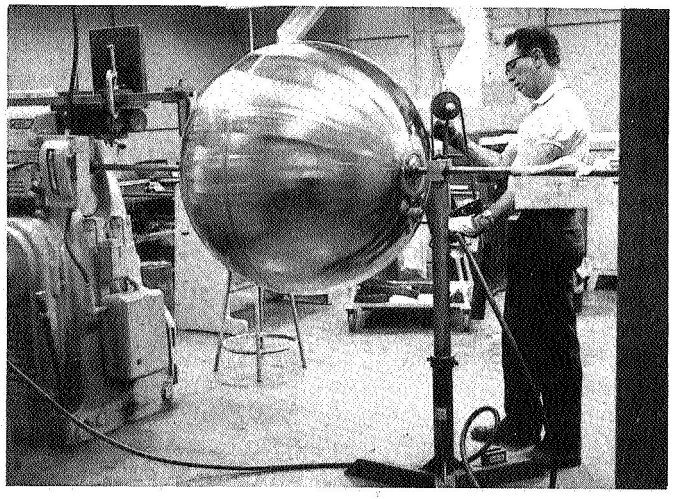

Figure C–27

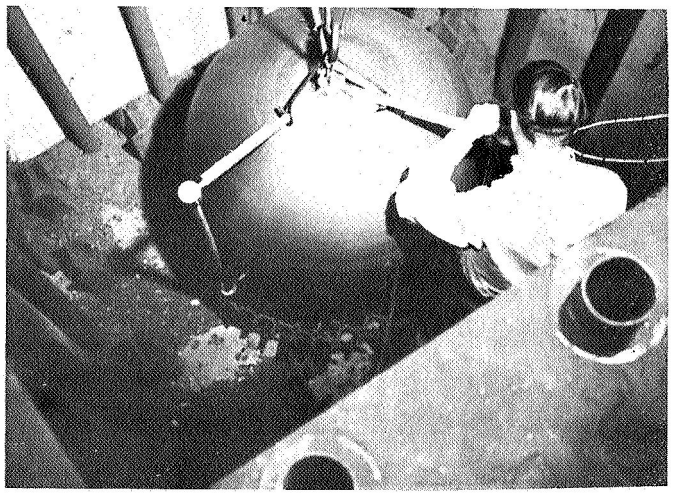

Figure C–28

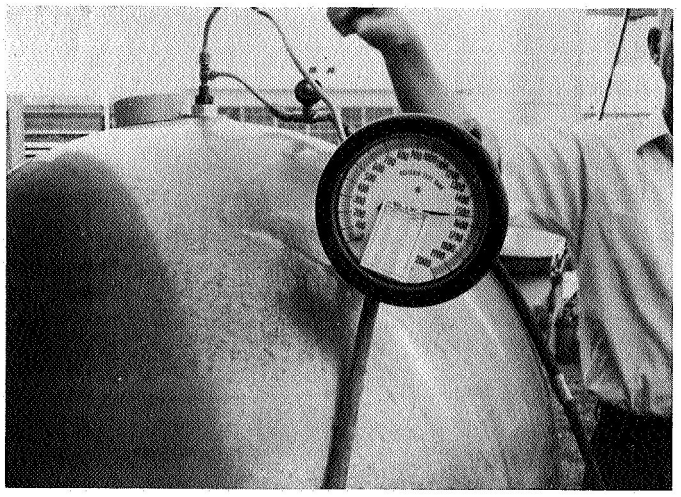

Figure C–29

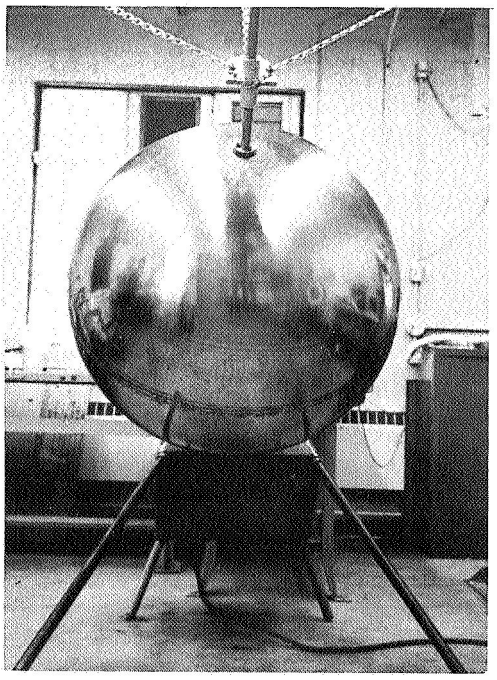

Figure C–30

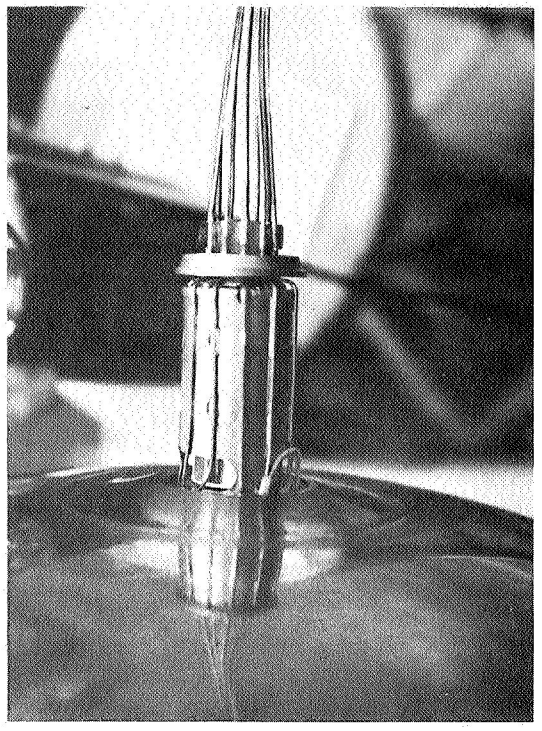

Figure C–31

Figure C–33

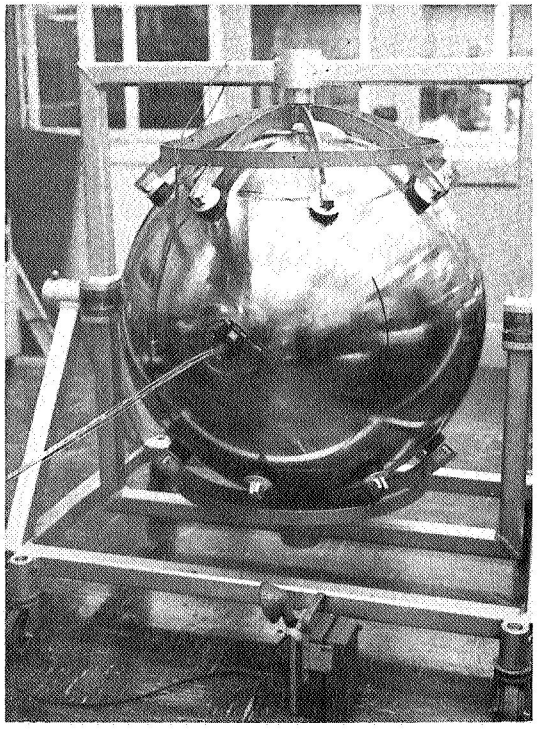

Figure C–32

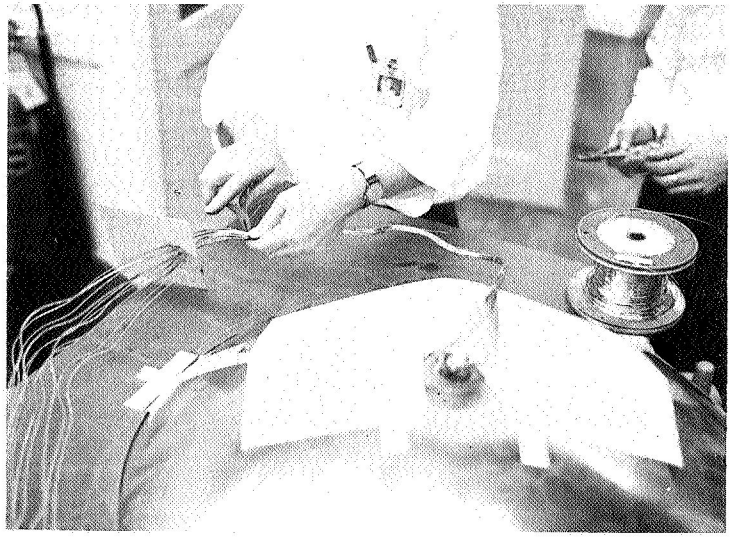

Figure C–34

2.3 Radiation Shield Assembly

The radiation shields were all formed from 6061 aluminum by the Bendix inturgescent process. After the hemispheres were formed, they were thoroughly inspected including a vidigage inspection to determine shell thickness and a dimensional check for height and diameter (figure C-35). After inspection the holding flanges were trimmed and eight hemispherical bumps at the bumper locations were formed in each of the hemispheres. These bumps were formed by a hydraulic press as shown in figures C-36 and C-37. The hemispheres were then checked to determine that the bumps were located properly. The holes for the bumpers, fluid tubes, etc. were then machined (figure C-38). Next, the double strip was attached to the girth of the bottom hemisphere of each shield pair. The shields were then fitted together (figure C-39) and the shield latch hold location was transferred from the upper shield to the doubler band. The four shield hemispheres along with the two outer shell hemispheres are shown in figure C-40. From this point on, the treatment of the inner shield differs from the outer shield. The outer shields were etch cleaned (figure C-41) and placed in a plastic bag and were ready for shipment to the vapor plater; however, the inner shields were next copper plated by electrodeposition so that the vapor cool line could be soldered to the inner surface. The vapor cool line is shown attached in figure C-42. (This photograph was taken after vapor plating.) After the vapor cool line was attached, the flux was removed by hot trichloro-ethylene vapors and a methyl alcohol rinse. The vapor cool line was then hydrostatically proof pressure tested to 1530 psig with Ucon. The shield was again cleaned with methyl alcohol and placed in plastic bag for shipment to the vapor plater.

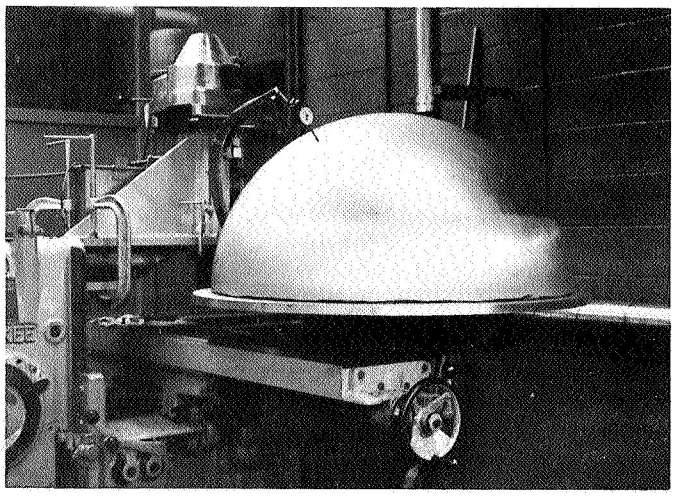

Figure C–35

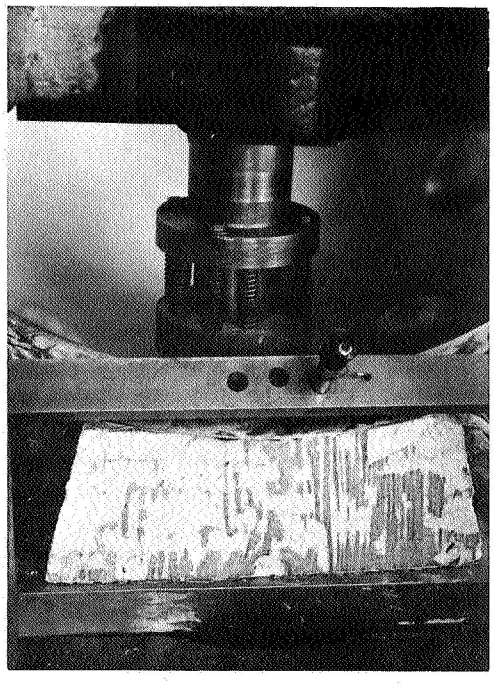

Figure C–37

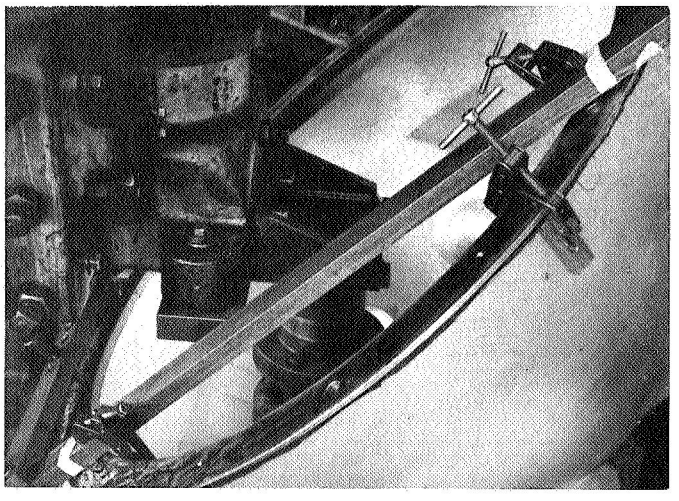

Figure C–36

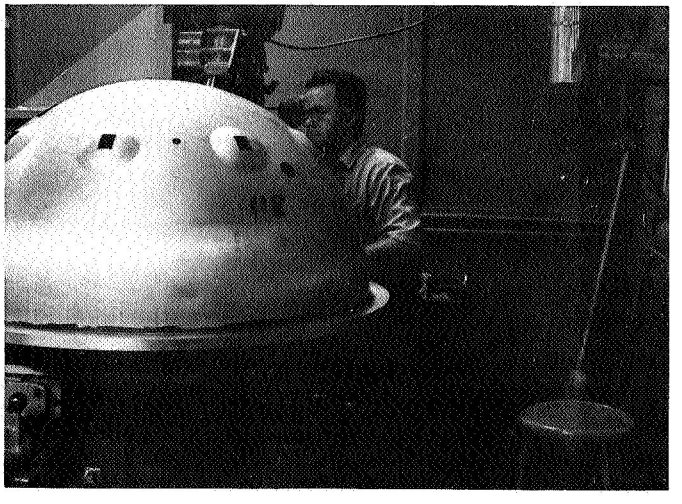

Figure C–38

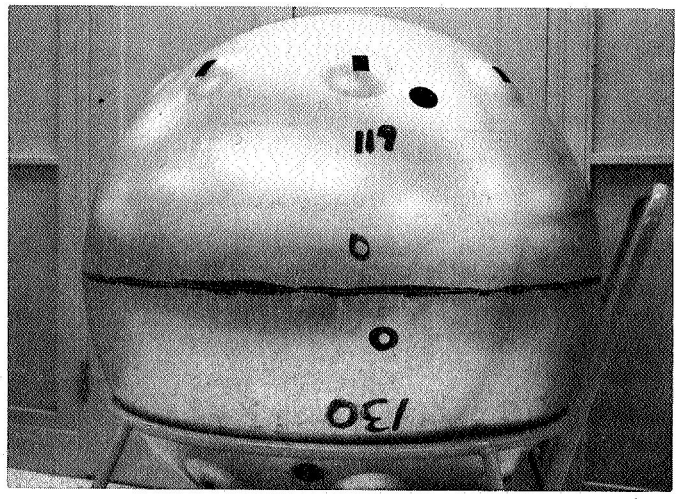

Figure C–39

Figure C–40

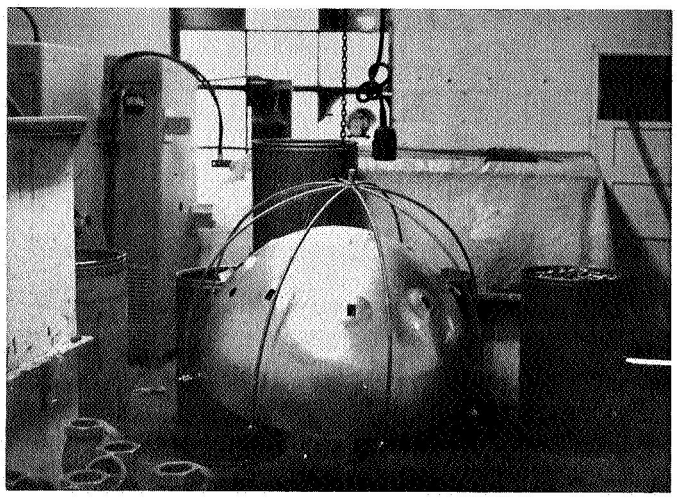

Figure C–41

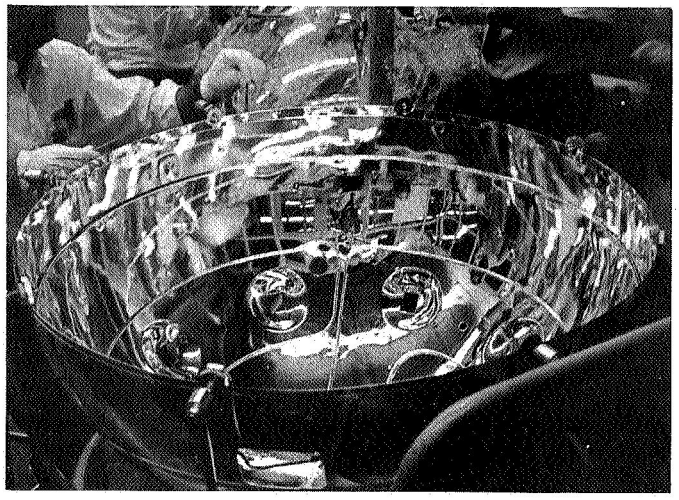

Figure C–42

2.4 Outer Shell Assembly

The outer shell hemispheres were manufactured from 6061 aluminum by the Bendix inturgescent forming process. The shells were thoroughly inspected including a vidigage to determine shell thickness and a dimension check for height and diameter. After checking, the hold flange was machined from the two hemispheres. The bottom hemisphere then received an offset lip and became the female half of the set; the upper or male half also received a slight offset to give a good fit to the female half. Both halves of the outer shell were then "bumpered" in the same manner as discussed under radiation shields. After the bumps were formed, the shells were placed in an oven on a vacuum table as shown in figures C-43 and C-44. They were evacuated and the temperature raised to 300° F. to insure against buckling during the bakeout period. Next, the holes for the rupture disc, tip-off, electrical, and fluid lines were machined into the shells. A practice machining is shown in figure C-45. When all of the holes had been machined in the burst disc, pump bracket, and ion pump, tip-off transitions were welded into the top outer hemisphere. Figure C-46 shows the location of these items, while a closeup of the pump bracket and ion pump (manufactured by Varian) is shown in figure C-47, and a closeup of the burst disc (manufactured by Black, Sivalls, & Bryson) from the inside of the outer shell is shown in figure C-48.

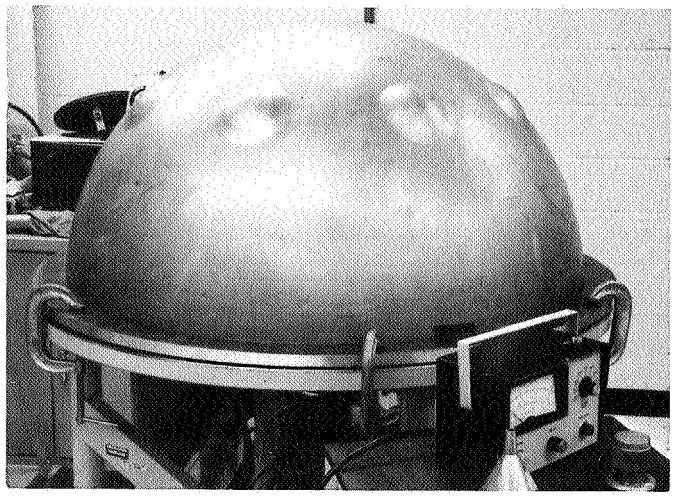

Figure C–43

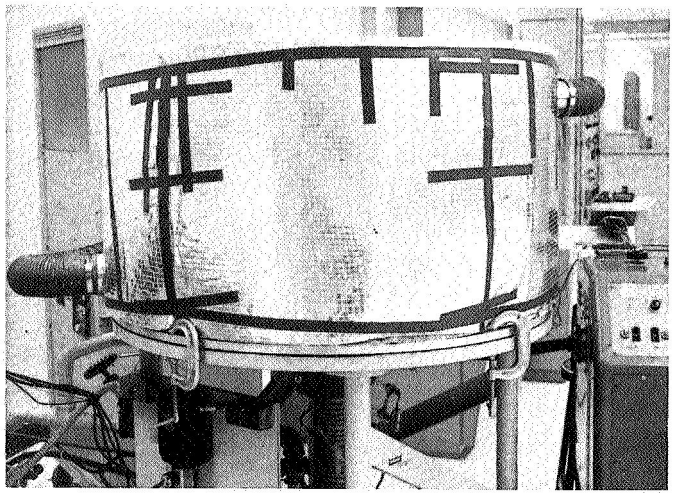

Figure C–44

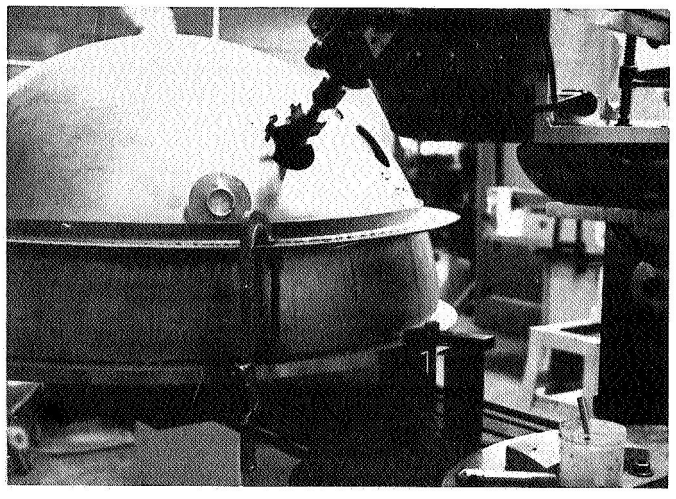

Figure C–45

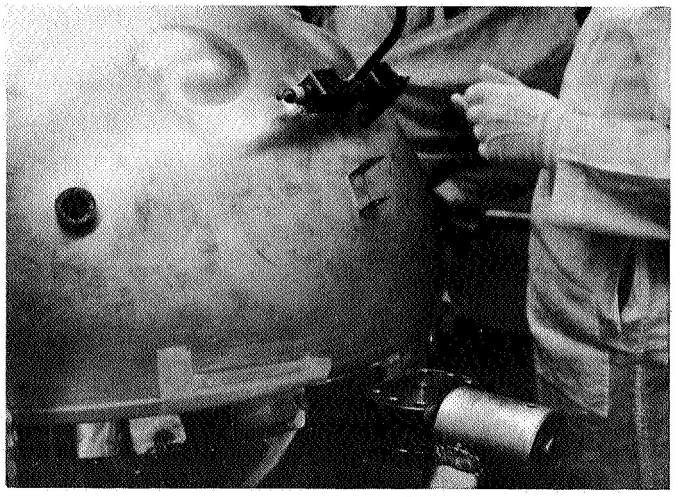

Figure C–46

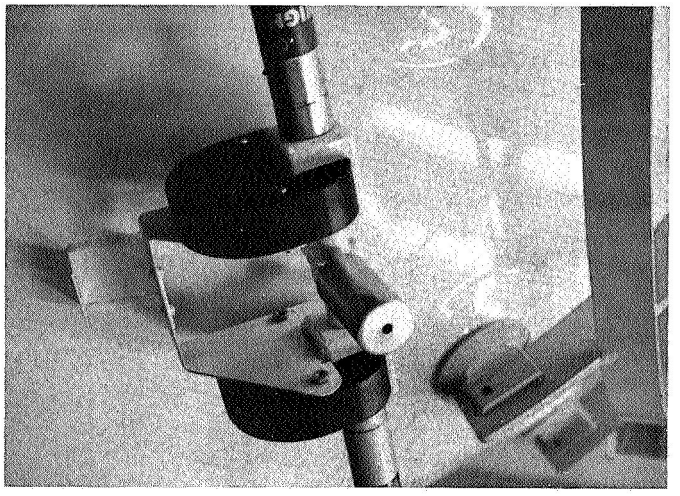

Figure C–47

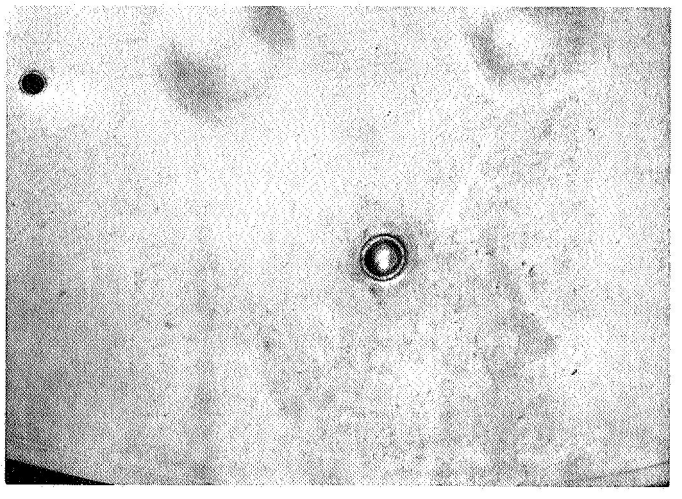

Figure C–48

2.5 Vapor Plating and Dewar Assembly

After all dewar subassemblies had been completed, the radiation shields, outer shells, and pressure vessel were shipped to Vacuum Metalizing, Van Nuys, California for application of the vapor plate. The radiation shields and the outer surface of the pressure vessel were plated inside and out with silver over an epoxy substrate. The inner surface of the outer shell was coated with epoxy and then copper plated.

The first step in preparing for assembly after the parts were returned was to remove the masking from areas that were not to be plated such as the bumpers and pigtails (figure C-49). Next, the stress pads were put in place and the bumper locators bent against the bumpers as shown in figure C-50. The inner shields were then put in place, the vapor cool line connections brazed, and the connections helium leak checked (figures C-51, C-52, and C-53). After the unit was leak checked, the outer shield and outer shells were installed (figure C-54). Welding of the girth of the outer shells was the next step (figure C-55) and then the electrical fittings and fluid fittings were welded into the outer shell (figure C-56). The vessel was again helium leak checked which made it ready for the evacuation-bakeout step.

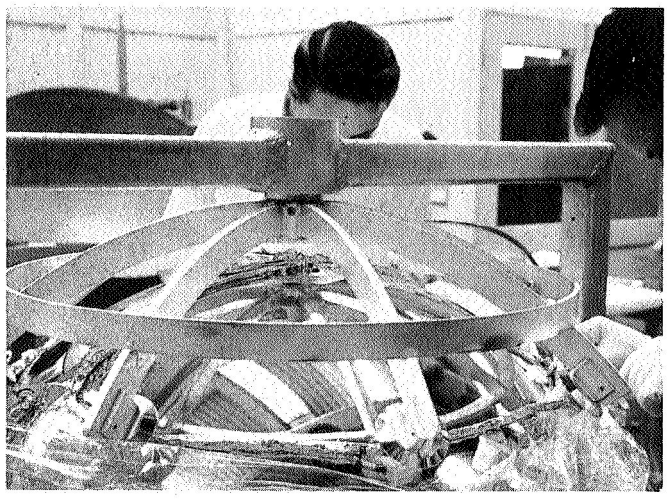

Figure C–49

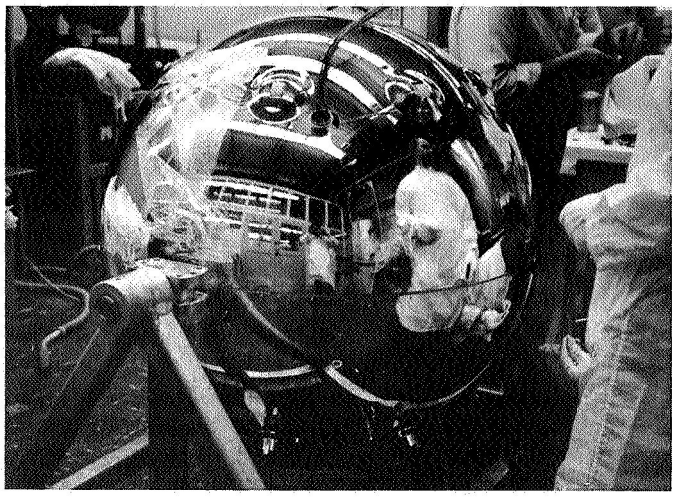

Figure C–51

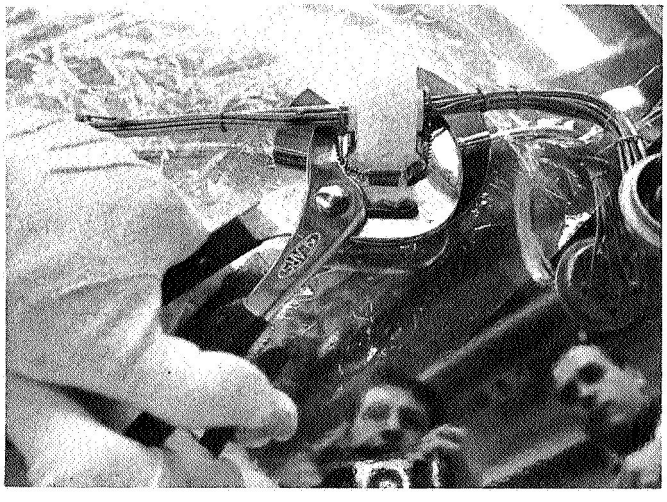

Figure C–50

Figure C–52

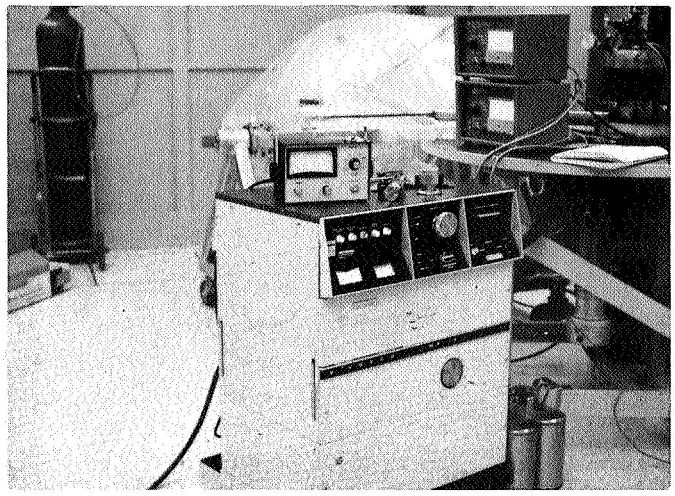

Figure C–53

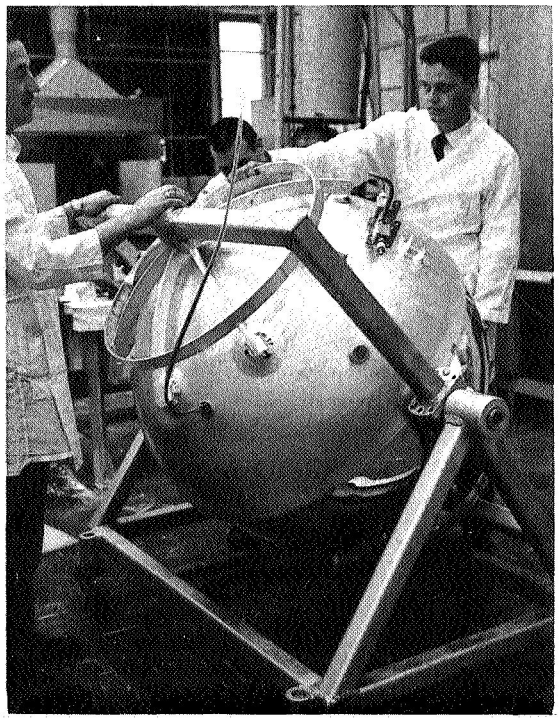

Figure C–54

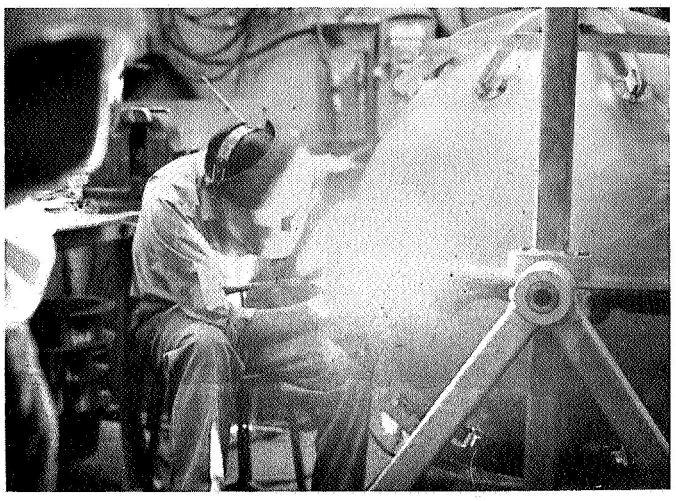

Figure C–55

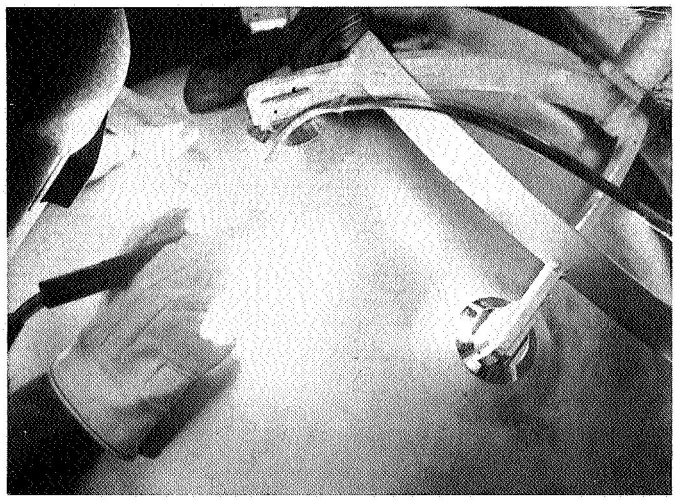

Figure C–56

2.6 External Hardware

All external hardware except for the ion pumps and the rupture disc was mounted on an aluminum panel attached to the assembly cart. The location of the panel on the bottle is shown in figure C-57, and the location of the various components on the panel is shown in figure C-58. The valves used for fill, vent, and vapor cool vent are Jamesbury ball valves (figure C-59). Two pressure switches manufactured by Southwestern Industries were mounted on the panel (figure C-60). A relief valve manufactured by The Bendix Corporation was used and is shown in figure C-61. The electrical leads excited from the outer shell as shown in figure C-62 were brought to terminal blocks (figure C-63). They were then mounted to the back side of the aluminum mounting panel. From the terminal blocks, wires were brought to the elctrical plugs as shown in figure C-64. Figure C-65 shows the quantity signal conditioner manufactured by Bendix. A system pressure gauge was mounted at the top of the panel (figure C-66). To control the operation of the heaters, fans, pressure switches, thermal cutoff switches, and to provide quantity readout, a control panel was supplied which is shown in figures C-67 and C-68.

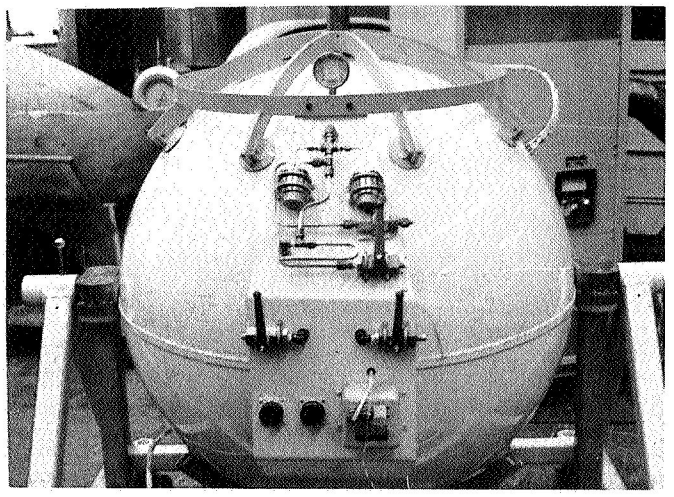

Figure C–57

Figure C–59

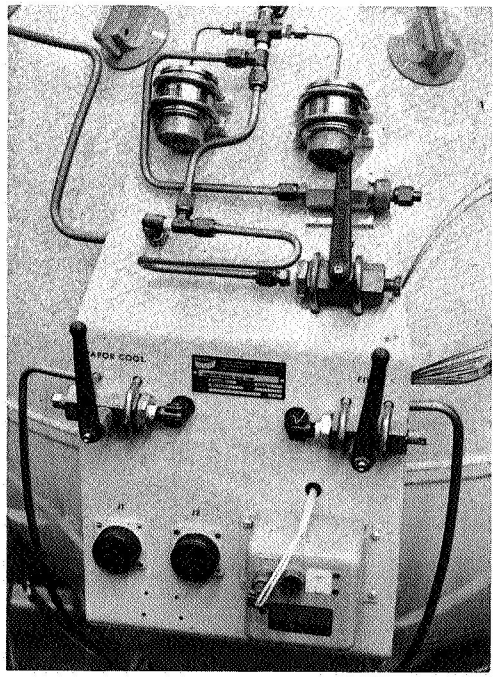

Figure C–58

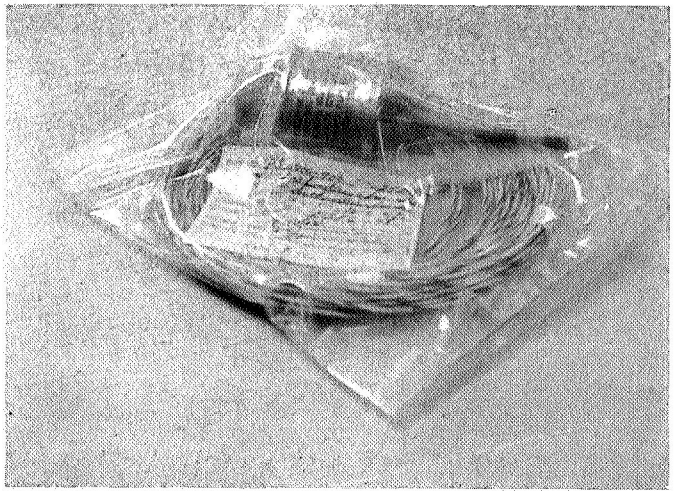

Figure C–60

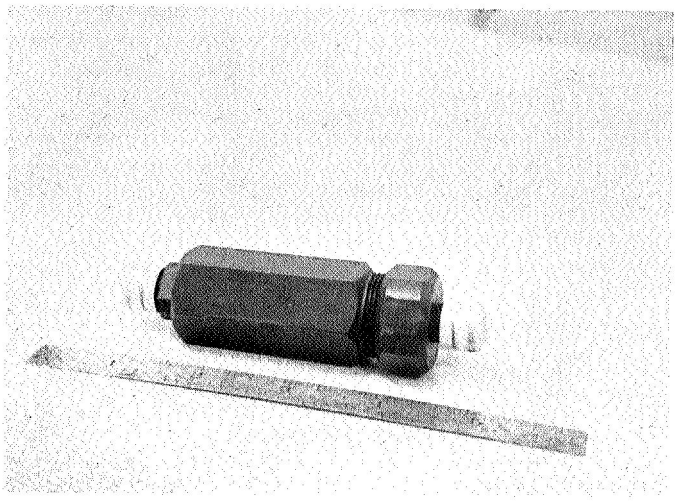

Figure C–61

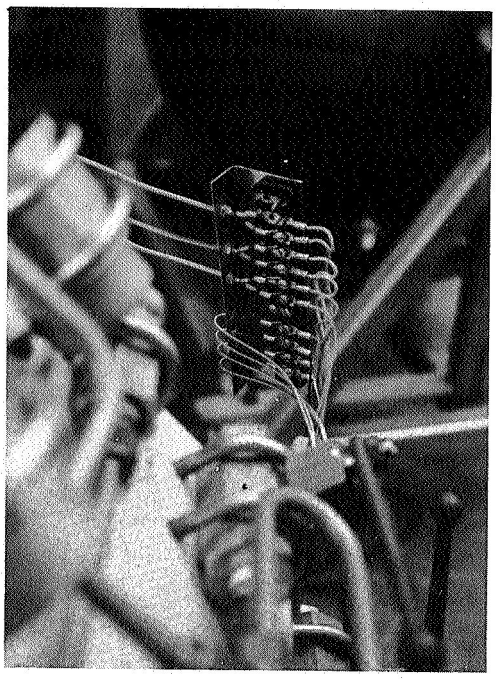

Figure C–63

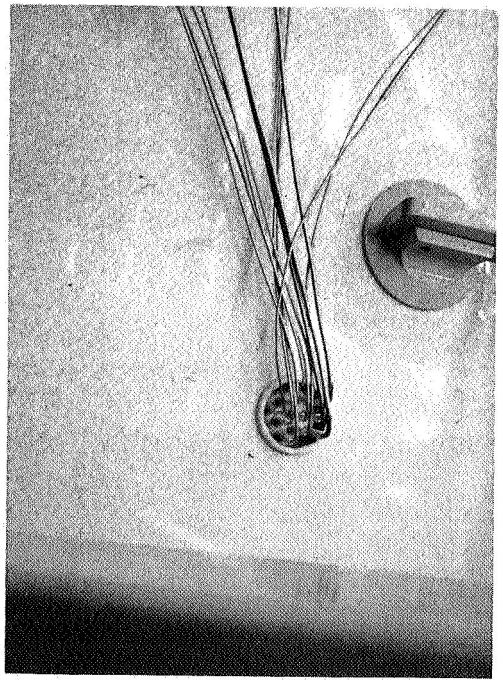

Figure C–62

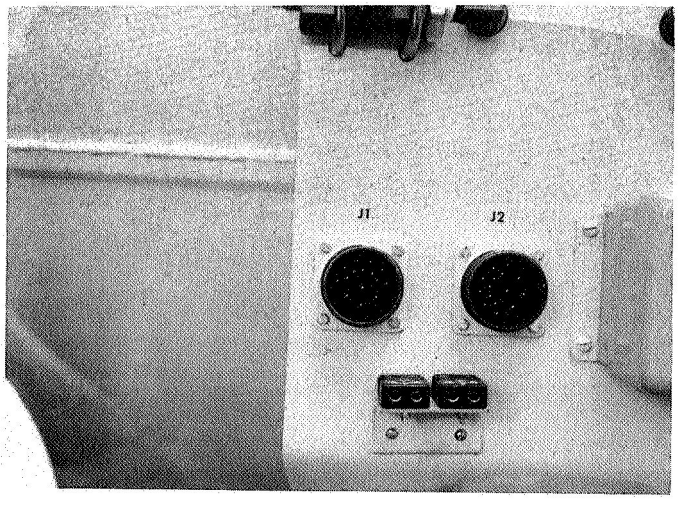

Figure C–64

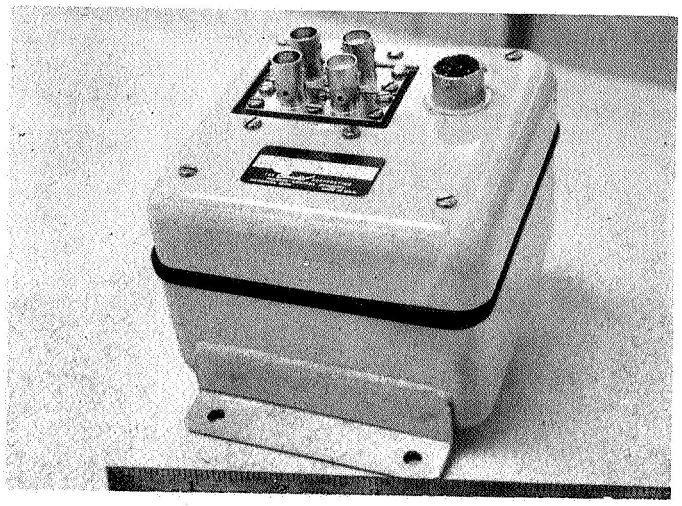

Figure C–65

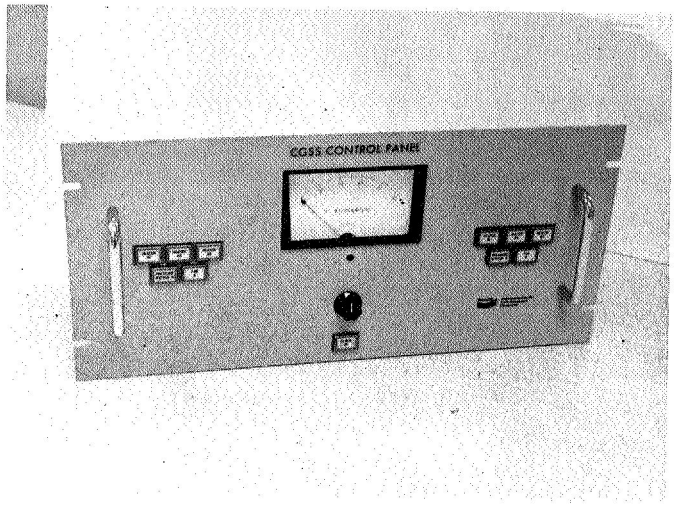

Figure C–67

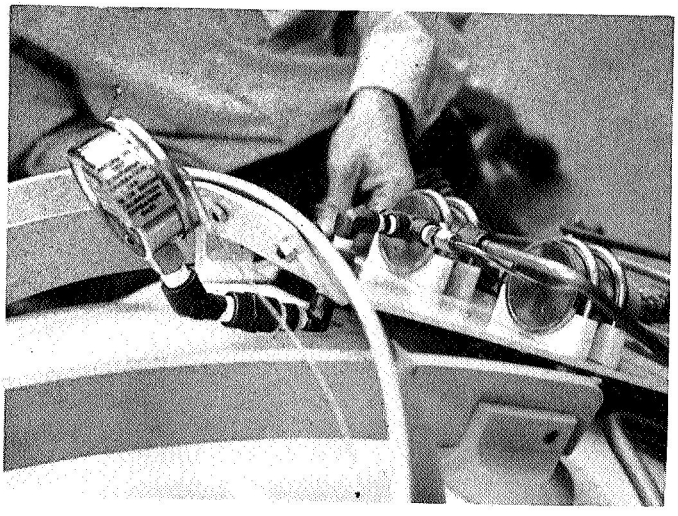

Figure C–66

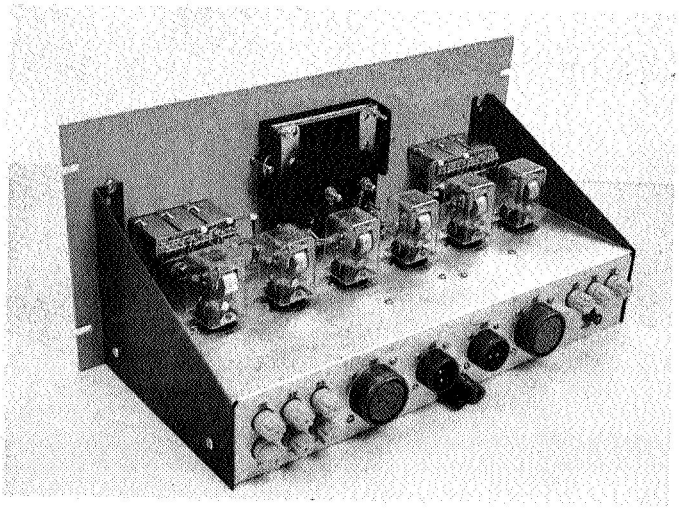

Figure C–68

2.7 Transport, Handling and Process Equipment

A number of different handling and processing fixtures were manufactured to facilitate buildup of the dewar. Some of these are shown in figure C-40 and figures C-69 thru C-80. Figures C-40 and C-69 illustrate three different types of transport and handling carts used. The carts in figure C-40 have a hand-carrying ring; carts in the foreground are made for carrying a single hemisphere or a pressure vessel sphere while carts in the background are designed to carry or store two hemispheres. Figure C-69 shows a cart and pressure vessel, the cart is similar to the single carts in Figure C-40, but doesn't have the separate carrying handle. Figures C-70 through C-72 illustrates the assembly and handling cart that was used throughout construction of the dewar. This cart was used for assembly as shown in figure C-71, welding as shown in figure C-72, rotating of the pressure vessel during vapor plating, as a support structure during proof testing and for rotating the dewar during the final cleaning with Ucon. Figure C-73 illustrates the tooling used for polishing the pressure vessel. Figures C-74 and C-75 show the heat treat support fixture and the electroclean and pickling fixture. The fixture used for holding and rotating the shields during vapor plating is depicted in figures C-75 and C-77. A similar fixture but with handles was used for electroplating the inner shields. Figures C-78 and C-79 show the simple fixtures made for forming the electrical leads and keeping them in proper orientation during forming. Figure C-80 illustrates the modified channel lock pliers used for banding the bumper retainers against the bumper.

Figure C–69

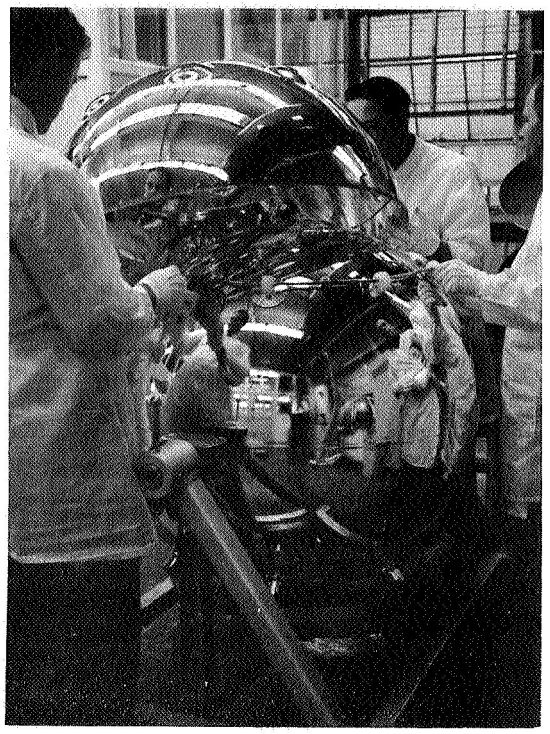

Figure C–71

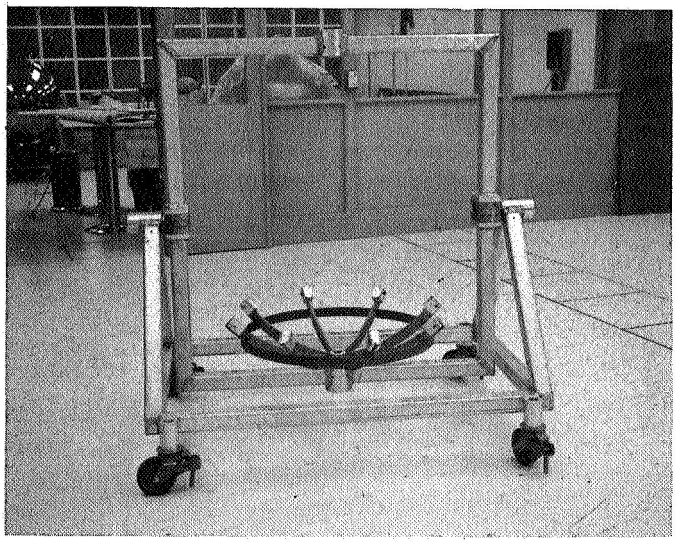

Figure C–70

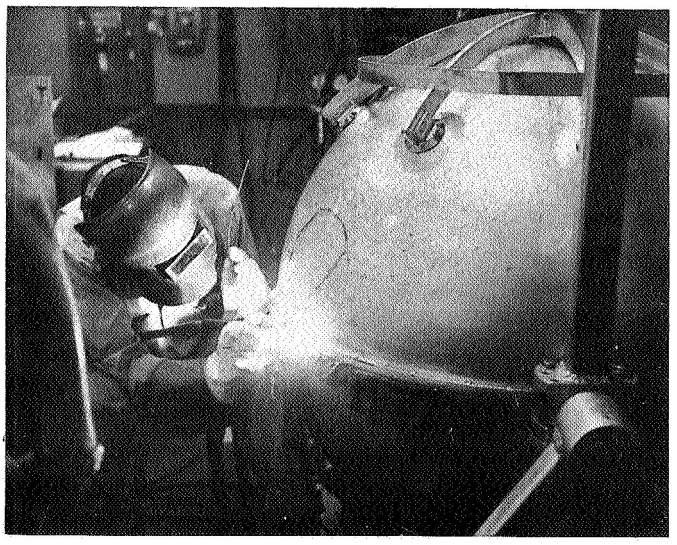

Figure C–72

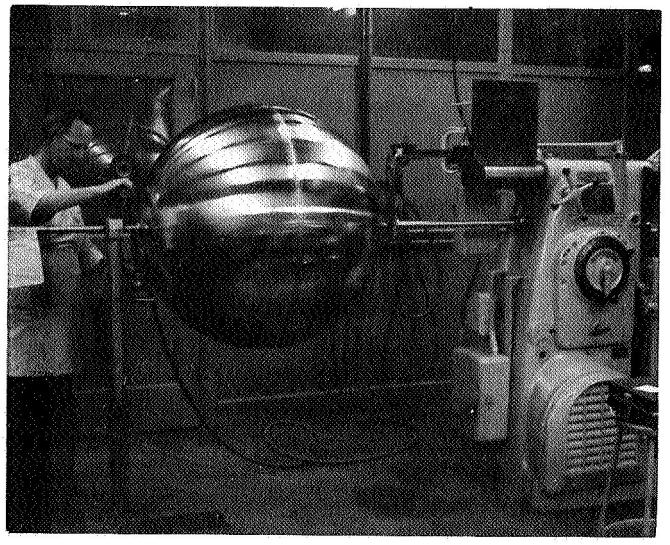

Figure C–73

Figure C–75

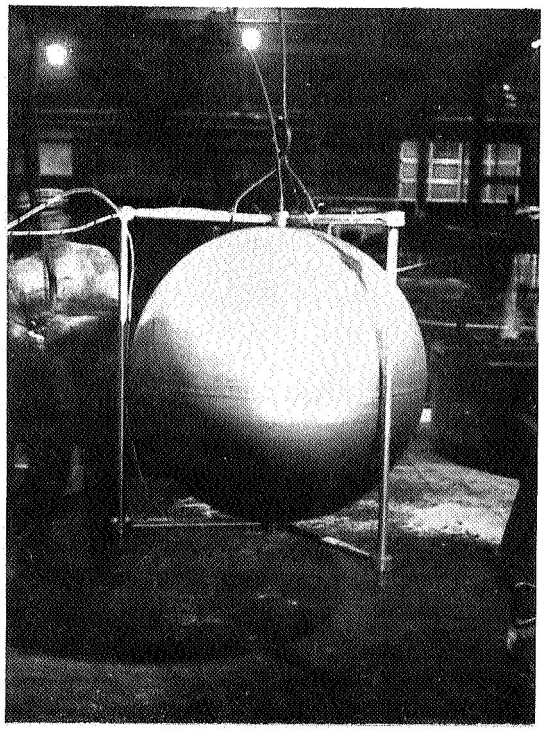

Figure C–74

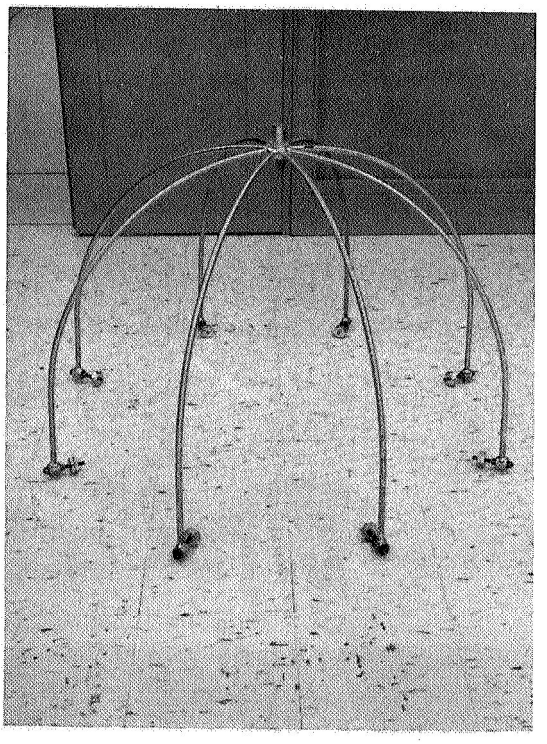

Figure C–76

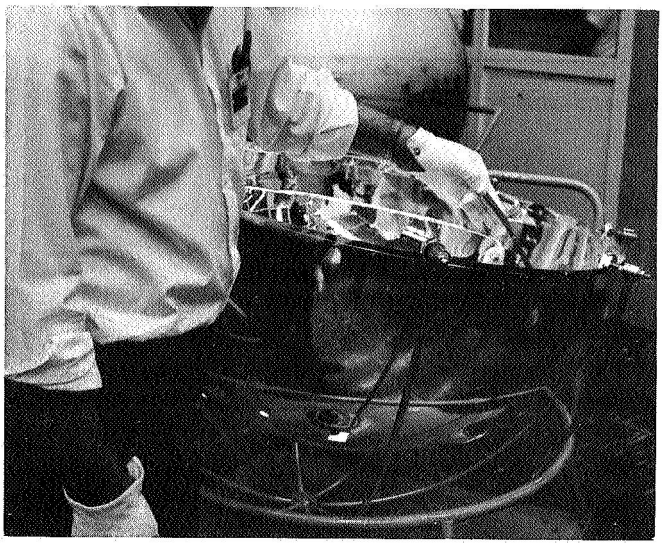

Figure C–77

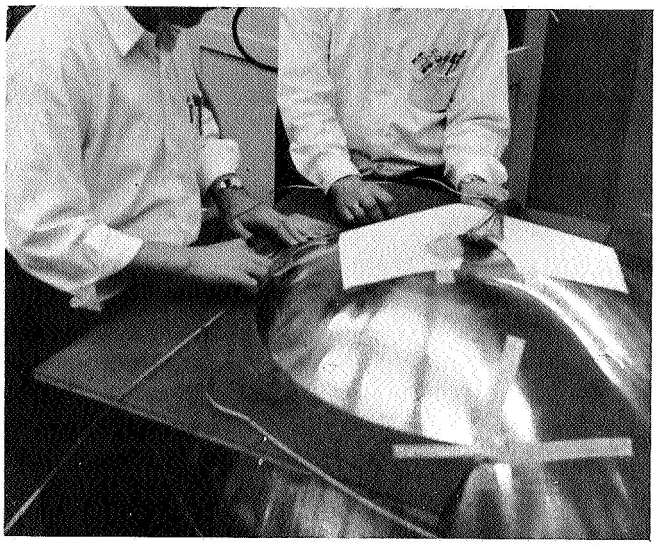

Figure C–79

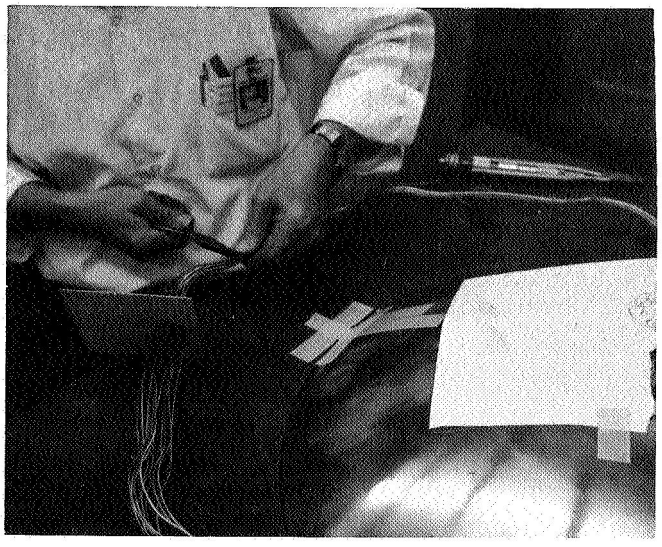

Figure C–78

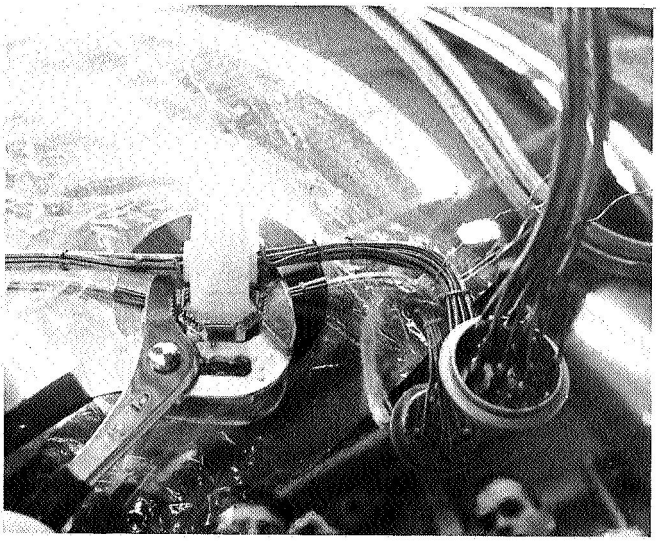

Figure C–80

2.8 Evaucation and Bakeout

The dewar was baked out during evaucation in the oven as shown in figure C-81. Pressure during evacuation was measured with a Veeco Ionization Gauge. Temperature was measured with four thermocouples attached to the girth of vessel and two thermocouples attached at the poles. The pressure in the vacuum space of the bottle was checked near the end of the evacuation period by means of the ion pumps. A mechanical vacuum pump and oil diffusion pump with liquid nitrogen cryo pumping the last few hours was used for evacuation. A close-up view of the evacuation tube and ion pump is illustrated in figure C-82. Figure C-83 depicts the dewar being filled with liquid nitrogen for a vented heat leak test immediately after tip-off.

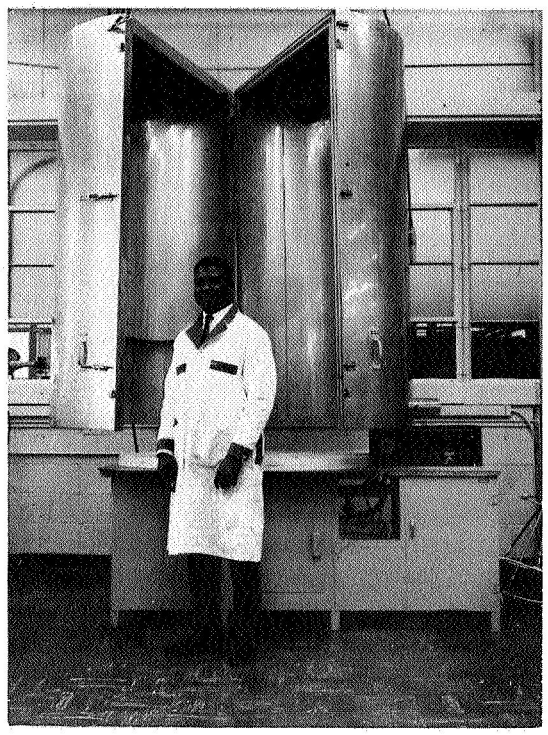

Figure C–81

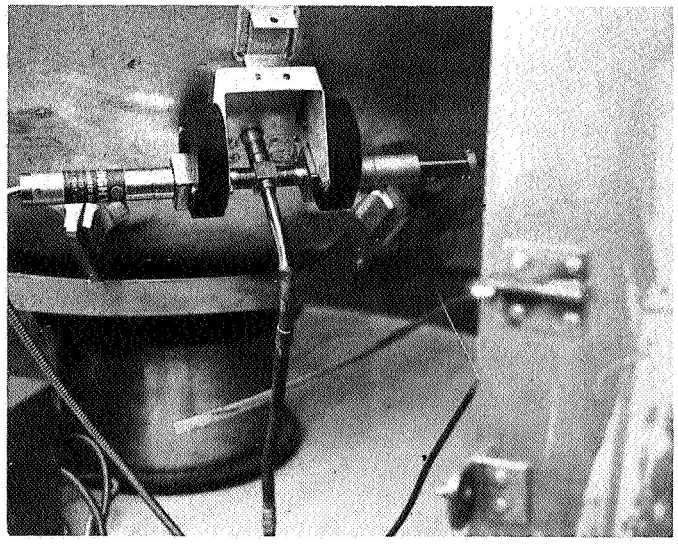

Figure C–82

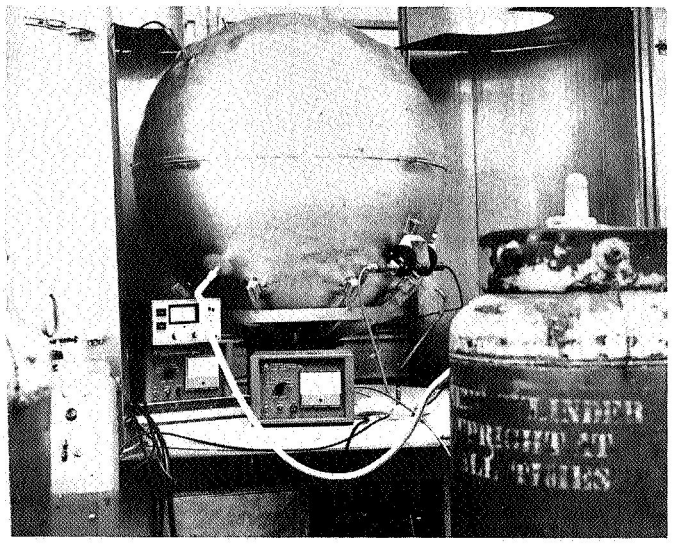

Figure C–83

SECTION D

Phase IV - Prototype Structural Model Fabrication

1.0 DEWAR FABRICATION

Fabrication of the structural model dewar vessel followed the same basic procedures discussed in Section C with a few exceptions.

Since the purpose of the structural model is to determine the structural integrity of the dewar, those features which are necessary for improving the thermal-physical attributes of a cryogenic storage system were not included. The features eliminated from the thermal model are:

(a) Vapor plating of the pressure vessel, shields and outer shells.

(b) Evacuation of the annulus and subsequent bakeout.

(c) Omission of all external components except the ion pumps.

To visually inspect the action of the shields and related assemblies in the annulus during vibration, a number of viewing holes were cut in the outer shell and shields. To determine the structural characteristics of the system an external cradle mount structure was designed and is described in para. 2.0.

2.0 EXTERNAL CRADLE MOUNT STRUCTURE

The mount structure was designed to interface with the 41.5 inch O.D. Cryogenic Gas Storage System (CGSS) tank and allow structural testing of the tank and mount structure assembly. The mount structure and tank assembly is shown in drawing 1621158.

2.1 Design Considerations

The mount structure design was based on the vibration, acceleration and shock environments presented in Exhibit B "Technical Specification Cryogenic Gas Storage System" from Request for Proposal # BG 621-M3-7-44P for CGSS Apollo Applications Program. The outline dimensions for the mount structure and tank assembly are within the space envelopes given in the North American drawing MH04-01002-134. This drawing defines clearance envelope space for installations in bays I, III and VI of the AAP-3 service module configuration from NR drawing 2743-12D.

The mount structure interfaces with the CGSS tank at the sixteen outer shell dimples which contact the support bumpers for the inner vessel. A clearance of 1.00 inch was allowed between the outer shell and the mount structure for additional insulation. The external interface mounting locations for the mount structure were positioned symmetrically about the mid plane of the tank. These mounting locations minimize bumper loads by providing inputs in the lateral (horizontal) direction which equalizes loads at the upper and lower bumper planes. The resulting mount structure design configuration is denoted as a cradle mount and is shown in drawing 1621158.

2.2 Description of Mount Structure

The mount structure consists of four basic parts as shown in drawing 1621158.

(a) Bumper Plane Rings (2 required), Upper and Lower - Each ring has a hollow triangular section.
(b) Bumper Cups (16 required) - The bumper cups mount into the bumper plane rings and interface in direct contact with the outer shell dimples.
(c) Cradle Legs (3 required) - The bumper plane rings are held together to restrain the tank by the 3 cradle legs.

(d) Vibration Isolators (6 required) - Barry Controls' Part No. NC-4300-T10 - The cup type vibration isolators are used to attenuate the high frequency vibration inputs.

2.3 Materials, Fabrication Processes and Assembly

The mount structure is constructed from aluminum parts formed from 6061 flat sheet material. The bumper plane ring and the portion of the legs adjacent to the ring are welded together to provide a rigid assembly common to the top and bottom of the structure. The center portion of the structure is a separate welded assembly. The bumper cups are installed in the bumper ring assemblies which are positioned on the top and bottom of the tank. The center portions of the legs on the structure are positioned between the upper and lower bumper ring assemblies. The gaps remaining between the mating parts are measured, and the shims and screws are installed to preload the mount structure around the tank. The final assembly is shown in drawing 1621158.

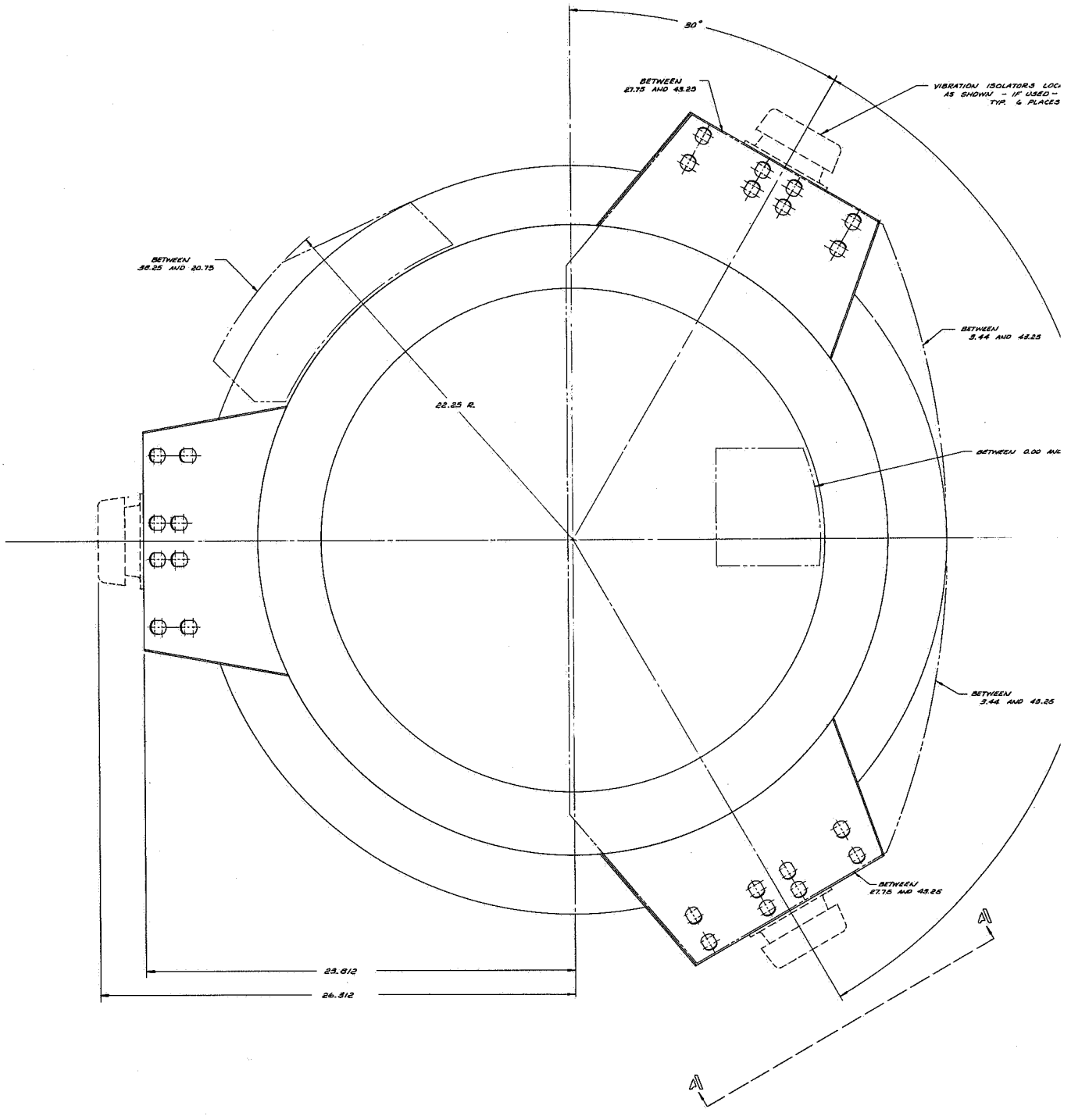

FOLDOUT FRAME 1

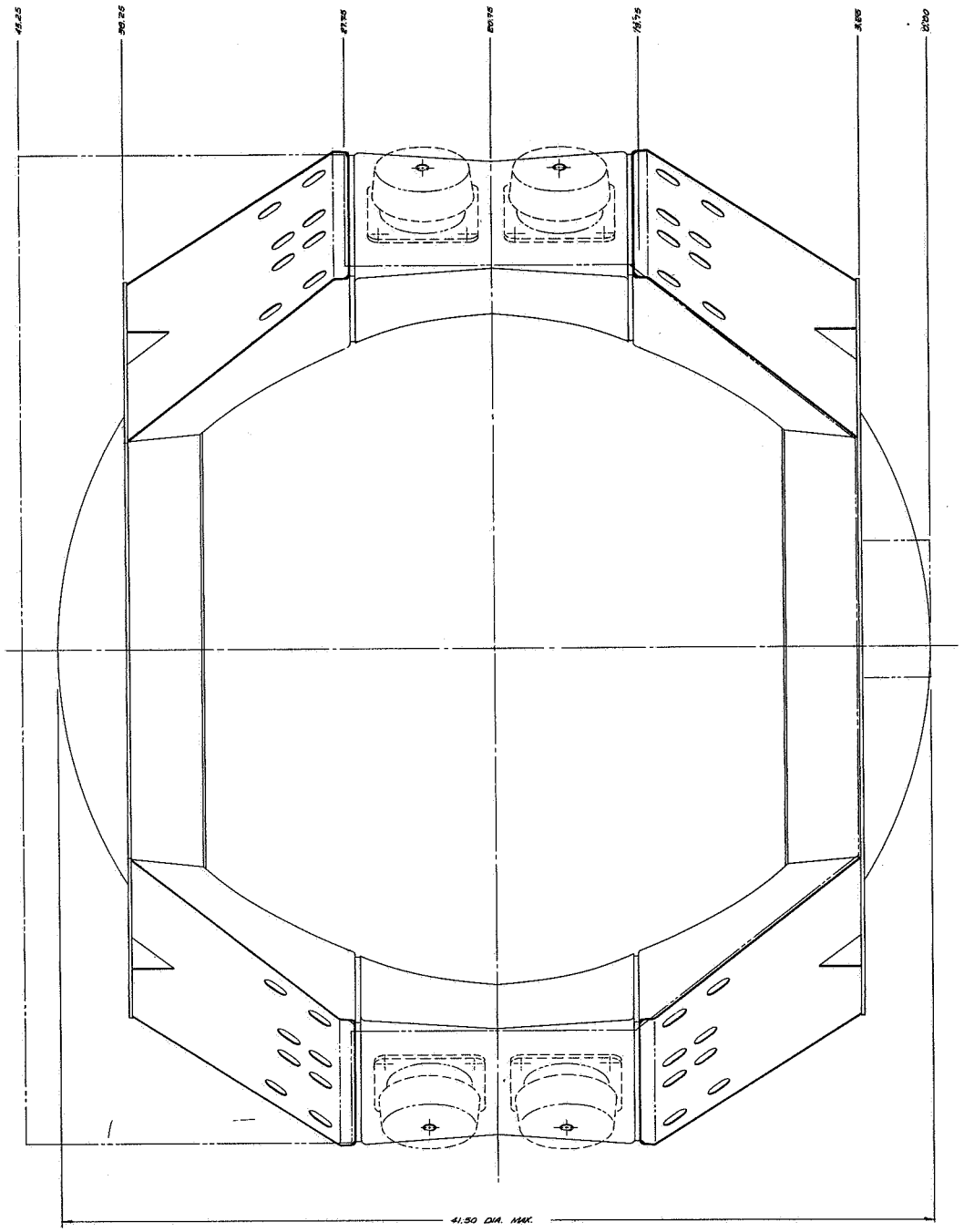

FOLDOUT FRAME 2

REVISIONS				
ZONE	LTR	DESCRIPTION	DATE	APPROVED
	A	NUMEROUS REVISIONS	2/28/62	R.S.D.

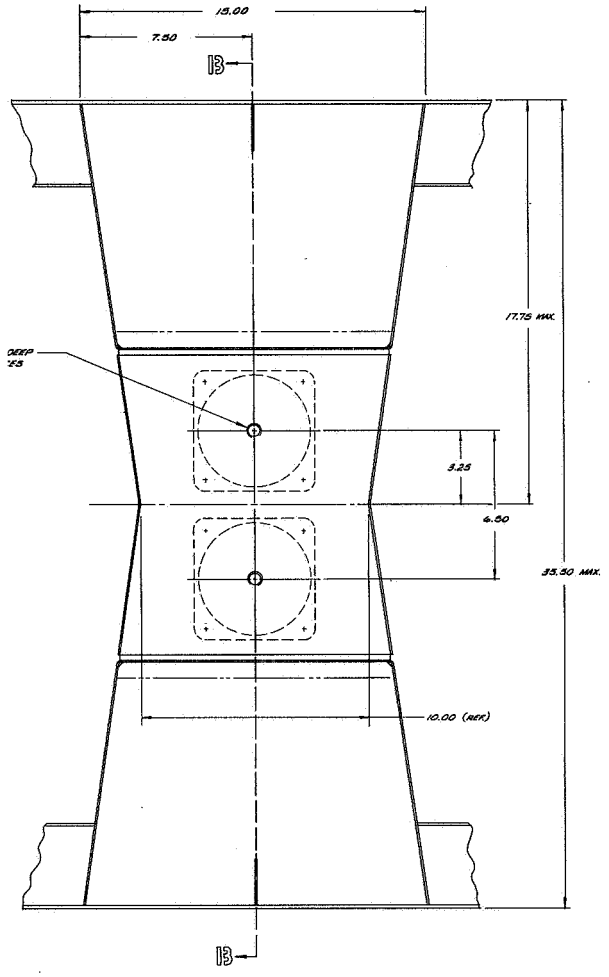

VIEW A-A
- ROTATED 30° CLOCKWISE -
CRYO TANK OMITTED

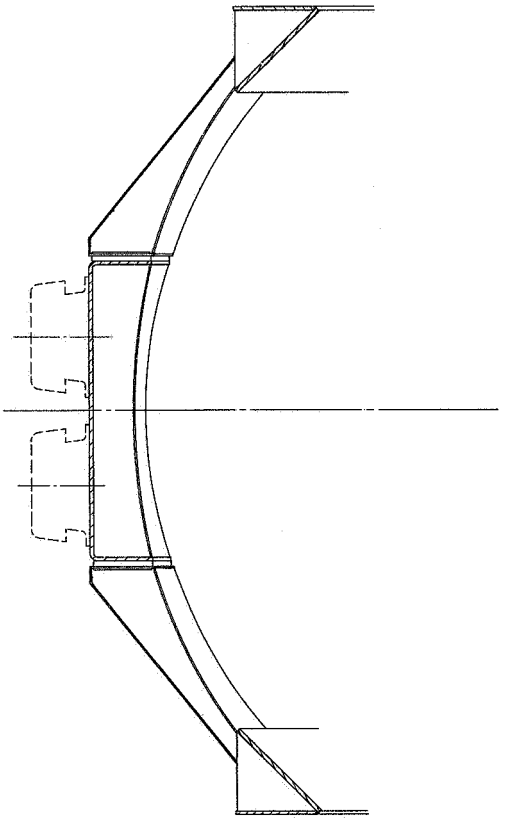

SECTION B - B

1621158-1
PART No.

	R. BJORNAS	2-8-62

THE Beech CORPORATION
PIONEER-CENTRAL DIVISION
DAVENPORT, IOWA, U.S.A.

INTERFACE CLEARANCE ENVELOPE - CGSS SYSTEM

CODE IDENT. NO.	SIZE	DWG. NO.
99251	J	1621158

SCALE 1:2 SHT.

FOLDOUT FRAME 3